Acoustic Data Analysis of the OpenHydro Open-Centre Turbine at FORCE

Final Report

Submitted to:
Sarah Rocks
OpenHydro

Authors:
Bruce Martin
Christopher Whitt
Loren Horwich

28 June 2018

P001292-002
Document 01588
Version 3.0b

JASCO Applied Sciences (Canada) Ltd
Suite 202, 32 Troop Ave.
Dartmouth, NS B3B 1Z1 Canada
Tel: +1-902-405-3336
Fax: +1-902-405-3337
www.jasco.com

Document Version Control

Version	Date	Name	Change
1.0	2018 Mar 28	B. Martin	Draft released to client for review.
2.0	2018 Apr 11	B. Martin	Final released to client.
3.0b	2018 Jun 27	C. Whitt	Updated version released to client. Includes static spectrograms in Section 4.1.

Suggested citation:

Martin, B., C. Whitt, and L. Horwich. 2018. *Acoustic Data Analysis of the OpenHydro Open-Centre Turbine at FORCE: Final Report.* Document 01588, Version 3.0b. Technical report by JASCO Applied Sciences for Cape Sharp Tidal and FORCE.

Disclaimer:

The results presented herein are relevant within the specific context described in this report. They could be misinterpreted if not considered in the light of all the information contained in this report. Accordingly, if information from this report is used in documents released to the public or to regulatory bodies, such documents must clearly cite the original report, which shall be made readily available to the recipients in integral and unedited form.

Contents

Figures

Tables

Executive Summary

Cape Sharp Tidal (CST), a joint venture of Emera Ltd and OpenHydro, is evaluating the potential for generating electrical power from tidal water flow with OpenHydro's Open-Centre Turbine technology. A demonstration project is currently being conducted at the Fundy Ocean Research Centre for Energy (FORCE) test site in the Minas Passage, NS. The demonstration project aims to improve the turbine technology for long-term efficient generation of electricity from tidal currents and to understand and assess the potential effects of turbines on the environment. As required under the Environmental Assessment (EA) Approval, CST and FORCE developed Environmental Effects Monitoring Plans (EEMPs) to address the predictions of the EA. A key element of the EEMPs is the potential effects of turbine sound on fish and marine mammals.

The scope for the turbine sound component of the EEMPs is two-fold: 1) investigations to determine the best way to record operational and ambient sounds in the Minas Passage (both short and long term); and 2) subsequent data analysis to characterize the tidal turbine sound relative to the existing environment.

Acoustic data collection at the FORCE test site has been ongoing since 2012. Comprehensive measurements began in fall 2016 when CST deployed the first grid-connected Open-Centre Turbine on 7 Nov 2016, in the FORCE Crown Lease Area (the study area, Figure 1). After a six-month engineering evaluation, the turbine was disconnected from its subsea cable in April 2017, recovered in June 2017, and taken to Saint John, NB, for further design improvements. During the engineering evaluation, long-term acoustic recordings were made with hydrophones mounted on the turbine platform, as well as an autonomous hydrophone housed in a protective flow-shield on the seabed 167 m from the turbine. Short-term drifting hydrophone measurements were made before the turbine was installed on 18 Oct and 20 Oct 2016, and with the turbine in place on 27 Mar 2017. Two methods of hanging the hydrophone below the drifting float were evaluated: one with an 'S'-shaped catenary cable and one with an elastic cable and baffles to minimize movement.

This report, jointly funded by CST and FORCE, analyzes the 2016–2017 short- and long-term data to:

1. Compare tidal turbine sound to flow noise and how it depends on current speed, turbine state, and measurement method.
2. Estimate the possible effects of the turbine sound on marine life.
3. Evaluate the relative utility of instrument configurations to be used moving forward when measuring the effects of new turbine configurations on the acoustic environment.
4. Provide guidance on methodologies for performing acoustic measurements near tidal turbines and processing of acoustic data to mitigate effects of flow noise.

Based on these measurements, we find that at most frequencies the turbine has a lower source level than vessels that might be typical in the area. For porpoises, the sound amplitude of vessels and the turbine will be similar at similar ranges, and we can expect that pressure-sensing fish will detect and be affected by vessels at 7–10 times the range as the turbine.

The estimated ranges for sound to have various effects on animals is summarized in Table 1 and discussed in Section 4.3.

Table 1. The typical and maximum ranges to the selected thresholds for effects on marine life.

Acoustic effect	Typical range (m)	Maximum range (m)
Fish disturbance	< 30	30
Herring masking	500	1000
Porpoise masking	300	800
Porpoise TTS after 24 h	200	500

From these measurements we observed that autonomous recorders near the seabed provided the best data quality and best characterization of the turbine and ambient sound through all tidal and turbine operating states. Drifter measurements provided useful validation of turbine sound at various ranges but were insufficient to develop a model of the turbine sound in all tidal and operating states. Drifter hydrophone suspensions must include an effective means of isolating the hydrophone from surface wave action, and drifters should have a GPS logger attached to record the location at least twice per minute. Hydrophones on the turbine platform need to be more carefully isolated from flow noise and electrical noise.

Based on the results, we recommend:

- Autonomous recorders in high-flow shielded moorings be considered as the primary method of assessing turbine sound levels.
- Cabled hydrophones on turbine platforms should be located as close as possible to the seabed, and they should be protected by a stream-lined flow-shield.
- The sound signature of the Open-Centre Turbine should be re-assessed during the next deployment.
- At least one lunar cycle of ambient sound should be recorded before or after the next deployment, to quantify the ambient sound levels at all current speeds. An Acoustic Doppler current profiler should be deployed at the same time as the acoustic recorder.
- The detection performance for porpoise should be compared during a simultaneous deployment of the autonomous recorder and the turbine mounted hydrophones.

1. Introduction

To evaluate the potential for generating electrical power from tidal water flow with OpenHydro's Open-Centre Turbine technology, Cape Sharp Tidal (CST) is conducting a demonstration project at the Fundy Ocean Research Centre for Energy (FORCE) test site in the Minas Passage, NS. As part of the Environmental Assessment (EA) Approval, CST and FORCE developed Environmental Effects Monitoring Plans (EEMPs). A key element of the EEMPs is the potential effects of turbine sound on fish and marine mammals.

The turbine sound component of the EEMPs aims to: 1) determine the best way to record short- and long-term operational and ambient sounds in the Minas Passage and 2) analysis the collected data to characterize the tidal turbine sound relative to the environment.

Acoustic data collection at the FORCE test site has been ongoing since 2012. Comprehensive measurements began in fall 2016 when CST deployed the first grid-connected Open-Centre Turbine on 7 Nov 2016 in the study area (Figure 1). During an engineering evaluation, long-term acoustic recordings were made with hydrophones mounted on the turbine platform, as well as an autonomous hydrophone housed in a protective flow-shield on the seabed 167 m from the turbine. Short-term drifting hydrophone measurements were made before the turbine was installed and with the turbine in place.

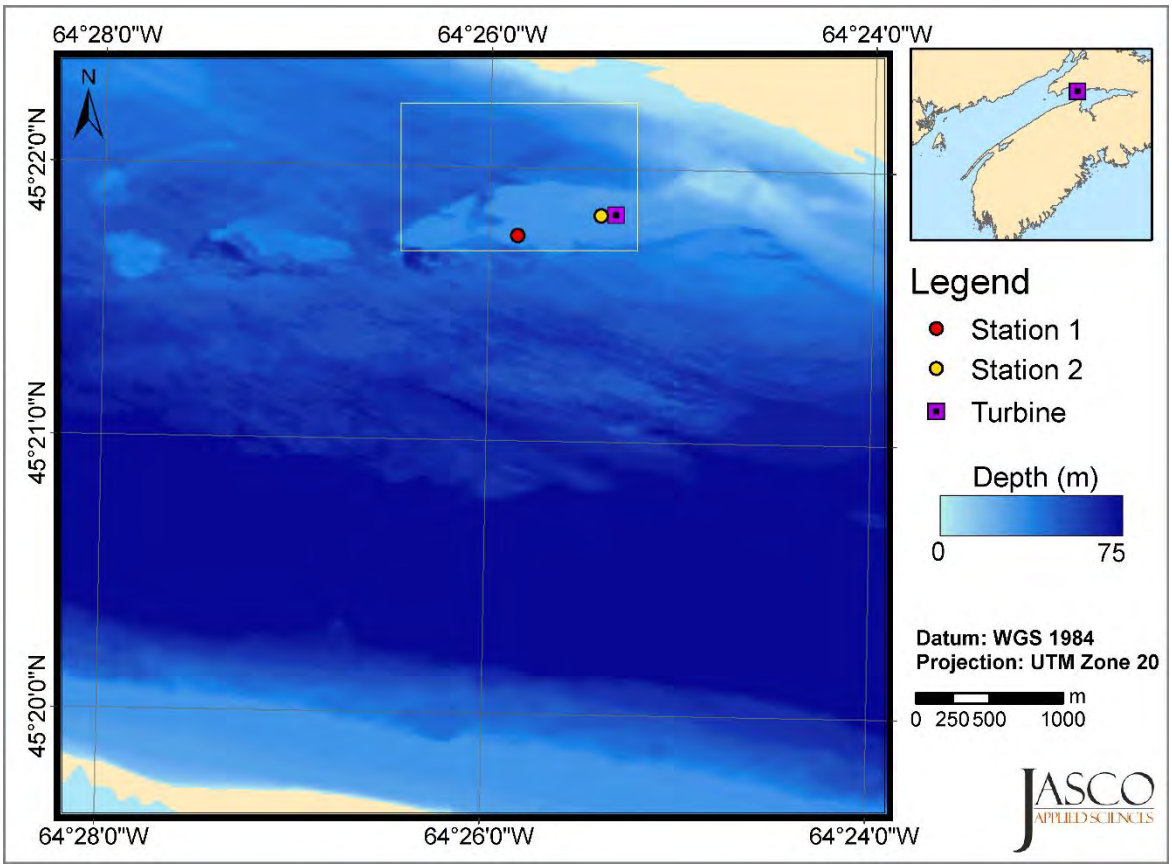

Figure 1. The study area, including locations of turbine and acoustic recorders at two 'stations'. Station 1 was the control site 680 m from the turbine. Station 2 was 167 m from the turbine. The FORCE test site is outlined in yellow.

This report analyzes the 2016–2017 short- and long-term data to:

1. Compare tidal turbine sound to flow noise and how it depends on current speed, turbine state, and measurement method. Specifically, to:
    a. Characterize the frequency content (i.e., spectrum) of the flow noise in relation to that of the tidal turbine sound and its correlation with the current speed.
    b. Determine the cut-off frequency below which the flow noise contaminates the acoustic measurements.
    c. Compare the received sound spectra between recording methods (drifting hydrophones versus hydrophones on the turbine platform versus autonomous recorders on the seabed).
2. Estimate the possible effects of the turbine sound on marine life. Specifically, to:
    a. Determine the total received sound level, as a function of frequency, for each increment of the tidal cycle,
    b. Determine the source level of the turbine as a function of frequency, tidal states, and turbine states,
    c. Determine the range from the turbine where the sound has the potential to injure marine life, and
    d. Determine the range from the turbine where the sound has the potential to mask biologically relevant sounds.
3. Evaluate the relative utility of instrument configurations to be used moving forward when measuring the effects of new turbine configurations on the acoustic environment.
4. Provide guidance on methodologies for performing acoustic measurements near tidal turbines and processing of acoustic data to mitigate effects of flow noise.

This report is divided into two parts. The first part of the report contains:

- Section 2: A summary of underwater sound and the effects of sound on marine life.
- Section 3: A summary of the methods used to collect and analyze the acoustic data for this project.
- Section 4: High-level results that address items 1 and 2 above and a discussion of the results and guidance on future acoustic data collection efforts.

The second part of the report is comprised of technical appendices providing detailed analysis results that support the summaries in the main report.

2. Effects of Underwater Sound on Marine Life

Underwater sound in the ocean is generated by four types of sources [1, 2]:

1. Natural geologic sources: Earthquakes, breaking waves, rain, ice, and sediment moving in high current conditions.
2. Man-made sources: Ships, sonars, seismic airgun surveys, and in-water activities such as drilling, pile-driving, dredging, and generating power.
3. Biologic sources: A wide variety of marine life makes and listens to sounds for social communicating, mating, mother-calf bonding, foraging, avoiding predators, and selecting habitat.
4. Measurement artifacts: Signals that are not caused by sound propagating in the water but instead are the result of how the measurements are made, including signals generated by water flowing around a hydrophone (flow noise), electrical noise from recording hardware, and sounds reflecting off recorders or moorings, which add to the sound travelling from the source to the hydrophone.

Different sources of sound can overlap in time, location, and frequency. The capacity for marine life to perceive and be affected by a sound depends how the sound's frequency content overlaps with the animal's hearing range (see Section 2.3). As a result, a source's frequency range is often used as the primary characteristic for assessing its possible effects (Figure 2).

The subsections below introduce how marine life uses underwater sound, the hearing capabilities of marine life, and the effects of sound on marine life. For more information on these topics that is geared toward a general audience, we recommend the website *Discovery of Sound in the Sea* (https://dosits.org).

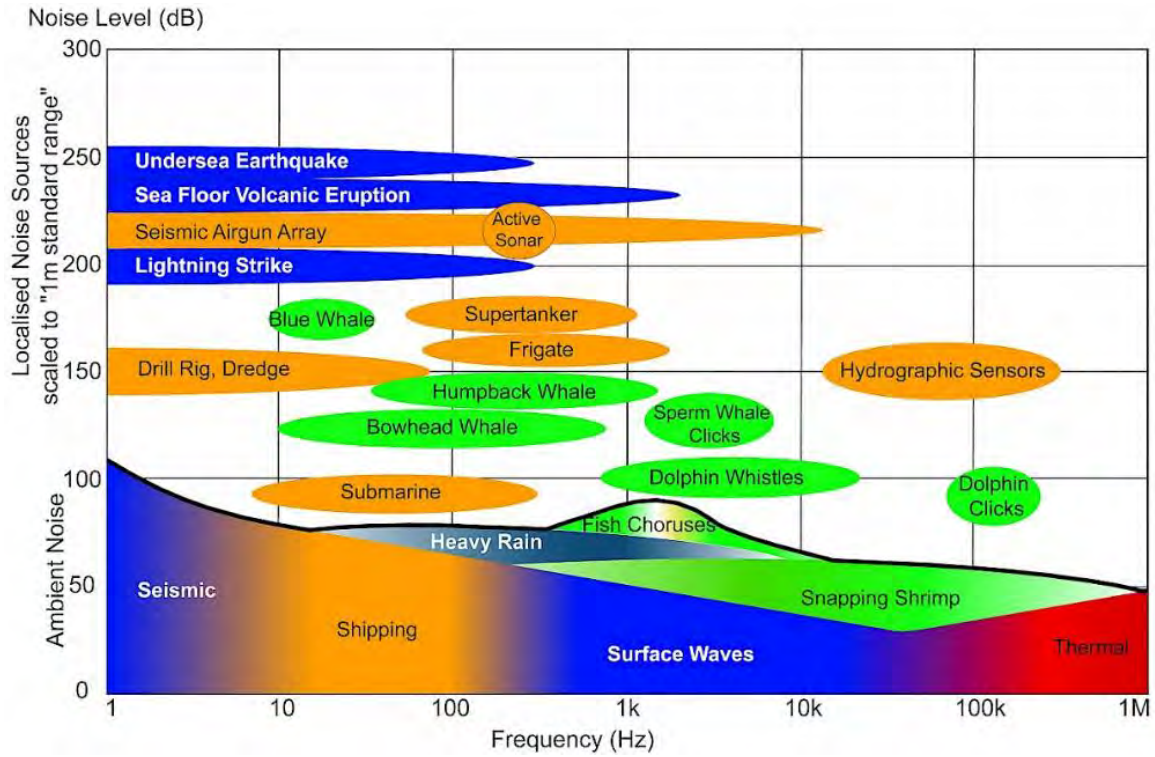

Figure 2. Sounds in the ocean. The spectral level of typical sound source, when measured at 1 m from the source, and the typical ambient noise levels measured by a recorder. Yellow sound sources are man-made, blue are geologic, and green are biologic. Thermal noise is the limit of what can be measured at high frequencies due to electronic self-noise (from https://www.ospar.org/work-areas/eiha/noise).

2.1. How Marine Life uses Underwater Sound

Hearing is one of the most important senses for marine life because light does not penetrate very far into the ocean. Sounds that are ecologically relevant to marine animals include conspecific calls, predator and prey sounds, natural sounds used for orientation, and echolocation calls from odontocetes (toothed whales) [3].

We know that marine mammals use sound for foraging and navigating [4-6], social communicating [e.g. 7], mother-calf bonding [8], and mating displays [9]. Populations of odontocetes that live together, such as dolphins, beluga, and pilot whales, have signature whistles that identify individuals to the group. Many populations of odontocetes have dialects used to communicate within their group, including sperm whale 'codas' [10] and the whistles of killer whales [11]. The Minas Passage is frequented by harbour porpoise that use the Passage as a feeding area. Porpoise emit a very high frequency echolocation click (~130 kHz) and listen for the echoes to navigate and to find food [12, 13].

All fish and sea turtles have hearing organs, and all individuals measured to date responded to sound in some way [14]. In fish, there have been multiple evolutions of sound production for courtship and agonistic displays [15], which implies a significant advantage is gained by being able to produce sound. Some reef fish select or avoid habitat based on sound [16], and it appears that both coral and fish larvae use the intensity and transient content of the soundscape to select settlement locations [17, 18]. This shows that sound is important to these species at all life stages. Invertebrates also produce and perceive sound. For example, oysters have a valve closing response to sound [19], as do scallops, which also make distinctive 'cough' sounds associated with clearing sediment from their valves [20]. Snapping shrimp generate bubbles by rapidly moving their claws; these bubbles are believed to be used for signalling and hunting. These sounds vary widely in space and time [21]. Lobsters and many other crustaceans sense sound and generate sounds that are believed to be associated with breeding [22].

2.2. Hearing Capabilities of Marine Life

The potential effects that a sound could have on an animal depend greatly on how well the animal can hear the sound. Marine mammals have two ears whose structure is very similar to that of land mammals. Their ears are sensitive to acoustic pressure in the water. Different groups of mammals have evolved their hearing for specific purposes, and they hear at different frequencies and with different minimum sound levels.

Marine fish have different hearing structures—three dense masses of bone, called otoliths, that respond differently to sound waves than the tissue around them. As a result, fish hearing is sensitive to the acceleration of the water caused by a sound rather than the acoustic pressure. In most cases, particle acceleration is only large enough to be perceived very close to a sound source [23]. Some fish, however, have adaptations that connect their swimbladder to the otoliths, which enhances their sensitivity to sound pressure. Fish and sea turtles can be organized into five large groups with respect to hearing and sensitivity to man-made sounds. The groups, arranged in order from most to least sensitive are: 1) fish with swimbladders involved in hearing, 2) fish with swimbladders not involved in hearing, 3) fish without swimbladders, 4) sea turtles, and 5) eggs and larvae. The grouping of the key species for the Minas Passage monitoring programs are shown in Table 2.

Table 2. Hearing groups of fish in the Minas Passage.

Hearing group	Key species in the Minas Passage
Fish with swimbladders involved in hearing	Atlantic herring (*Clupea harengus*) Alewife/Gaspereau (*Alosa pseudoharengus*) River herring (*Alosa aestivalis*) Shad (*Alosa sapidissima*)
Fish with swimbladders not involved in hearing	Atlantic salmon (*Salmo salar*) Atlantic cod (*Gadus morhua*) Pollock (*Pollachius pollachius*) Silver hake (*Merluccius bilinearis*) Red hake (*Urophycis chuss*) Striped bass (*Morone saxatilus*) Atlantic sturgeon (*Acipenser oxyrhynchus*)
Fish without swimbladders	Mackerel (*Scomber scombrus*) Wolffish (*Anarhichas lupus*) Sea raven (*Hemitripterus americanus*) Grubby (*Myoxocephalus aenaeus*) Summer flounder (*Paralichthys dentatus*) Witch flounder (*Glyptocephalus cynoglossus* Lump fish (*Eumicrotremus spp.*) Plaice (*Hippoglossoides platessoides*) Spiny dogfish (*Squalus acanthias*) Thorny skate (*Amblyraja radiata*) White shark (*Carcharodon carcharias*)

Invertebrates have a different sensory organ called a statocyst that is also believed to be sensitive to acceleration from water movement, gravity, and sound; however, there is limited data on the response of these structures.

The hearing sensitivity of a species, the threshold of hearing (akin to the level at which a sound becomes audible) as a function of frequency, is commonly referred to as an audiogram. Figure 3 shows examples of sound pressure audiograms for fish (left) and odontocete mammals (i.e., toothed whales (right) and harbour porpoises). Herring are fish whose swimbladders are involved in hearing and, as a result, they can sense acoustic pressure at relatively low levels over a wide frequency range. In contrast, salmon, cod, and dab (a flatfish) have swimbladders that are not involved in hearing and are therefore less sensitive to acoustic pressure. Their audiograms are elevated compared to those of herring and span a smaller frequency range. The odontocete audiograms show a wide range of sensitivities across species, but in general odontocetes are most sensitive in the range of 20 kHz and above, which is the band they use for echolocation. Their sensitivity at 200 Hz is lower than that of the salmon. Sea turtles have hearing like that of salmon shown in Figure 3 (left). Shark hearing is restricted to low frequencies (less than ~400 Hz), [e.g., 24], and, because they lack swimbladders, shark hearing relies on detecting the particle motion aspect of sound. There are no audiograms for marine invertebrates, but invertebrates lack air-filled cavities so these groups are presumed to respond primarily to particle motion, and only at low frequencies.

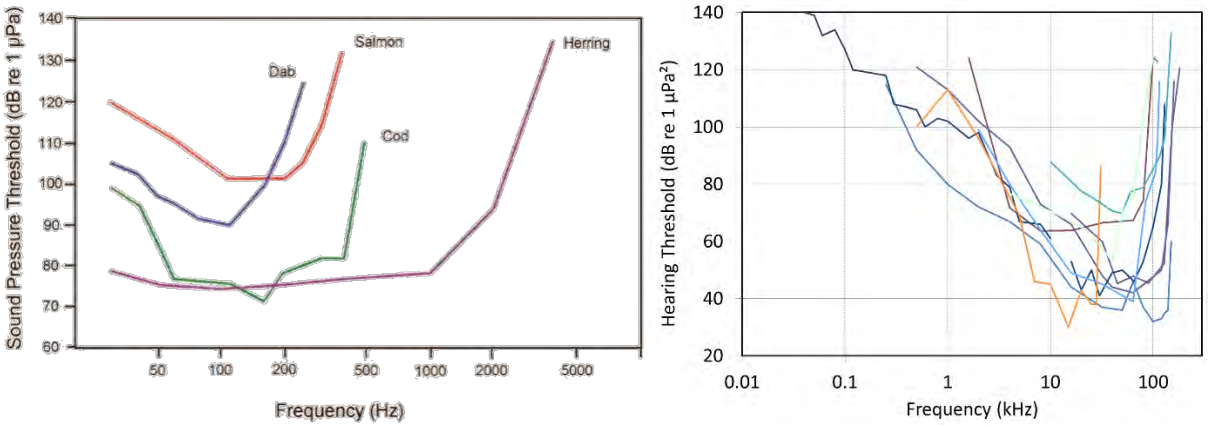

Figure 3. Example audiograms for fish (left [25]) and odontocete mammals (right, courtesy of H. Yurk and C. Gomez, extracted from the literature).

When determining potential effects of a sound source, audiograms are used to inform the process of frequency weighting received sound. Frequency weighting scales the importance of sound components at particular frequencies according to an animal's sensitivity to those frequencies. For human hearing, we use the 'A-weighting' auditory weighting function to filter sounds before estimating the effects [26]. The weighting function is an inversion of the audiogram (or equal-loudness curves when they exist), normalized to have a gain of zero at the frequencies of peak sensitivity. For marine mammal hearing, species are separated into five hearing groups, each with its own auditory weighting function (Figure 4). These weighting functions, developed by Finneran [27], are based on detailed analysis of existing audiogram data and other inputs and have been incorporated into the Technical Guidance issued by American regulators for assessing effects of noise on marine mammals [28]. No such generalized weighting functions exist for fish or invertebrates; however, inverted audiograms (i.e., Figure 3, left) have been used for individual species.

To determine the potential effects of tidal turbine sounds on relevant species, sound levels are compared with known thresholds for effects, or compared to ambient sound levels. In this analysis, we compare the high-frequency cetacean (e.g., porpoise) marine mammal weighted sound and the herring auditory filter-weighted sound pressure levels to the weighted background sound levels. We did this because porpoise and herring are the two most sound-sensitive species in the study area.

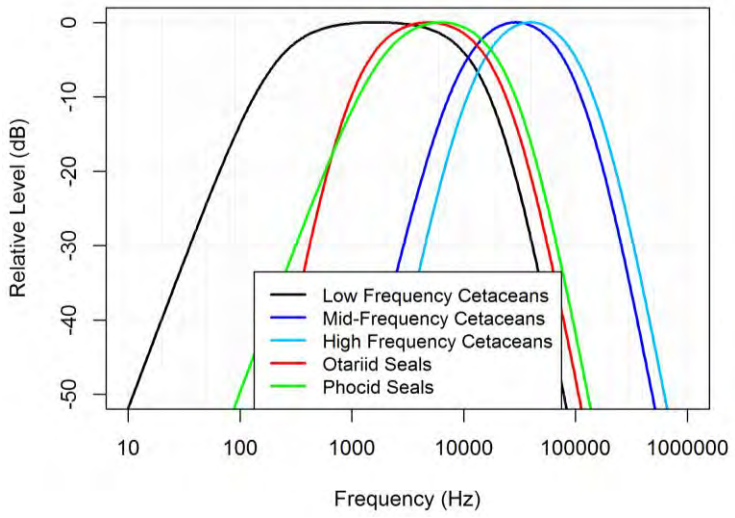

Figure 4. Auditory weighting functions for the marine mammal hearing group [28]. Low-frequency cetaceans include the large baleen whales (e.g., blue, fin, and humpback whales). Mid-frequency cetaceans are dolphins, sperm whales, and beaked whales that whistle and echolocate in the band of ~1000–80000 Hz. High-frequency cetaceans are dolphins, sperm whales, and porpoises that echolocate at ~130 kHz. Otariid seals are sea lions and fur seals, whereas phocid seals are considered 'true' seals, characterized by short fore flippers and the absence of external ears.

2.3. Effects of Underwater Sound on Marine Life

Short- and long-term studies of passive acoustic data in conjunction with observations of marine life behaviour have shown a wide range of impacts of man-made underwater sound on marine life. In general, impulsive sounds (brief, intermittent sound with a rapid rise and decay) have greater potential to damage hearing than non-impulsive sounds (broadband sound without a high peak pressure with rapid rise) because of their short rise time and high pressures . Non-impulsive sounds may present greater masking potential and greater behavioural effects due to their, typically, longer duration signals. Examples of observed effects of impulsive sounds include: diversion of migrating of bowhead whales around seismic surveys [29]; a change in bowhead whale calling rates in response to seismic surveys [30]; porpoise avoiding areas within 20 km of impact pile driving [31, 32]; seismic survey noise affecting scallops, lobsters, and zooplankton months after exposure [33, 34]; alarm and startle reactions in fish and squid to seismic surveys [35]; a variety of responses by benthic animals to substrate borne vibrations [36]; beaked whales responding and stranding when exposed to naval sonars [37-39]; blue whales changing behaviour and calling patterns when exposed to naval sonars [40, 41] or seismic surveys [42]; pile driving sounds injuring fish [43, 44]; blue mussels changing their metabolic state when exposed to pile driving [45]; and a marked difference in beaked whale echolocation clicks in the presence of vessels with active echosounders [46].

Known effects of non-impulsive sounds include: small boat noise affecting the settlement of larvae fish [47], affecting fishes orientation responses [48], and increasing fish cortisol (stress) levels [49]; vessel noise restricting the communication space for baleen whales [50]; vessel noise reducing the communication space of mating cod and haddock [51]; fish avoiding or changing behaviour in the presence of vessels [14, section 7.5.5] and stress hormones decreasing in right whales when shipping was reduced after 9/11 [52]. Adverse effects from noise on marine fish may also in turn affect other ecosystem components that rely on marine fish as a food source.

The effects of sound on humans and animals is generally visualized as a series of four zones, or concentric rings, around the sound source (Figure 5). In Zone 1, the sound exposure leads to barotrauma injury [for examples see 53] or permanent threshold shift (PTS), meaning that hearing is damaged and does not recover. In Zone 2, the sound exposure causes a temporary threshold shift (TTS) where hearing recovers after some duration (e.g., the morning after a rock concert). In Zone 3, the sound source masks

the ability of an animal to hear another sound of importance (e.g., conspecifics, predators, prey, environmental queues). In Zone 4, the sound is still audible and may evoke a behavioural response (e.g., orientation, movement) or physiological response (e.g., stress hormones).

The first noise mitigation regulations based on noise thresholds were based on keeping the sound pressure level below the level associated with measured injuries to the hearing of marine life [54-56]. Evidence has since demonstrated that the total sound exposure level and the peak sound pressure levels are better indicators of injury than the sound pressure level [14, 57]. As a general rule, noise regulations are imposed on human activities to minimize injury to marine mammals and other endangered marine life rather than to reduce disturbance [58]. Understanding the effects of acoustic disturbance remains an important area of research [59, 60].

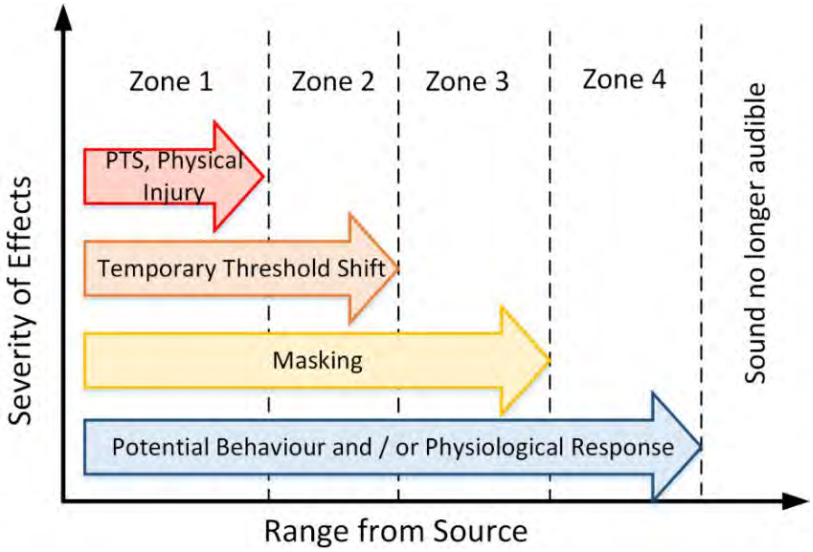

Figure 5. General principles of noise exposure (after Dooling, Leek and Popper [61]).

For assessing the potential of a project, such as the development of tidal energy in the Minas Passage, to affect marine wildlife it is useful to have numeric thresholds to compare with the project's emitted sounds. For fish, Canadian regulations include the protection of fish and fish habitat under the federal *Fisheries Act* and additional protection of specific species under the *Species at Risk Act.* No numeric thresholds are specified. Our best available information on effects of underwater noise on fish indicates that exposure to a sound pressure level of 158 dB re 1 µPa for 12 hours (194 dB re 1 µPa²·s sound exposure level) can cause temporary shifts in hearing thresholds (TTS) for fish with swimbladders [62], and exposure to a sound pressure level of 170 dB re 1 µPa for 48 hours (220 dB re 1 µPa²·s sound exposure level) causes recoverable injury for fish with swimbladders [63]. For behavioural reactions, 150 dB re 1 µPa² sound pressure level is often cited as the threshold for effects, as well as the minimum sound level at which injury effects begin to accumulate (known as 'effective quiet'), and it is assumed to apply to all hearing groups [64].

For marine mammals, Canadian regulations focus on critical habitats for species that are listed under Schedule 1 of the *Species at Risk Act;* the only noise thresholds that are specified apply to these habitats. American regulatory criteria provide the best available guidance for assessing potential hearing injury to marine mammals. The criteria use weighted functions based on frequency hearing range of the species (Figure 4) and calculate a daily sound exposure level (SEL; total daily sound energy) for predicting injury. For near continuous sound sources, such as tidal turbines, the daily exposure limit for porpoise is 153 dB re 1 µPa²·s to avoid temporary hearing threshold shifts, and 173 dB re 1 µPa²·s to avoid permanent hearing threshold shifts [28].

3. Methods

Collection and analysis of turbine and ambient sound used both long-term and short-term recording methods. Long-term acoustic recordings are weeks to months in duration using hydrophones that are held stationary on the turbine platform or on the seabed nearby. Short-term acoustic recordings are made using drifters that move with the currents past the turbine. The drifters typically travel 2–3 km in 10 minutes. At a speed of 12 km/h (6.5 knots), a drifter would spend 1 minute within ±100 m of the turbine.

3.1. Data Collection

In accordance with the EEMPs, CST and FORCE gathered extensive acoustic data during the deployment of the Open-Centre turbine from November 2016 to June 2017. This data set includes:

- Drifting hydrophone measurements made by FORCE on 18 and 20 Oct 2016 before the turbine was installed. Two types of drifters were evaluated—a drifter with a catenary 'S' shaped hydrophone suspension and a drifter with a simple elastic rope and damper to minimize hydrophone vertical movement. The drifter with the catenary used a JASCO AMAR recorder in a duty cycled setting sampling at 32 and 375 kHz (see technical details in Appendix A.1.4). The drifter with the elastic rope and damper used an Ocean Sonics icListen recorder sampling at 512 kHz (see technical details in Appendix A.1.3).
- Ocean Sonics icListen hydrophones were mounted on the turbine platform and transmitted their data to shore, as indicated in the 2017 EEMP annual report, up until cable disconnection in April 2017. The sample rates varied from 32 to 512 kHz over the measurement period (see technical details in Appendix A.1.2).
- An autonomous acoustic recorder (JASCO AMAR) in a specially designed high-flow mooring recorded data at the seabed 167 m from the turbine from 18 Nov 2016 to 19 Jan 2017. The JASCO AMAR recorder used a duty cycled setting sampling at 32 and 375 kHz (see technical details in Appendix A.1.1).
- Drifting hydrophone measurements made by FORCE on 27 Mar 2017 with the turbine free-spinning during a flood tide. The simple elastic-rope and damper drifter was used for these measurements. These measurements used an Ocean Sonics icListen recorder sampling at 512 kHz (see technical details in Appendix A.1.3).

Two autonomous recorders were originally deployed near the turbine. The second autonomous recorder was intended as a control measurement to capture ambient sound. That recorder was not recovered. We were able to extract enough information about ambient sound from the first autonomous recorder to sufficiently distinguish turbine sound from ambient sound and develop a model of turbine sound.

For contextual comparison of the Minas Passage measurements to the sound levels in the wider project area, the results of a four-month acoustic recording underneath the shipping lanes at the Grand Manan Basin are provided. Details of the measurement equipment configurations, calibrations, and mooring designs are contained in Appendices A.1 and A.2.

To help interpret the acoustic data, current speed and direction were measured at the turbine platform continuously during the deployment and CST logged turbine state data throughout the evaluation. The turbine states are categorized as: not-spinning, free-spinning, and generating.

3.2. Data Analysis

The objectives of this data analysis were to determine the frequency band affected by flow noise, the frequency band of the sounds emitted by the Open-Centre Turbine, and then comparing how these bands changed with turbine operating state, current speeds, and measurement technique (drifters versus turbine-mounted hydrophones versus autonomous bottom-mounted hydrophones), as well as investigate the potential relationship between turbine sound and marine life. The acoustic metrics used for these analyzes were 1-minute broadband sound pressure level (SPL), pressure spectral density, and decidecade-band SPL (see Appendix A.3). The decidecade sound pressure levels were weighted to also provide the high-frequency cetacean (Figure 4) and herring-auditory-filter weighted (Figure 3) sound pressure levels. We used 1-minute statistics to match the time resolution of the current speed and turbine state data set. One-minute averaging also smooths the random effects of turbulence and sediment movement sounds.

The metrics used throughout this report are *level* quantities. This means that they are ten times the logarithm of an acoustic measure divided by its reference value, and the units have the form 'dB re 1 μPa^2'. A result, a 10 dB increase in the level is equivalent to multiplying the acoustic measurement by 10. Details of the acoustic metrics are provided in Appendix A.3.

An automated odontocete click-detector (see Appendix A.7) was used to find periods when porpoise were vocalizing in the long-term data sets.

The analysis results were used to train models that provide the source level of the turbine as it changed with frequency, operating state, and current speed. Generalized Additive Models (GAMs) were used for the source levels modelling (see Appendix A.5), along with simplified acoustic propagation models (see Appendix A.6).

3.3. Data Quality

All JASCO instrumentation used in this study were calibrated before and after each use (see Appendix A.2). Data from other instrumentation were analyzed according to manufacturer-supplied calibration information. Calibrations were validated after data collection and before data analysis to verify instrument performance, as a standard part of JASCO's ISO 9001 Quality Management System. During processing and analysis, relevant ISO standards were used for acoustic metrics (see Appendix A.3).

4. Results

This section addresses the first two questions identified in Section 1. Recommendations for future measurement programs are contained in Section 4.3. Detailed results are contained in Appendix B, Appendix C, and Appendix D.

In this analysis, the current speeds are in units of normalized current speed, which is the percent of maximum current. To help interpret the acoustic measurements, it is important to note that the current speeds in the ebb tide are ~70% of those in the flood tide. The maximum daily current speed depends on the long-term tidal cycle and can vary from 65–100% of the absolute maximum (see Appendix B.1).

4.1. Comparing Tidal Turbine Sound to Flow Noise and Dependence on Current Speed, Turbine State, and Measurement Method

The data indicates that turbine sound is dependent on the current speed and the operating state of the turbine. Flow noise depends on the measurement method and current speed. Overall, the turbine and flow sound levels increase with the current speed and are higher in the flood tide than the ebb tide, similar to the current speeds.

In Figure 6, the full recording period of the autonomous seafloor AMAR recorder has been aligned so that the left edge of the data is at high tide. The first ~6 hours of the recording are median pressure spectral densities for each minute of the ebb tide, and the last ~6 hours are for the flood tide. The data from Figure 6 are presented slightly differently in Figure 7, which shows the decidecade sound pressure levels as a function of time since high tide and turbine state. From these figures, we identify four frequency bands of interest:

1. Primary flow noise: Up to ~60 Hz is dominated by flow noise (for the autonomous seafloor recorder). Increasing current speed increases both the magnitude of the flow noise effects and the range of frequencies affected.
2. Turbine Band 1: From ~60–250 Hz, there is a band of sound generated by the turbine in both free-spinning and generating states that intensifies with current speed.
3. Turbine Band 2: From ~600–1600 Hz, there is a band of sound from the turbine that is present only in the generating state. The amplitude of this sound does not depend on current speed.
4. Turbine Band 3: From ~3000–4500 Hz, there is a band of sound that is only present during the generating state whose amplitude depends weakly on current speed.

The data in Figure 7 has gaps in the generating and free-spinning curves near slack tide and in the not-spinning curves during the flood tide. This is due to the operating parameters for the turbine during the engineering evaluation: at least 15% normalized current was required to start the turbine spinning, and the turbine was always at least free-spinning during high current flows.

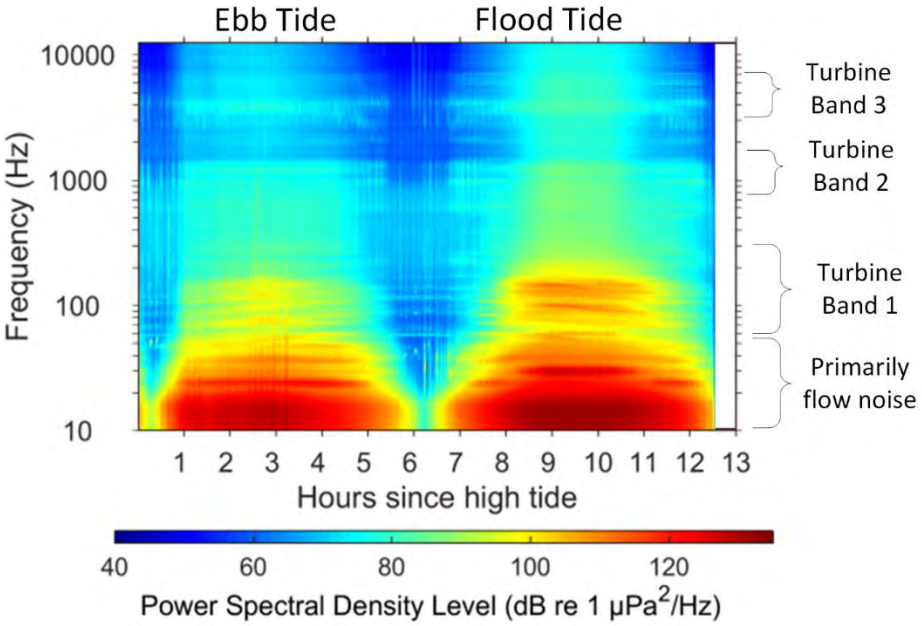

Figure 6. Pressure spectral density versus tidal increment time as measured by the AMAR 167 m from the turbine 18 Nov 2016 to 19 Jan 2017. The horizontal axis is time in hours since high tide.

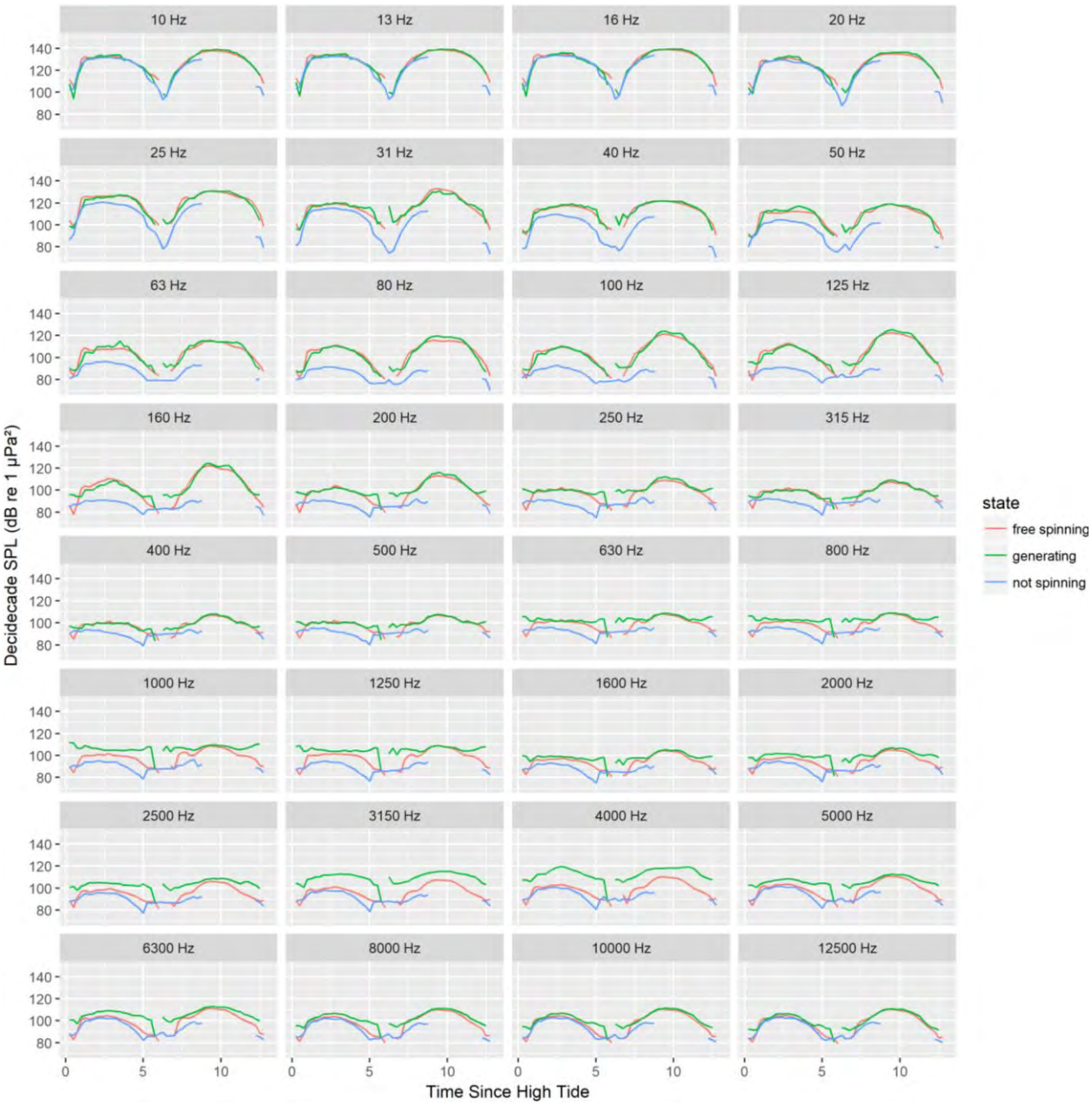

Figure 7. Median decidecade band SPL for each decidecade using data from the autonomous AMAR 167 m from the turbine. The turbine state is shown by the curve colours.

Figures 8 and 9 provide examples of the sounds created by the Open-Centre turbine. The generating state produced broadband rasping sounds (Figure 8). The free-spinning operating state produced a knocking and vibrating sound, as well as tones in the 50–200 Hz range (Figure 9). Throughout the recordings, occasional impulsive sounds were observed, possibly produced by sediment striking the metal housing of the turbine or the recorder (e.g., at ~15 sec in Figure 9). The examples in Figures 8 and 9 are typical of sounds in the different operating states and how the sound transitioned between states. However, a wide variety of onsets and transitions were found. These depended on how the OpenHydro engineers configured the turbine control centre, which was tested and evaluated during these recordings.

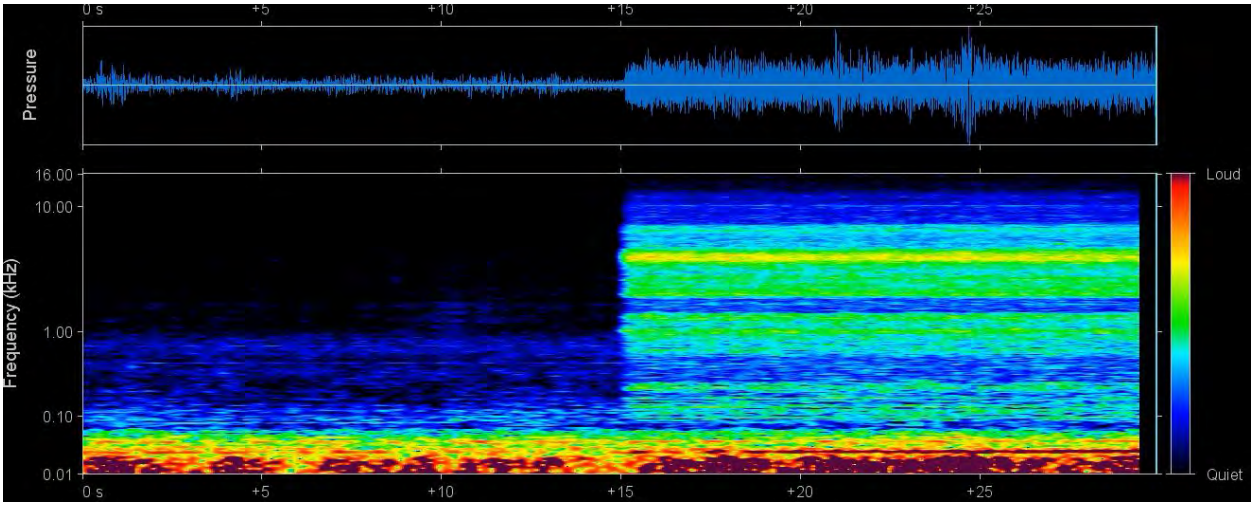

Figure 8. Spectrogram from 30 second MP4 movie containing the sound recorded by the AMAR 167 m from the OpenHydro turbine when it switched from not spinning to generating in a 20% normalized speed flood current at 14:39 on 17 Jan 2017.

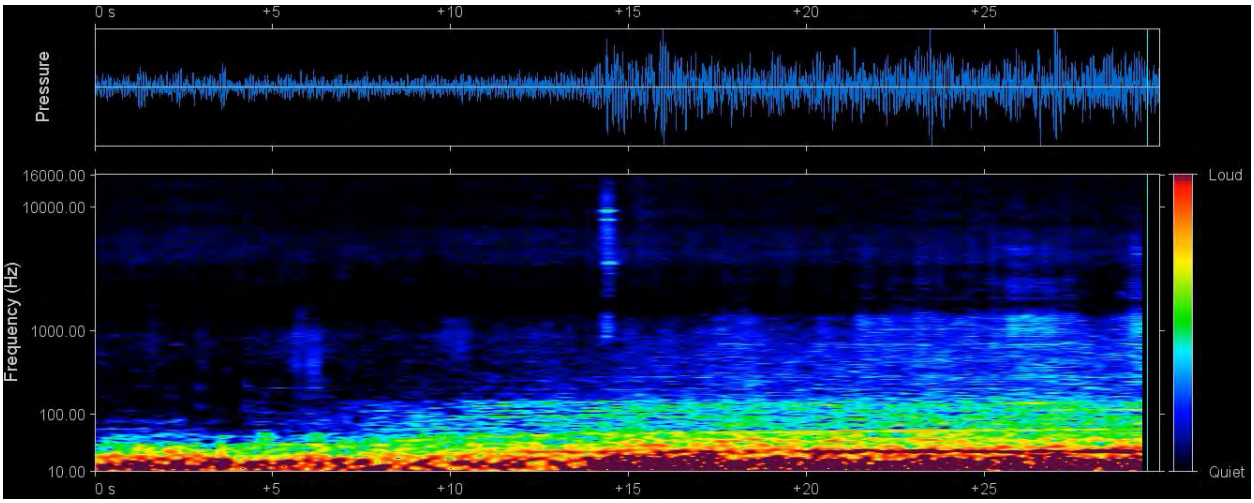

Figure 9. Spectrogram from 60 second MP4 movie containing the sound recorded by the AMAR 167 m from the OpenHydro turbine when it switched from not spinning to free wheeling in a 50% normalized speed ebb current at 21:29 on 5 Dec 2019. The knocking/vibrating sound at the end of the clip was typical for the free-spinning state.

To determine how the measurement method affects the flow noise, we compared median pressure spectral densities as an indicator of the effectiveness of different long-term recording positions (Figure 10). In Figure 10, two spectra are shown from the hydrophones on the turbine platform—the hydrophone on the forward-port leg of the platform and the hydrophone on top of the turbine (hydrophone

mounting arrangements are shown in Figure 27). These are compared to the seabed AMAR located 167 m from the turbine, the icListen drifter data from 27 Mar 2017, and reference data from the outer Bay of Fundy. Turbulent flow noise is expected to have a slope of frequency$^{-5/3}$; this noise is included in Figure 10 for comparison [65, 66].

The similarity of slope of all the measured data to the frequency$^{-5/3}$ line at low frequencies shows that all recording methods considered are affected by flow noise to varying degrees. For frequencies greater than 60 Hz, the autonomous AMAR data appears to be representative of sounds in the water rather than flow noise. The autonomous, shielded, and bottom mounted location of AMAR was 5–20 dB quieter than the hydrophone in the forward-port location, and 10–40 dB quieter than the turbine top location. The icListen drifter data from 27 Mar 2017 had similar median sound levels to the AMAR from ~90–1000 Hz; however, we found that there was vertical movement noise up to ~150 Hz when comparing sound levels as a function of current speeds. Above 1000 Hz, measured sound levels in the Minas passage were up to 5 dB higher than the outer Bay of Fundy because of sediment impact noise hitting the instrumentation or surrounding structures. The sediment noise may have had higher levels on recordings made above the seabed compared to the autonomous bottom mounted recorder.

The analysis of the turbine sound levels used the autonomous recordings because flow noise affected a much wider range of frequencies on the turbine platform hydrophones. The 63 Hz decidecade was chosen as the lowest frequency band where the turbine sound levels were sufficiently above the flow noise for analysis.

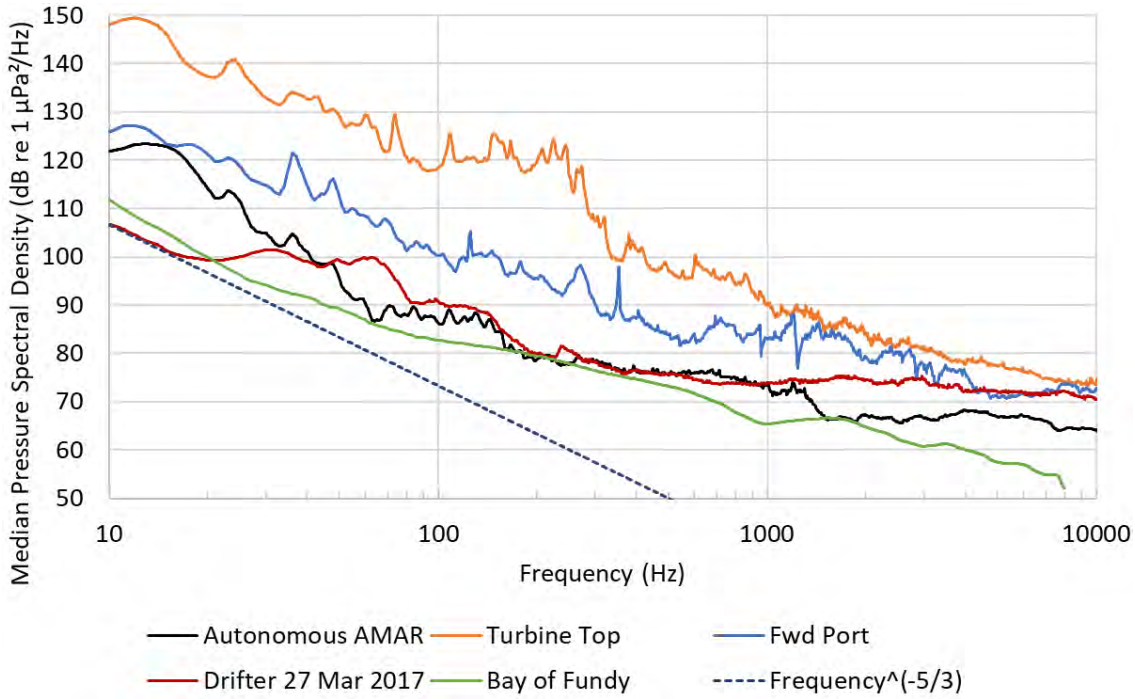

Figure 10. Median pressure spectral densities for three different long-term recording positions, as well as the icListen drifter measurements from 27 Mar 2017

4.2. Turbine Sound Level Modelling

We used the data from the autonomous recorder to train models of the decidecade received sound pressure levels that depended on the current speed for each of the operating states (not spinning, free spinning, and generating), as well as the two current directions (ebb and flood). Figure 11 shows examples of the predicted levels from the model and how they compare to the median decidecade sound pressure levels from the outer Bay of Fundy. The model analysis shows:

- The sound levels in all three turbine states does not depend strongly on the current direction, only on the current speed.
- The ambient conditions in the Minas Passage at frequencies below 1 kHz are up to 25 dB quieter than the sound levels in the outer Bay of Fundy.
- The turbine emits a band of sound in 60–250 Hz range in the generating and free-spinning states that increases by 20–30 dB as the current speeds increases.
- The turbine emits a band of sound in the 1000–1250 Hz range while generating that is nearly constant sound level, regardless of currents speeds.
- The turbine emits a band of sound in the 3150–4000 Hz while generating whose sound levels increase by ~10 dB as the current speed increases.
- The free spinning state is 5–25 dB quieter than the generating state, especially at low current speeds.
- At normalized currents of 80%, the sound levels are 10–30 dB above the levels recorded in the outer Bay of Fundy.

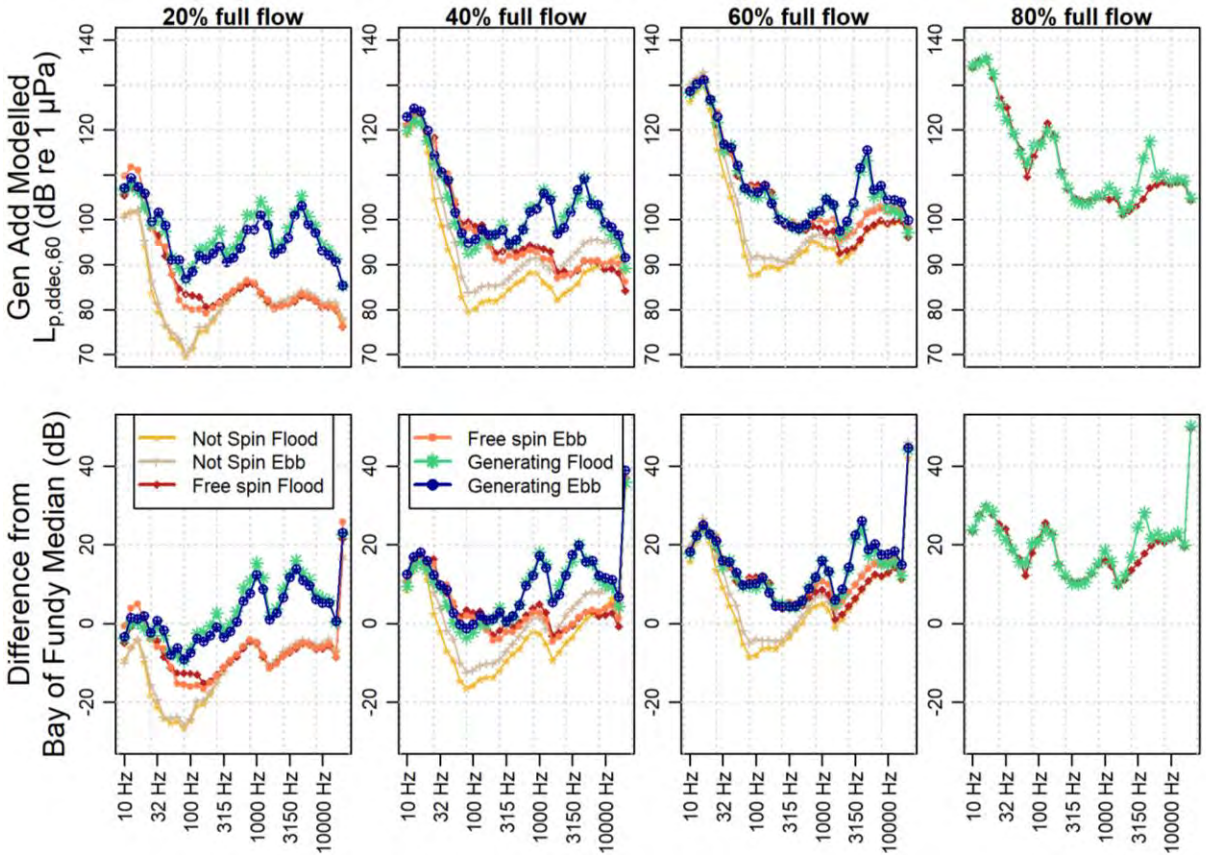

Figure 11. General additive modelled decidecade sound pressure levels received at the autonomous AMAR for normalized current speeds of 20, 40, 60, and 80% of full flow. (Top row) the modelled sound pressure levels. (Bottom row) the difference between the median decidecade sound pressure level measured under the shipping lanes in the Bay of Fundy and the conditions measured in the Minas Passage

The models were validated by looking at boxplots of their predictions compared to the measurements. The not-spinning case had the largest measured-modelled errors of ~−3 dB for turbine speeds below ~25% of full speed, which is due to the presence of additional sound sources (such as wind and waves) that are not part of the models. As the current speeds increase above 25% of full speed, the models have ~0 dB mean error compared to the measurements and progressively smaller interquartile ranges as the speed increases. This implies that the turbine sound becomes highly predictable as the speed increases and it is well characterized by the autonomous recordings (Appendix C.2.2).

The model was then converted to a *source level* model by adding $20 \cdot \log_{10}(167\ \text{m})$ to the received levels since the recorder was 167 m from the turbine. The source level model was then verified by using it to predict the expected sound levels from the icListen drifter during the drift that passed closest to the turbine on 27 Mar 2017. Using a restricted frequency band of 63–400 Hz, the agreement was excellent, both for the background noise levels and the turbine levels (see Appendix D.1).

We recommend only the source level model of turbine sound for specific frequency ranges and flow speeds. The measured data did not allow a useful model to be created for other conditions. For the free-spinning case, the valid frequency range of the model is the 63–400 Hz decidecade bands, and the model is only recommended for normalized flow speeds from 20–100%. For the generating case, the valid frequency range is the 63–10000 Hz decidecade bands, and the model is only recommended for normalized flow speeds from 20–70%.

Appendix D.3 presents spreadsheets that contain the median modelled sound pressure levels as a function of decidecade band and normalized flow speed.

4.3. Ranges to Effects of Sound on Marine Life

The verified source level model estimated ranges to thresholds for possible effects on marine life:

- The range where sound levels drop below the fish behavioural effects threshold (150 dB re 1 µPa²).
- The range where the herring auditory filter weighted sound levels drop below the median herring auditory filter weighted ambient noise levels for the Minas Passage.
- The range where the high-frequency cetacean (HFC) marine mammal hearing weighted sound pressure levels drop below the HFC weighted ambient sound levels.
- The range where the daily HFC weighted sound exposure level drops below the temporary threshold shift (TTS) criteria of 153 dB re 1 µPa²·s.

We found that:

- The turbine sound only exceeds the threshold for behavioural disturbance to fish (150 dB re 1 µPa²) at ranges less than 30 m and only at the highest current speeds on the flood tide (Figure 12).
- The range where the turbine could be audible to herring, or mask sounds a herring could hear, was less than 1000 m (upper inter-quartile values in Figure 13). For most turbine states and current speeds, the range was less than 500 m.
- The range where the turbine could be audible to porpoise, or mask sounds porpoises could hear, was less than 800 m (Figure 14). Ranges were generally less than 300 m in the generating state. In the free-spinning state, the turbine did not generate sound levels in the porpoise hearing frequency band that were measurable above ambient sediment noise at a range of 167 m (at the autonomous recorder).
- The range where the turbine could cause TTS in porpoises, if one stayed beside the turbine for 24 hours, was 150–250 m on most days and increased to 500 m during spring tides (Figure 15).

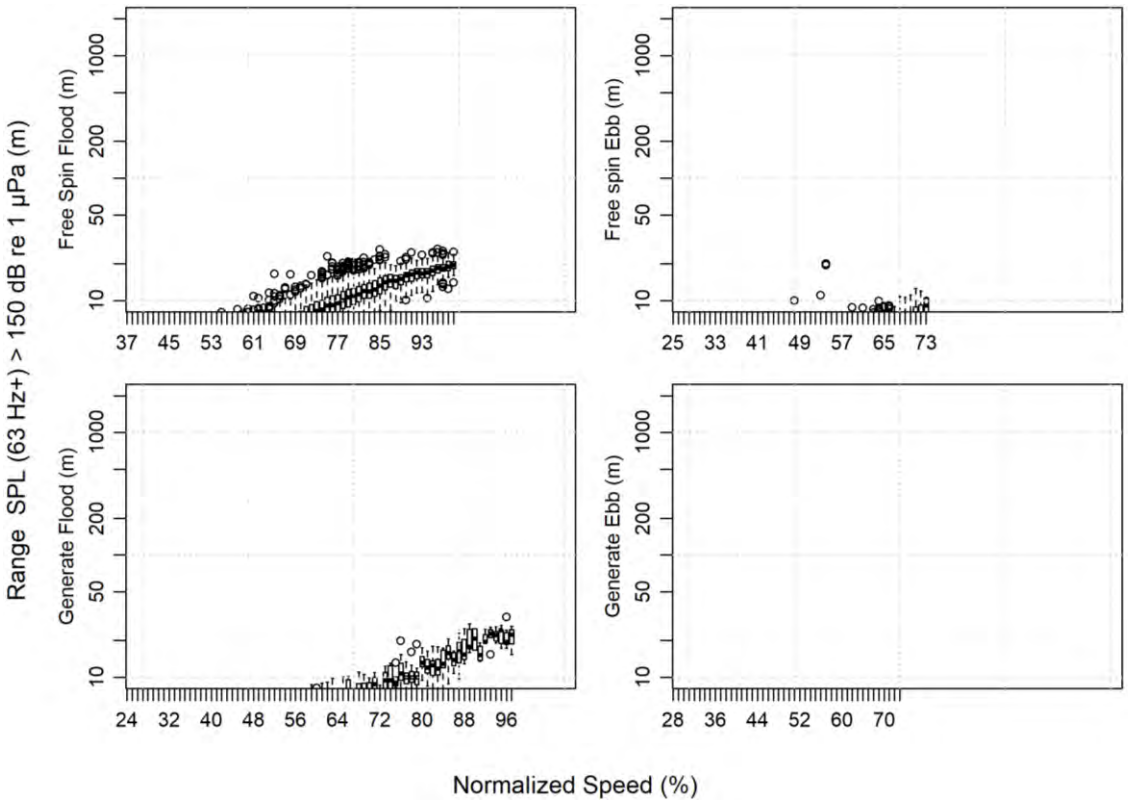

Figure 12. Threshold ranges for possible behavioural disturbance to fish.

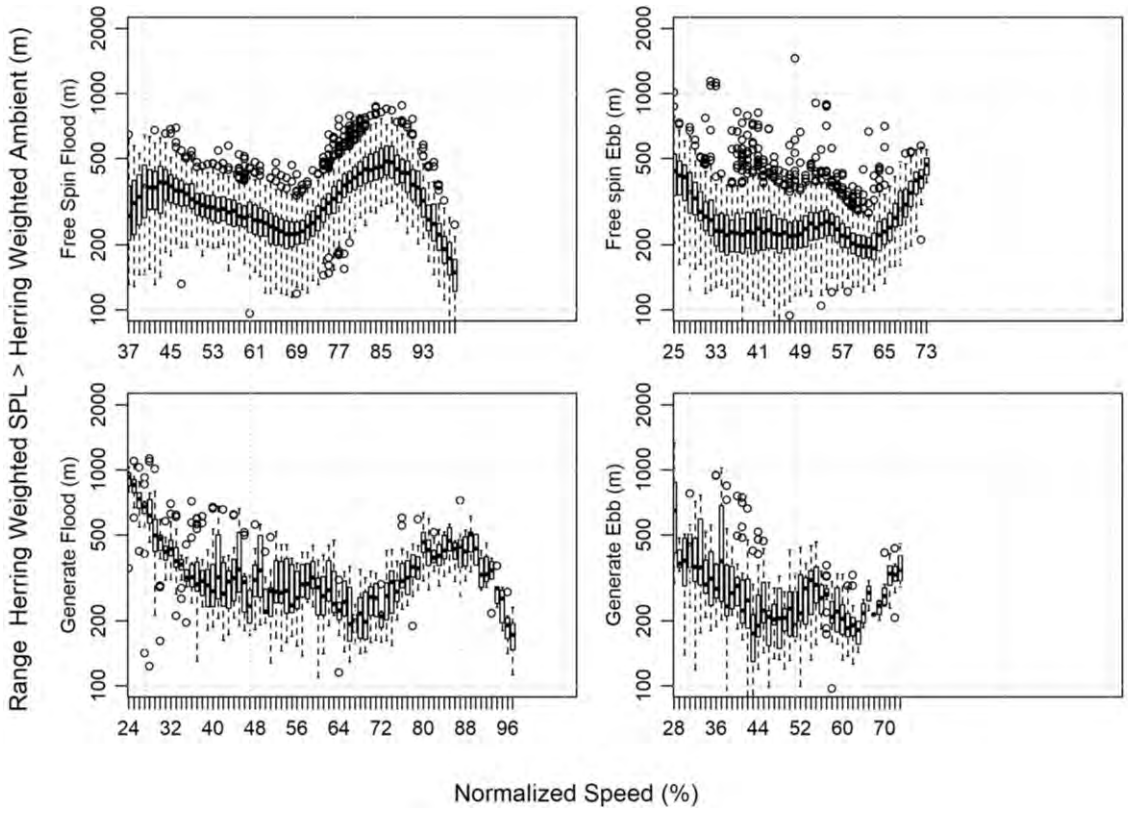

Figure 13. Threshold ranges where the herring-weighted turbine sound exceeds ambient herring weighted background.

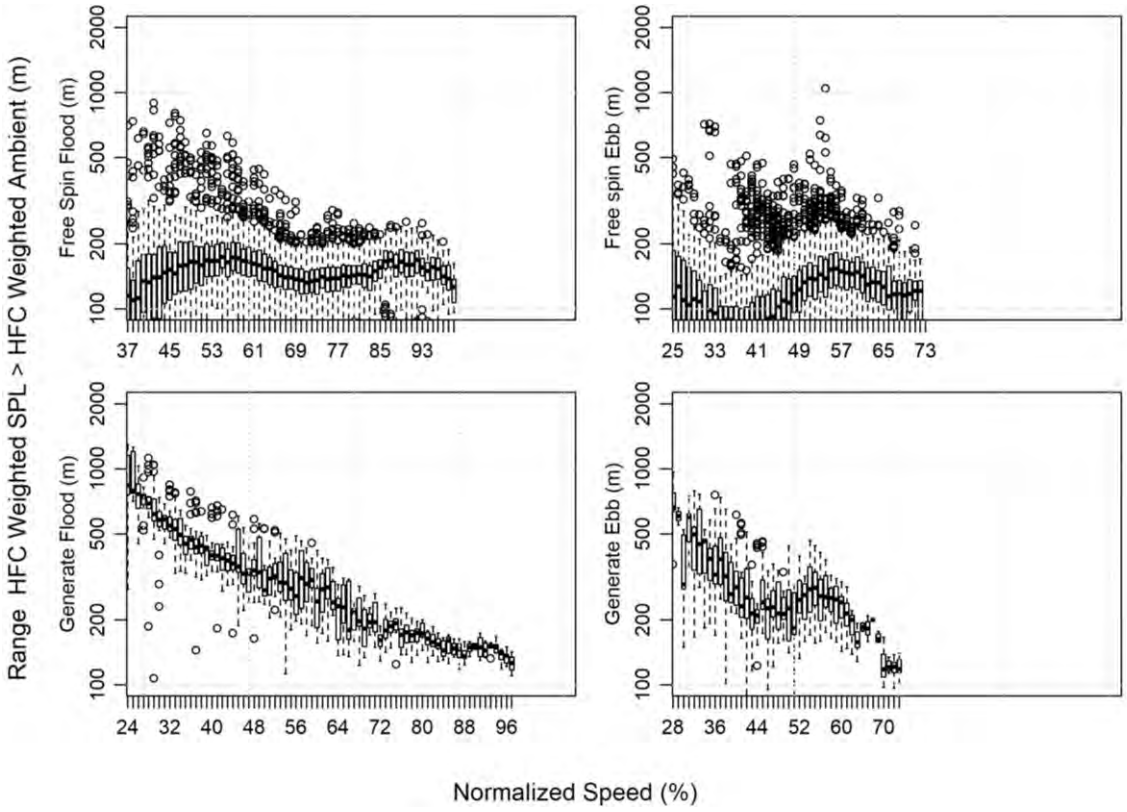

Figure 14. Threshold ranges where the high-frequency cetacean auditory-filter weighted turbine sound exceeds the high-frequency cetacean auditory-filter weighted background.

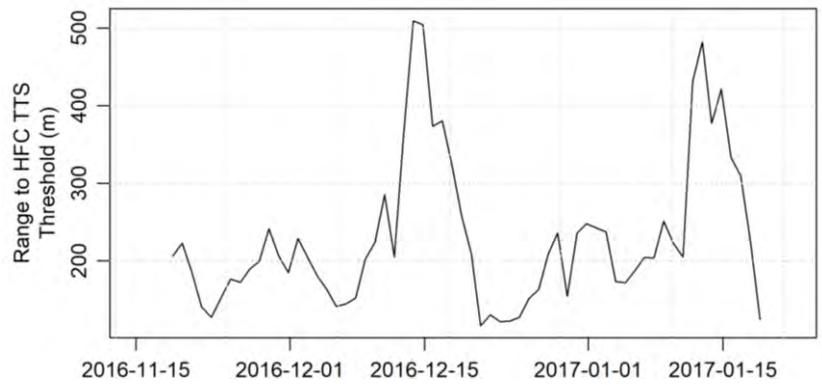

Figure 15. High-frequency cetacean weighted daily sound exposure levels and range to possible temporary threshold shift (TTS). Porpoises would need to stay within this range of turbine for a full 24 hours to accumulate enough acoustic energy for the onset of temporary hearing injury.

5. Discussion

5.1. Open-Centre Turbine Sound, Ambient Sound and Typical Vessels

We have compared the turbine sound to a typical fishing vessel at 10 knots and a typical tugboat at 10 knots (Figure 16) [67] to put the amplitude of turbine sound in context of other sounds typical of the area. Below 4 kHz, the turbine has a lower source level than the vessels. In the generating case, the 4000 Hz decidecade has a similar source level as the typical vessel. Since the maximum source level of the turbine is ~165 dB re 1 µPa² and the vessels are ~180 dB re 1 µPa² at low frequencies, we can expect that pressure-sensing fish will detect and be affected by vessels at 7–10 times the range as the turbine. For porpoises, the sound amplitude of vessels and the turbine will be similar at similar ranges.

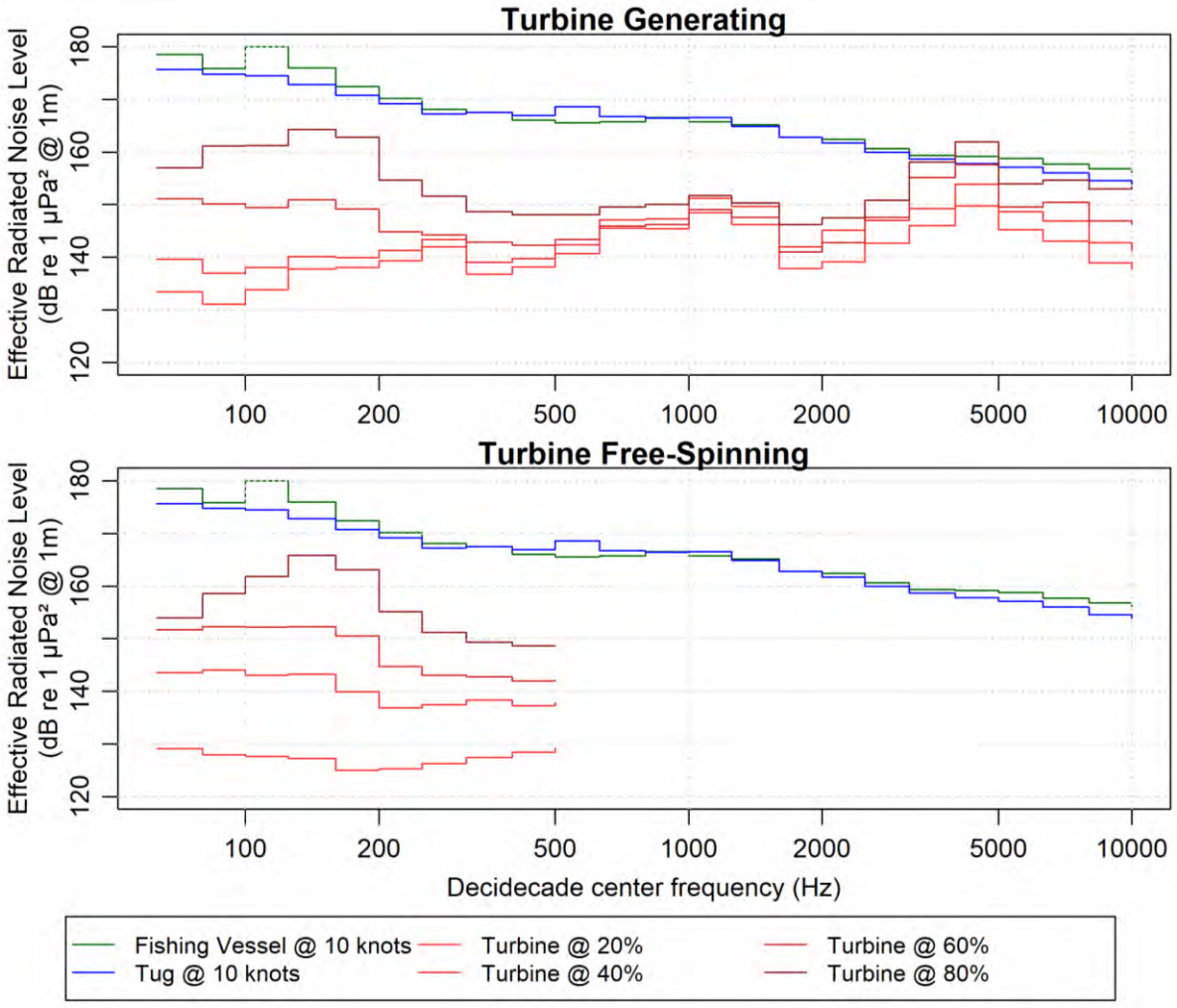

Figure 16. Comparing the turbine source levels to typical fishing and tugboat source levels at 10 knots. Above 400 Hz the turbine does not generate sounds in free-spinning mode that are measurable above background at 167 m.

Table 3. Comparing broadband and weighted effective radiated noise levels (dB re 1 µPa² @ 1 m)

Vessel class	Broadband effective radiated sound level (63 Hz–10000 Hz generating & vessels, 63–400 Hz free spinning)	Herring audiogram weighted (including sound below 63 Hz for all sources)	High-frequency cetacean weighted
Free spinning 40% current speed	153	160	--
Generating 40% current speed	160	158	144
Free spinning 80% current speed	170	173	--
Generating 80% current speed	171	173	155
Fishing vessel @ 10 knots	186	186	155
Tug @ 10 knots	184	184	153
Recreational @ 12 knots	172	164	155
Large ferry @ 20 knots	194	194	158
Tanker @ 14 knots	191	192	154
Container @14 knots	190	192	156

Notes: 63 Hz is the lowest frequency that is consistently above flow noise for the autonomous recorder. The free-spinning turbine only emits sound in the band of 63–400 Hz (which does not overlap with the high-frequency cetacean auditory filter; see Figure 4).

5.2. Turbine Sounds and Marine Life

We cannot say what the effects of sound were, only what the effects of turbine sound on marine life might be. The estimated ranges for sound to have various effects on animals is summarized in Table 1. Results are presented in Section 4.3 and Appendix D.2.

In general, the range from the turbine to each of the identified thresholds is typically much shorter than the maximum range. This is because turbine and ambient sounds are at a maximum only at peak current speeds at spring tides, for short periods of time during the day, and only for a few days each lunar cycle.

The typical and maximum ranges for each threshold described in Table 1, Section 4.3, and Appendix D.2 are shown in subsequent figures to illustrate the ranges relative to the size of the Minas Passage. Figure 17 shows the range until the sound decreases to below the threshold for behavioural disturbance to fish. At the scale shown in Figure 17, the range is indistinguishable from the turbine location. Figure 18 shows the range until sound decreases below the threshold for masking any sound a herring could hear. Figure 19 shows the range until turbine sound levels decrease below the level audible to porpoises, or mask sounds porpoises could hear. Figure 20 shows the range where the turbine could cause TTS in porpoises, if one stayed within that range for 24 hours.

The range where the turbine could cause TTS in porpoises was calculated by accumulating the sound exposure level over multiple tide cycles, so it accounts for variations in both turbine sound and ambient sound. To exceed the exposure threshold would require an individual animal to stay within that range for the entire 24 hours. It is highly unlikely that a porpoise would remain near the turbine for longer than one hour, and therefore TTS is not expected to occur.

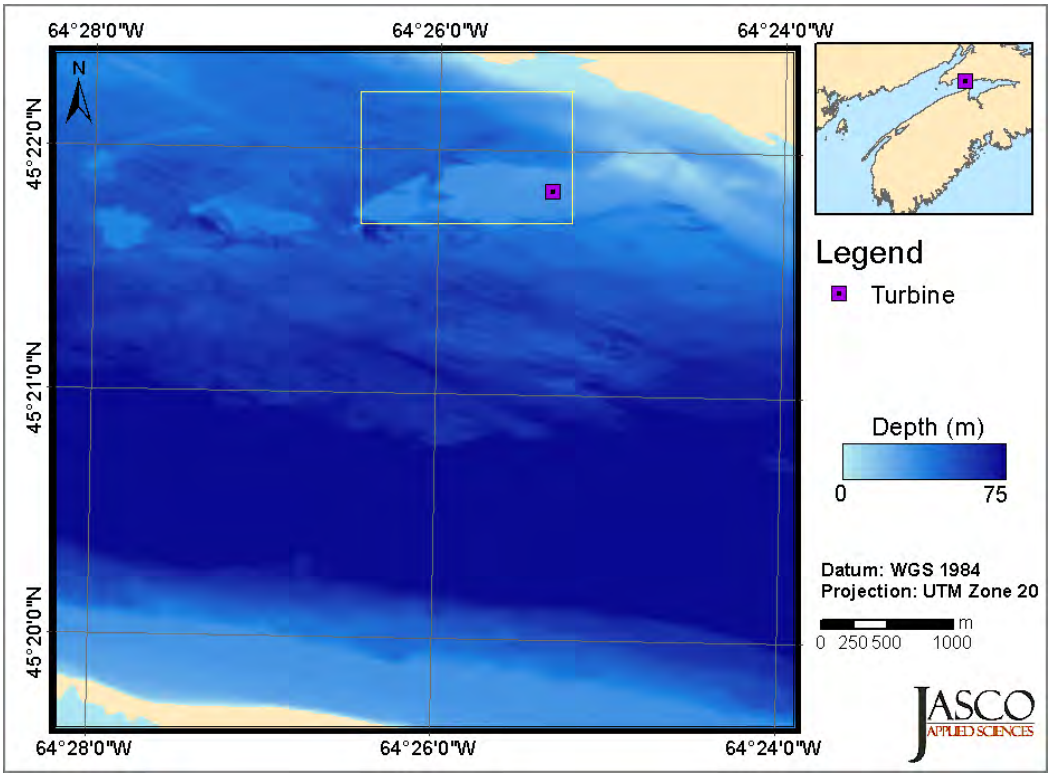

Figure 17. The range for the turbine sound to drop below the threshold for behavioural disturbance to fish. The inner ring is the typical range. The outer ring is the maximum range at spring tides, once per lunar cycle.

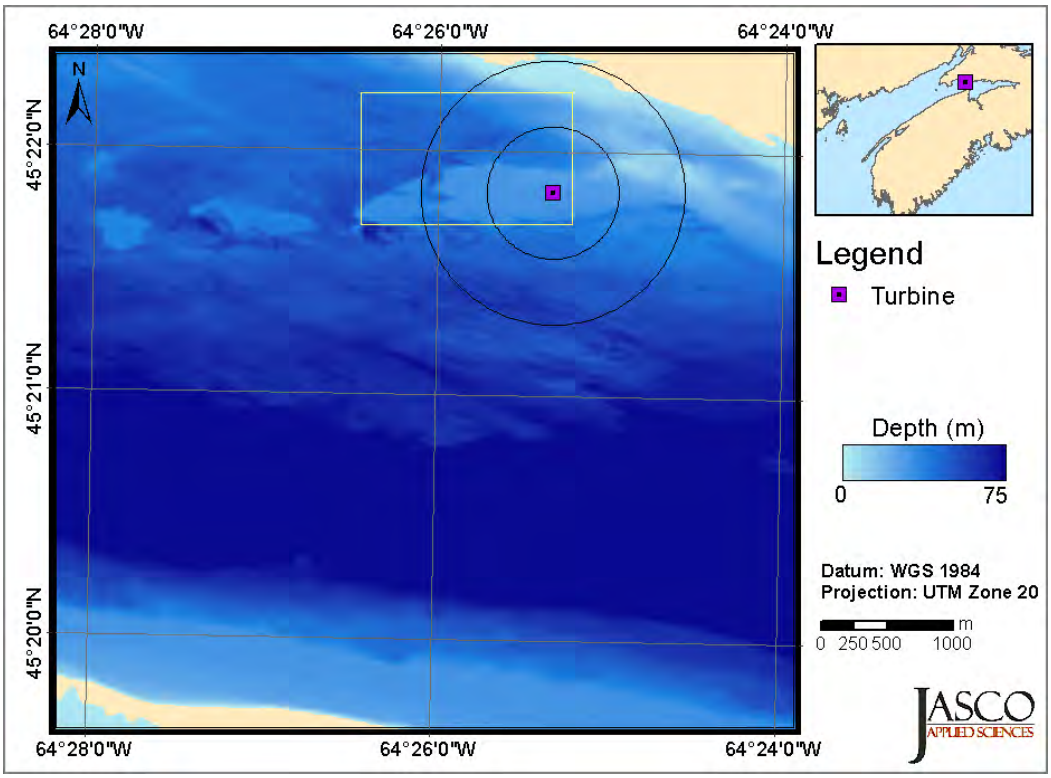

Figure 18. The range for the turbine sound to drop below the threshold for herring masking. The inner ring is the typical range. The outer ring is the maximum range at spring tides, once per lunar cycle.

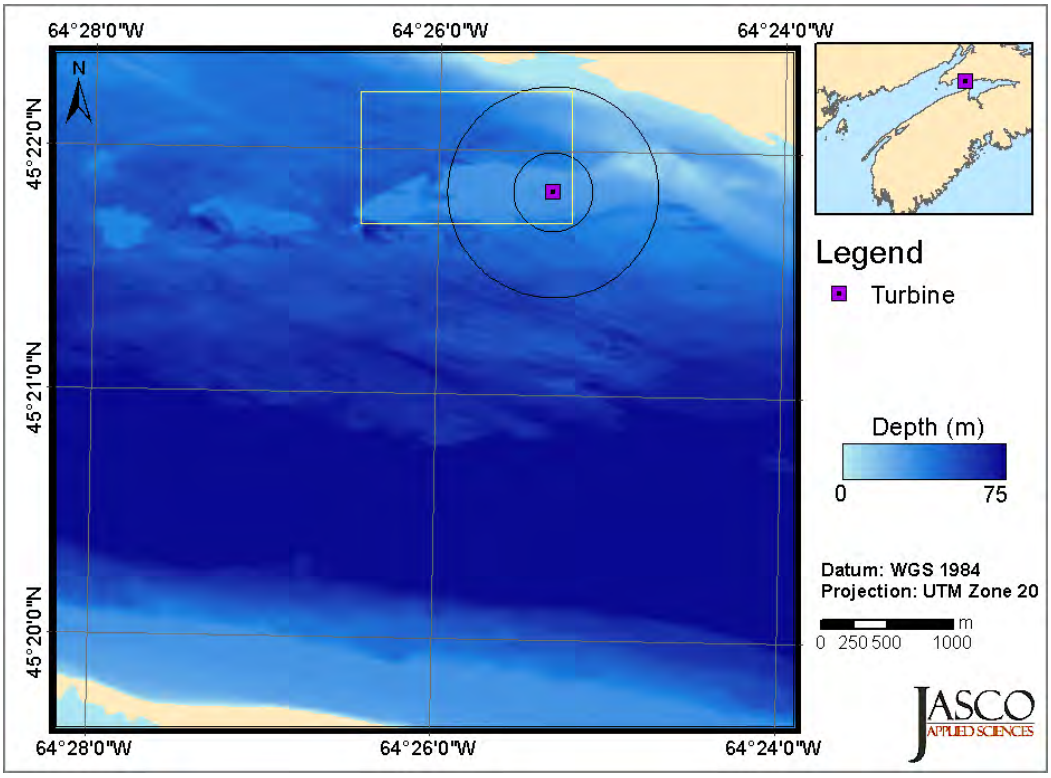

Figure 19. The range for the turbine sound to drop below the threshold for porpoise masking. The inner ring is the typical range. The outer ring is the maximum range at spring tides, once per lunar cycle.

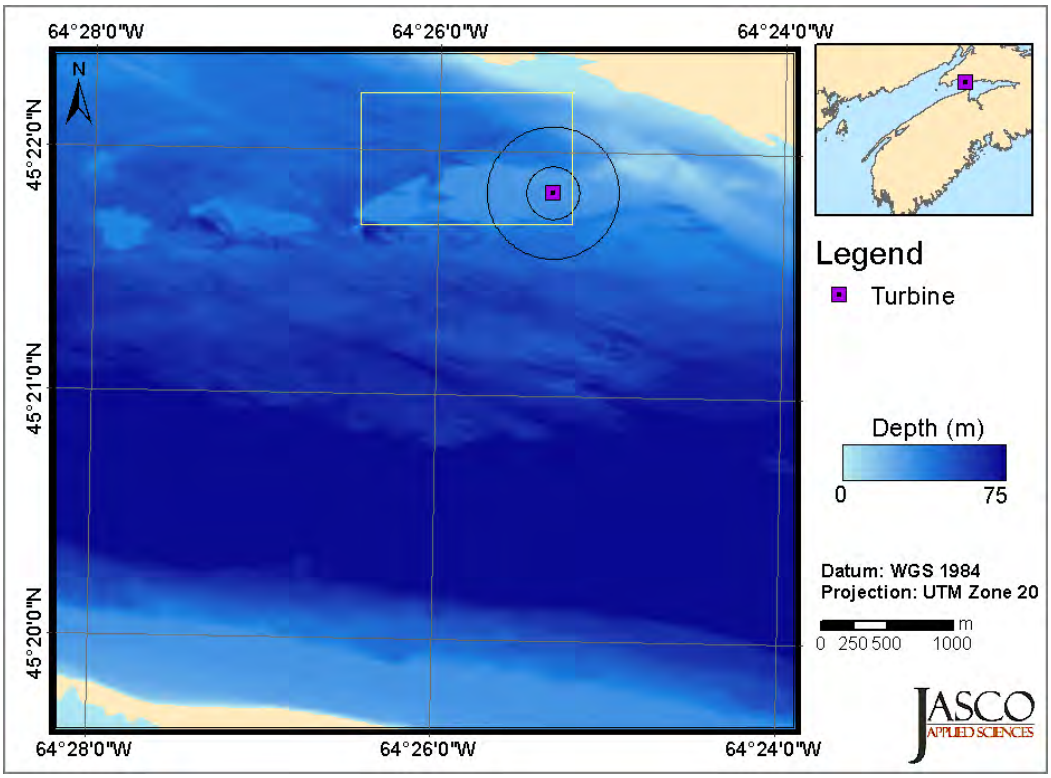

Figure 20. The range for the turbine sound to drop below the threshold for porpoise TTS. The inner ring is the typical range. The outer ring is the maximum range at spring tides, once per lunar cycle.

5.3. Relative Utility of Different Measurement Methods

Appendices B.2, B.3, B.4, and C.1 contain numerous comparisons between the measurement methods that show:

- The value of drift measurements is in obtaining the sound level versus range to validate source level models.
- Ignoring the drifter suspension, either acoustic recorder (Ocean Sonics icListen or JASCO AMAR) is suitable for drift measurements.
- Drifter suspensions must include an effective means of isolating the hydrophone from surface wave action. The relatively simple elastic isolation used on the Ocean Sonics icListen drifter in this study was inadequate for measurements below 150 Hz on 27 Mar 2017 because waves and weather caused flow noise that masked the sounds being measured. Data quality with the elastic hydrophone suspension was acceptable on 20 Oct 2017, because weather was calmer on that day.
- Drifters must have a GPS logger attached to record the location at least twice per minute; higher logging rates are recommended
- Hydrophone(s) on the turbine platform had much higher flow noise levels than the drifters and the autonomous recorder, and the effects were larger when the hydrophone was higher in the water column.
- The flow noise for some positions of hydrophones on the turbine platform hydrophones varied according to the current direction. Noise was louder when the hydrophone was downstream of turbine, even for the not-spinning turbine state (i.e., during the ebb tide for the forward-port hydrophone).
- Hydrophones on the turbine platform need to be more carefully isolated from electrical noise.
- Porpoise detections varied by time period. Porpoises were detected sporadically by the autonomous AMAR in November and December 2016 and detected regularly in cabled icListen data from 24 Mar to 13 Apr 2017. Simultaneous measurements are needed to determine if the differences are due to recording method, recording location, or recording time frame.

Based on the results, we recommend:

- Autonomous recorders in high-flow shielded moorings be considered as the primary method of assessing turbine sound levels. A recording of at least one full lunar cycle should be made while simultaneously logging of the current speed and turbine state. The 1-minute decidecade sound levels should be used to train generalized additive models of the turbine source levels, which can then be used to predict 1) the range where the turbine sound could injure marine life and 2) the range where the turbine is audible above background. $20\log_{10}$(range) acoustic propagation attenuation models are adequate around tidal turbines in the Minas Passage.
- Drifters should be used occasionally to measure the sound level versus range to the turbine to verify the sound level models developed from the autonomous recorders.
- Cabled hydrophones on turbine platforms should be located as close as possible to the seabed, and they should be protected by a stream-lined flow-shield.

5.4. Additional Recommended Measurements of the Open-Centre Turbine

In summer 2018, the Open-Centre Turbine will be redeployed in the Minas Passage. It is possible that the sound signature of the turbine will change, and it should therefore be re-assessed. As well, the turbine platform hydrophones mounts have been updated, increased protection has been provided, and the transmission system has been updated. We recommend that CST use this next deployment to address the following points related to acoustic monitoring of the turbine:

- Record the soundscape in the Minas Passage for at least one lunar cycle before deploying the turbine using an autonomous recorder. This baseline measurement will quantify the ambient sound levels at all current speeds. An Acoustic Doppler current profiler should be deployed at the same time as the acoustic recorder. We suggest the following duty cycle:
  - 64 kHz for 300 seconds
  - 375 kHz for 60 seconds
  - Sleep for 300 seconds.

  An autonomous AMAR will record for 120 days on this duty cycle. This cycle will record both more time and a wider bandwidth than the measurement in 2016 by using only one hydrophone instead of two to conserve storage space. The purpose of 64 kHz data is to check if the turbine emits any sounds above 10 kHz that have been missed in the earlier analysis (with a 32 kHz sampling rate). The 375 kHz sampling is intended for porpoise detection.
- Assuming the autonomous recorder remains deployed after turbine installation, the data should be used to develop a source level model for the refurbished turbine.
- The detection performance for porpoises should be compared for the simultaneous deployment of the autonomous recorder and the turbine mounted hydrophones.
- Consider applying flow shields to at least one of the lower-level turbine mounted hydrophones (Figure 27, locations 1, 2, or 4) to compare with the autonomous recorder as well as the locations that are not shielded.
- Consider making measurements of the turbine using two autonomous recorders, one that is perpendicular to the turbine, as was done previously, and one that is in-line with the turbine to check if the axial source levels are higher.
- A different suspension mechanism (Figure 21) that places the hydrophone at 5–8 m depth should be evaluated. Two types of drifters have been used at the FORCE test site to date. The icListen-based drifters are easy to deploy and have shallow draught, but they tend to have high levels of surface wave noise. The AMAR-based drifters solve the surface noise problem but are too cumbersome for rapid deployment. They also would place the hydrophone at 15 m depth, which could tangle with the turbine at low tide.
- During the next round of reporting, consider performing a literature review that compares the Open-Centre Turbine measurements with other devices worldwide to determine if any other measurement techniques might provide better results, a simpler implementation, or both.
- During the analysis and reporting of the next measurements, consider reporting the pressure spectral densities as a function of current speed with confidence intervals around each curve (e.g., Figure 22). This will demonstrate statistical validity of the characterization of the turbine sound and support the conclusion that reported sound levels are truly representative of the turbine sounds.

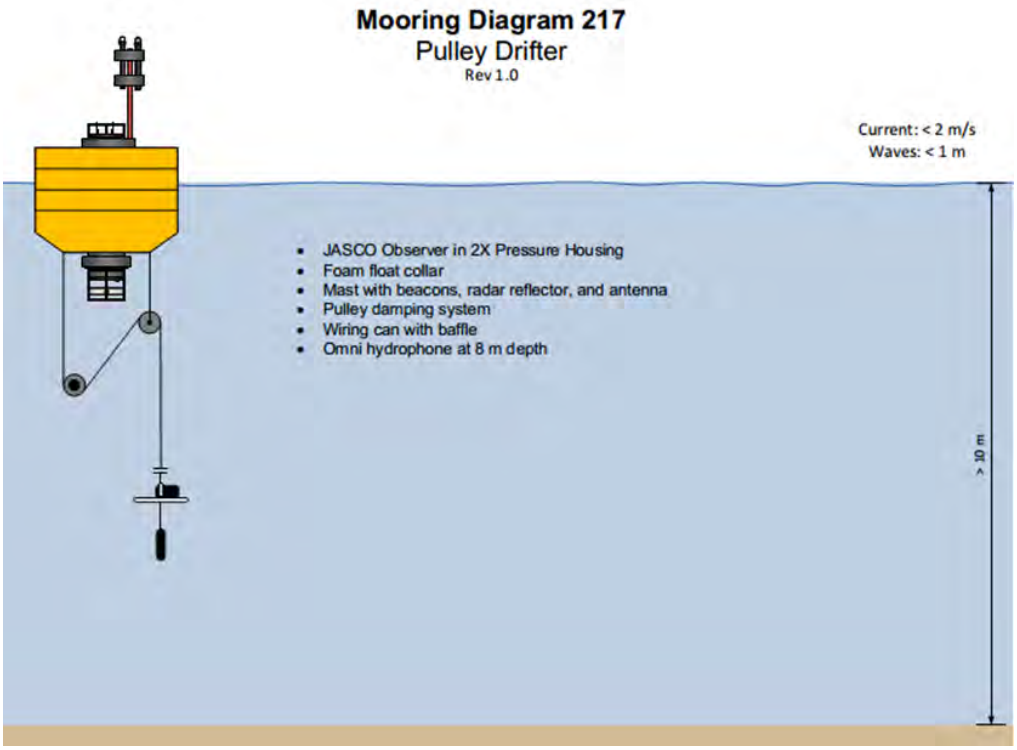

Figure 21. Proposed pulley drifter with localization beacons.

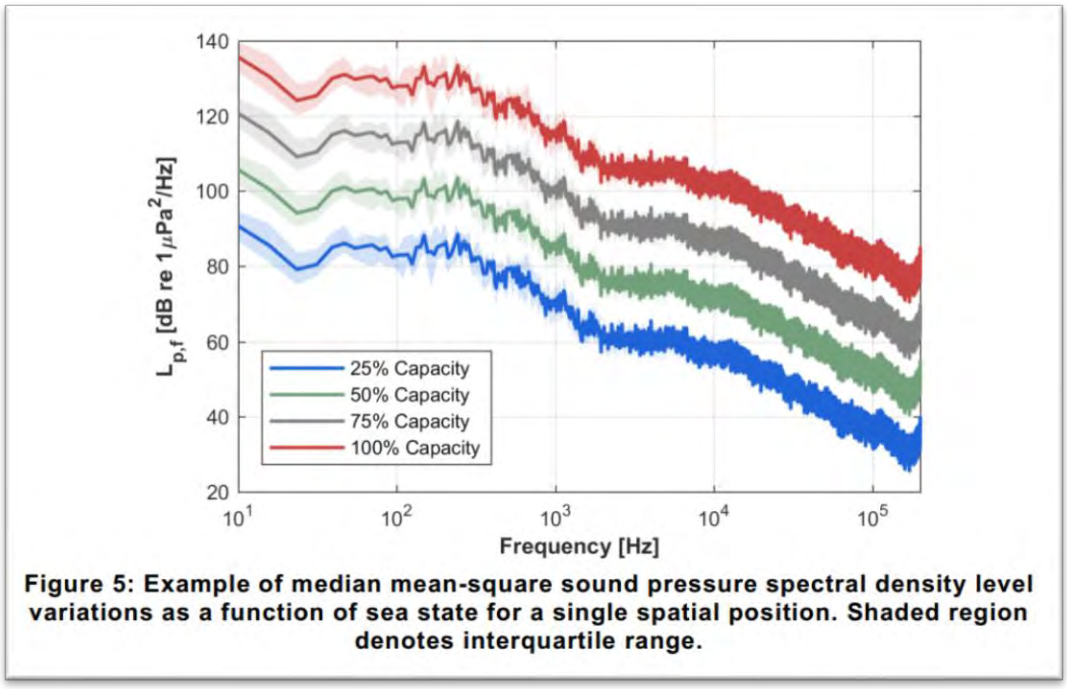

Figure 22. Example of turbine pressure spectral densities as a function of current speed, with interquartile confidence intervals [Figure 5 from IEC 68].

Literature Cited

1. Cato, D.H. (2008) Ocean ambient noise: Its measurement and its significance to marine animals. Proc. Inst. Acoust 30 (5), 1-9.

2. Pijanowski, B.C. et al. (2011) Soundscape Ecology: The Science of Sound in the Landscape BioScience 61 (3), 203-216.

3. Clark, C.W. et al. (2009) Acoustic masking in marine ecosystems: Intuitions, analysis, and implication. Mar Ecol Prog Ser 395, 201-222.

4. Au, W.W.L. et al. (1974) Measurement of echolocation signals of the Atlantic bottlenose dolphin, *Tursiops truncatus* Montagu, in open waters. J Acoust Soc Am 56 (4), 1280-1290.

5. Madsen, P.T. et al. (2004) Echolocation clicks of two free-ranging, oceanic delphinids with different food preferences: False killer whales *Pseudorca crassidens* and Risso's dolphins *Grampus griseus*. J Exp Biol 207 (11), 1811-1823.

6. Payne, R. and Webb, D. (1971) Orientation by means of long range acoustic signaling in baleen whales. Ann. N. Y. Acad. Sci. 188, 110-142.

7. Whitehead, H. and Rendell, L. (2014) The Cultural Lives of Whales and Dolphins, University of Chicago Press.

8. Dombroski, J.R.G. et al. (2016) Vocalizations produced by southern right whale (*Eubalaena australis*) mother-calf pairs in a calving ground off Brazil. J Acoust Soc Am 140 (3), 1850-1857.

9. Payne, R.S. and McVay, S. (1971) Songs of humpback whales. Science 173 (3997), 585-597.

10. Weilgart, L. and Whitehead, H. (1997) Group-specific dialects and geographical variation in coda repertoire in South Pacific sperm whales. Behav Ecol Sociobiol 40 (5), 277-285.

11. Ford, J.K.B. et al. (2011) The role of acoustics in defining killer whale populations and societies in the Northeastern Pacific Ocean. J Acoust Soc Am 129 (4), 2605-2605.

12. Au, W.W.L. et al. (1999) Transmission beam pattern and echolocation signals of a harbor porpoise (*Phocoena phocoena*). J Acoust Soc Am 106 (6), 3699-3705.

13. Teilmann, J. et al. (2002) Characteristics of echolocation signals used by a harbour porpoise (*Phocoena phocoena*) in a target detection experiment. Aquat. Mamm. 28, 275-284.

14. Popper, A.N. et al. (2014) Sound Exposure Guidelines for Fishes and Sea Turtles: A Technical Report prepared by ANSI-Accredited Standards Committee S3/SC1 and registered with ANSI, ASA Press.

15. Parmentier, E. et al. (2017) Multiple exaptations leading to fish sound production. Fish Fish 18 (5), 958-966.

16. Parmentier, E. et al. (2015) The influence of various reef sounds on coral-fish larvae behaviour. J Fish Biol 86 (5), 1507-1518.

17. Piercy, J.J. et al. (2016) The good, the bad, and the distant: Soundscape cues for larval fish. In The Effects of Noise on Aquatic Life II (Popper, A.N. and Hawkins, A. eds), pp. 829-837, Springer.

18. Vermeij, M.J.A. et al. (2010) Coral larvae move toward reef sounds. PLoS. ONE 5 (5), e10660.

19. Charifi, M. et al. (2017) The sense of hearing in the Pacific oyster, *Magallana gigas*. PLoS. ONE 12 (10), e0185353.

20. Di Iorio, L. et al. (2012) Hydrophone detects cracking sounds: Non-intrusive monitoring of bivalve movement. J Exp Mar Biol Ecol 432-433, 9-16.

21. Lammers, M.O. et al. (2006) Temporal, geographic, and density variations in the acoustic activity of snapping shrimp. J Acoust Soc Am 120 (5), 3013-3013.

22. Pye, H.J. and Watson, W.H., III (2004) Sound detection and production in the American lobster, *Homarus americanus*: Sensitivity range and behavioral implications. J Acoust Soc Am 115 (5), 2486-2486.

23. Popper, A.N. et al. (2018) The importance of particle motion to fishes and invertebrates

Physical aspects of swimbladder function. The Journal of the Acoustical Society of America 143 (1), 470-488.

24. Nelson, D.R. (1967) Hearing thresholds, frequency discrimination, and acoustic orientation in the lemon shark, Negaprion brevirostris (Poey). Bull Mar Sci 17 (3), 741-768.

25. Hawkins, A.D. and Popper, A. (2014) Assessing the impacts of underwater sounds on fishes and other forms of marine life. Acoustics Today 10 (2), 30-41.

26. [NIOSH] National Institute for Occupational Safety and Health, Criteria for a recommended standard: Occupational noise exposure, U.S. Department of Health and Human Services, NIOSH, Cincinnati, Ohio, 1998, p. 122.

27. Finneran, J.J., Auditory weighting functions and TTS/PTS exposure functions for marine mammals exposed to underwater noise, Technical Report, 2016, p. 49.

28. [NMFS] National Marine Fisheries Service, Technical Guidance for Assessing the Effects of Anthropogenic Sound on Marine Mammal Hearing: Underwater Acoustic Thresholds for Onset of Permanent and Temporary Threshold Shifts, U.S. Department of Commerce, NOAA. NOAA Technical Memorandum NMFS-OPR-55, 2016, p. 178.

29. Richardson, W.J. et al. (1999) Displacement of migrating bowhead whales by sounds from seismic surveys in shallow waters of the Beaufort Sea. J Acoust Soc Am 106 (4), 2281-2281.

30. Blackwell, S.B. et al. (2015) Effects of Airgun Sounds on Bowhead Whale Calling Rates: Evidence for Two Behavioral Thresholds. PLoS. ONE 10 (6), e0125720.

31. Tougaard, J. et al. (2009) Pile driving zone of responsiveness extends beyond 20 km for harbor porpoises (*Phocoena phocoena* (L.)). J Acoust Soc Am 126 (1), 11-14.

32. Brandt, M.J. et al., Effects of offshore pile driving on harbour porpoise abundance in the German Bight. Assessment of Noise Effects. Final Report, Created by BioConsult SH GmbH & Co KG, IBL Umweltplanung GmbH, Institut für Angewandte Ökosystemforschung GmbH for Offshore Forum Windenergie, 2016.

33. Day, R., D. et al., Assessing the Impact of Marine Seismic Surveys on Southeast Australian Scallop and Lobster Fisheries. FRDC Project No 2012/008, Impacts of Marine Seismic Surveys on Scallop and Lobster Fisheries, Fisheries Ressearch & Development Corporation, University of Tasmania, Hobart, 2016, p. 159.

34. McCauley, R. et al. (2017) Widely used marine seismic survey air gun operations negatively impact zooplankton. Nature Ecology & Evolution 1, 1-8.

35. Fewtrell, J.L. and McCauley, R.D. (2012) Impact of air gun noise on the behaviour of marine fish and squid. Mar Pollut Bull 64 (5), 984-993.

36. Roberts, L. and Elliott, M. (2017) Good or bad vibrations? Impacts of anthropogenic vibration on the marine epibenthos. Sci Total Environ 595, 255-268.

37. Tyack, P.L. et al. (2011) Beaked whales respond to simulated and actual navy sonar. PLoS. ONE 6 (3), e17009.

38. D'Amico, A. et al. (2009) Beaked whale strandings and naval exercises. Aquat. Mamm. 35 (4), 452-472.

39. Deruiter, S.L. et al. (2013) First direct measurements of behavioural responses by Cuvier's beaked whales to mid-frequency active sonar. Biol Lett 9 (4), 1-5.

40. Goldbogen, J.A. et al. (2013) Blue whales respond to simulated mid-frequency military sonar. Proceedings of the Royal Society B 280 (1765), 1-8.

41. Melcon, M.L. et al. (2012) Blue whales respond to anthropogenic noise. PLoS. ONE 7 (2), 1-6.

42. Di Iorio, L. and Clark, C.W. (2010) Exposure to seismic survey alters blue whale acoustic communication. Biol Lett 6 (1), 51-54.

43. Halvorsen, M.B. et al. (2012) Effects of exposure to pile-driving sounds on the lake sturgeon, Nile tilapia and hogchoker. Proceedings of the Royal Society B: Biological Sciences 279 (1748), 4705-4714.

44. Casper, B.M. et al. (2013) Effects of exposure to pile driving sounds on fish inner ear tissues. Comparative Biochemistry and Physiology Part A: Molecular & Integrative Physiology 166 (2), 352-360.

45. Spiga, I. et al., Influence of Pile Driving on the Clearance Rate of the Blue Mussel, *Mytilus edulis* (L.), Proceedings of Meetings on Acoustics: Fourth International Conference on the Effects of Noise on Aquatic Life, Dublin, Ireland, 2016.

46. Cholewiak, D. et al. (2017) Beaked whales demonstrate a marked acoustic response to the use of shipboard echosounders. Royal Society Open Science 4 (12).

47. Simpson, S.D. et al. (2016) Small-Boat Noise Impacts Natural Settlement Behavior of Coral Reef Fish Larvae. In The Effects of Noise on Aquatic Life II (Popper, A. and Hawkins, A. eds), pp. 1041-1048, Springer.

48. Holles, S. et al. (2013) Boat noise disrupts orientation behaviour in a coral reef fish. Mar Ecol Prog Ser 485, 295-300.

49. Spiga, I. et al. (2012) Effects of Short-and Long-Term Exposure to Boat Noise on Cortisol Levels in Juvenile Fish. In The Effects of Noise on Aquatic Life (Popper, A.N. and Hawkins, A. eds), pp. 251-253, Springer New York.

50. Hatch, L.T. et al. (2012) Quantifying loss of acoustic communication space for right whales in and around a U.S. National Marine Sanctuary. Conserv Biol 26 (6), 983-994.

51. Stanley, J.A. et al. (2017) Underwater sound from vessel traffic reduces the effective communication range in Atlantic cod and haddock. Scientific Reports 7 (1), 14633.

52. Rolland, R.M. et al. (2012) Evidence that ship noise increases stress in right whales. Proceedings of the Royal Society B: Biological Sciences.

53. Halvorsen, M.B. et al. (2012) Threshold for onset of injury in Chinook salmon from exposure to impulsive pile driving sounds. PLoS. ONE 7 (6), e38968.

54. [NOAA] National Oceanic and Atmospheric Administration (U.S.) (1998) Incidental taking of marine mammals; Acoustic harassment. Federal Register 63 (143), 40103.

55. [NMFS] National Marine Fisheries Service (US) and [NOAA] National Oceanic and Atmospheric Administration (1995) Small takes of marine mammals incidental to specified activities; offshore seismic activities in southern California: Notice of issuance of an incidental harassment authorization. Federal Register 60 (200), 53753-53760.

56. [FHWG] Fisheries Hydroacoustic Working Group, Agreement in Principle for Interim Criteria for Injury to Fish from Pile Driving Activities, 2008.

57. Southall, B.L. et al. (2007) Marine Mammal Noise Exposure Criteria: Initial Scientific Recommendations. Aquat. Mamm. 33 (4), 411-521.

58. Erbe, C. (2013) International regulation of underwater noise. Acoustics Australia 41 (1), 12-19.

59. King, S. et al. (2015) An Interim Framework for Assessing the Population Consequences of Disturbance. Methods in Ecology and Evolution 6 (10), 1150–1158

60. Shannon, G. et al. (2016) A synthesis of two decades of research documenting the effects of noise on wildlife. Biological Reviews 91 (4), 982-1005.

61. Dooling, R.J. et al. (2015) Effects of noise on fishes: What we can learn from humans and birds. Integr. Zool 10, 29-37.

62. Amoser, S. and Ladich, F. (2003) Diversity in noise-induced temporary hearing loss in otophysine fishes. J Acoust Soc Am 113 (4 Pt 1), 2170-9.

63. Smith, M.E. et al. (2004) Noise-induced stress response and hearing loss in goldfish (*Carrassius auratus*). J Exp Biol 207, 427-435.

64. Stadler, J.H. and Woodbury, D.P., Assessing the effects to fishes from pile driving: Application of new hydroacoustic criteria, Inter-Noise 2009: Innovations in Practical Noise Control, Ottawa, Canada, 2009.

65. Kolmogorov, A.N. (1991) The local structure of turbulence in incompressible viscous fluid for very large Reynolds numbers. Proceedings of the Royal Society of London. Series A: Mathematical and Physical Sciences 434 (1890), 9.

66. Bassett, C. et al. (2014) Flow-noise and turbulence in two tidal channels

A vessel noise budget for Admiralty Inlet, Puget Sound, Washington (USA). The Journal of the Acoustical Society of America 135 (4), 1764-1774.

67. MacGillivray, A. et al., Regional Ocean Noise Contributors Analysis: Enhancing Cetacean Habitat and Observation Program, Version 3.0. Technical report by JASCO Applied Sciences for Vancouver Fraser Port Authority, 2017.

68. [IEC] International Electrotechnical Commission, IEC TC 114. Marine energy – Wave, tidal and other water current converters, Part 40: Acoustic characterization of marine energy converters, Project number: IEC TS 62600-40 ED1, 2018.

69. [ISO] International Organization for Standardization, ISO/DIS 18405.2:2017. Underwater acoustics—Terminology, Geneva, 2017, p. 62.

70. Au, W.W.L. and Hastings, M.C. (2008) Principles of Marine Bioacoustics, Springer.

71. Wenz, G.M. (1962) Acoustic Ambient Noise in the Ocean: Spectra and Sources. J Acoust Soc Am 34 (12), 1936-1956.

72. Scharf, B. (1970) Critical bands. In Foundations of Modern Auditory Theory (Tobias, J.V. ed), pp. 157–202, Academic Press.

73. Saunders, J.C. et al. (1979) Frequency selectivity in bird and man: A comparison among critical ratios, critical bands and psychophysical tuning curves. Hearing Res 1 (4), 303-323.

74. ANSI S1.1-1994, American National Standard Acoustical Terminology, American National Standards Institute, New York, R2004.

75. Wood, S.N. (2004) Stable and efficient multiple smoothing parameter estimation for generalized additive models. Journal of the American Statistical Association 99 (467), 673-686.

76. Tollit, D. et al., Appendix D: Marine Mammal Detection Final Report (Detection of Marine Mammals and Effects Monitoring at the NSPI (OpenHydro) Turbine Site in the Minas Passage during 2010), Fundy Tidal Energy Demonstration Project: Environmental Effects Monitoring Report, Report by Sea Mammal Research Unit Ltd (SMRU) and Acadia Centre for Estuarine Research (ACER) for Fundy Ocean Research Centre for Energy (FORCE), 2011, p. 36.

Appendix A. Method Details

A.1. Recorder Configurations

A.1.1. AMARs–The Minas Passage and Outer Bay of Fundy

To measure sound pressure levels (SPL), two bottom-mounted Autonomous Multichannel Acoustic Recorders (AMARs, JASCO Applied Sciences) were deployed, Station 2 at a range of 167 m from the turbine as the measurement site and Station 1 at 680 m as a control site. The turbine was located at Easting: 388662 m, Northing: 5024422 m (UTM 20N).Due to the exceptionally high current in the area, hydrodynamic high-flow moorings were used with floats that submerged during tidal flows and surfaced at slack tide (Figures 24 and 25). The recorders were deployed near the OpenHydro turbine on 18 Nov 2016 (Table 4). Station 2 was retrieved on 19 Jan 2017, but Station 1 was not retrieved due to difficulties in locating the surface float of this unit. For the remainder of this document, the recorder at 167 m from the turbine will be referred to as the autonomous AMAR or autonomous recorder.

Each AMAR was fitted with two M36-V35-100 hydrophones (GeoSpectrum Technologies Inc.), sampling for 250 seconds at 32,000 samples per second (sps) giving an acoustic bandwidth of 10 to 16 kHz, with a nominal sensitivity of −165 dB re 1 V/µPa. Hydrophone 1 was located near the front, or 'bow' of the high flow mooring, and hydrophone 2 was located near the lifting plate at the centre of the high flow mooring (Figure 24). Hydrophone 1 also sampled for 65 seconds at 375,000 sps, giving an acoustic bandwidth of 10 to 187.5 kHz, also with a nominal sensitivity of −165 dB re 1 V/µPa. There was a 165 second sleep cycle in the recording schedule to preserve battery life and memory. The lower sample rate can capture most mechanical noise from the turbine and vessels, as well as potential vocalizations from most large marine mammals. The high sample rate can capture high-frequency vessel sound sources, such as sonars and acoustic positioning systems. It can also capture high-frequency echolocation clicks from marine mammals. Two hydrophones were used to determine if there were differences in flow-noise reduction inside the high flow mooring

A similar AMAR recorder to the ones used in the Minas Passage was deployed at 143 m water depth underneath the inbound Bay of Fundy shipping lane, adjacent to the North Atlantic Right Whale critical habitat (Table 4, Figure 26). This recorder is referred to as the outer Bay of Fundy recorder. Its data will be used as a reference for 'normal' conditions in the larger Bay of Fundy.

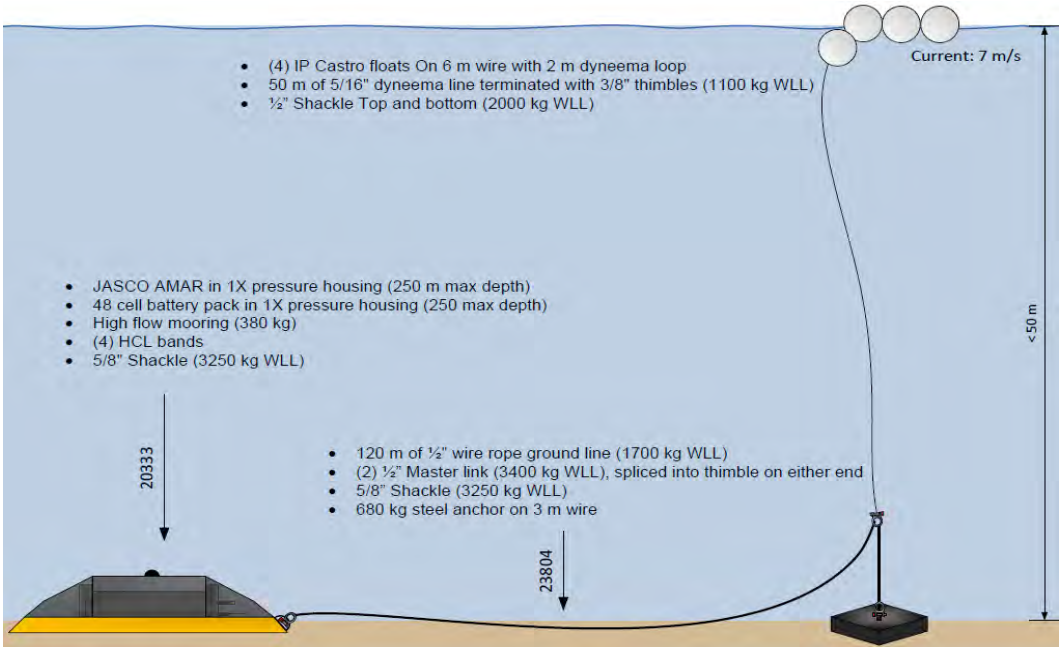

Figure 23. Configuration for the high-flow mooring.

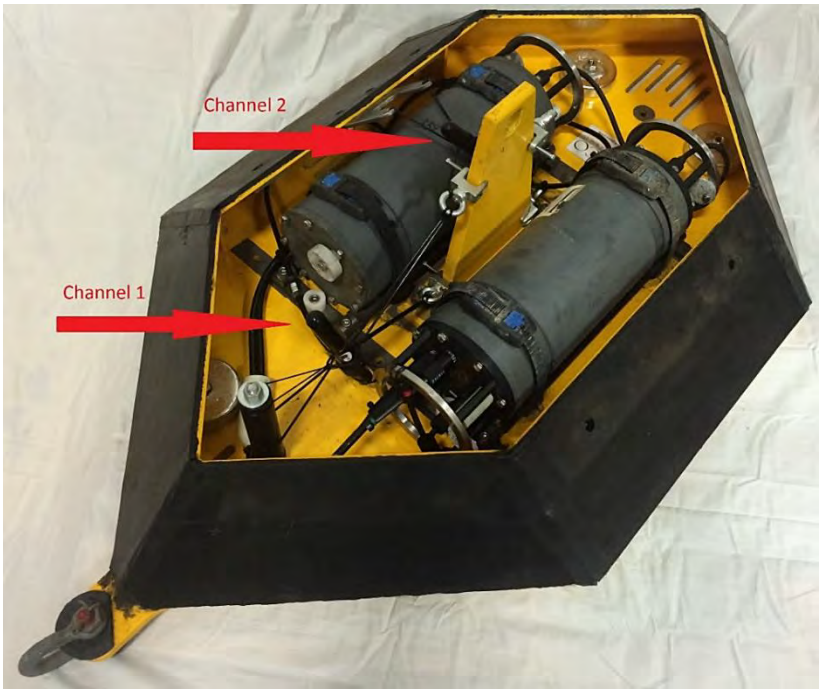

Figure 24. Inside the high-flow mooring. Hydrophones are shown with red arrows.

Figure 25. Cover of the JASCO High Flow Mooring. (Left) top view of the neoprene cover. (right) View from underneath showing cut-outs in the metal structure to allow for sound transmission.

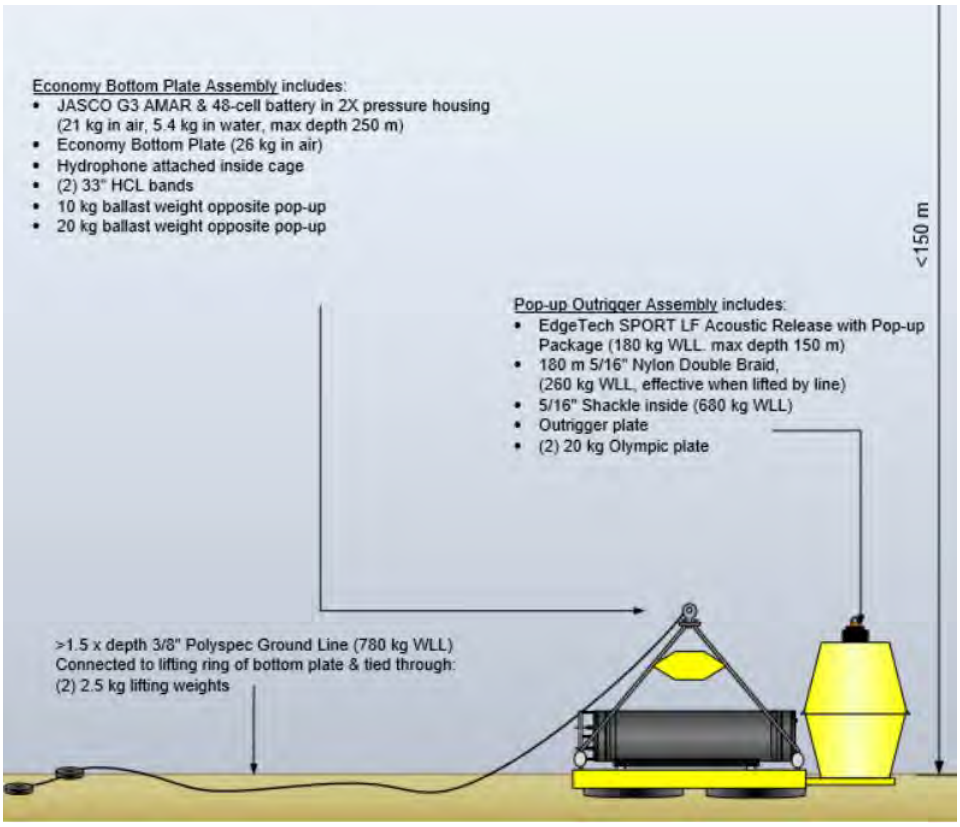

Figure 26. Mooring configuration used in the outer Bay of Fundy.

Table 4. Recorder locations and deployment details from the OpenHydro study. Sensor depths are relative to mean high water.

Device	Latitude (N)	Longitude (W)	Deployment	Retrieval	Horizontal range from source (m)	Sensor depth (m)
AMAR 200, Station 2	45° 21' 49.51 N	64° 25' 24.78 W	18 Nov 2016	19 Jan 2017	167	43
AMAR 227, Station 1	45° 21' 45.12 N	64° 25' 50.88 W	18 Nov 2016	Not retrieved	680	46
Outer Bay of Fundy AMAR Stn 1	44° 33' 46.50' N	66° 20' 9.90' W	3 Dec 2015	28 Apr 2016	--	143

A.1.2. icListen Real-time data stream

Four icListen Smart Hydrophones (Ocean Sonics Ltd.) were secured to the turbine platform (Figure 27) and interfaced to the fibre optic data cable connecting the turbine platform to shore. The data from the icListen was recorded at the visitor's centre in Parrsboro, NS, and used for subsequent analysis, including this report. Of the four hydrophones installed on the platform, only Hydrophone 1 (icListen 1404) provided data throughout the turbine deployment (Table 5). Data from two of the hydrophones were not transmitted due to issues with the telemetry system, and one hydrophone suffered physical damage. The telemetry system on the turbine platform, as well as physical protection for the hydrophones, have been improved in anticipation of the turbine's redeployment.

icListen 1404 in the Forward-Port location sampled at 32 kHz until 8 Mar 2017, increased in sample rate to 64 kHz until 24 Mar 2017, and then increased again to 512 kHz until turbine recovery on 13 Apr 2017.

The icListens were equipped with hydrophone ceramics from GeoSpectrum Technologies Inc. and had a nominal sensitivity of −169 dB re 1V/µPa.

Table 5. Data from the turbine-mounted icListen.

icListen ID	Data start	Data end
Hydrophone 1–1404–Forward-Port	12 Nov 2016	13 Apr 2017
Hydrophone 2–1407–Forward-Starboard	8 Nov 2016	9 Nov 2016
Hydrophone 3–1405–Top	10 Nov 2016	20 Nov 2016
Hydrophone 4–1406–Aft	--	--

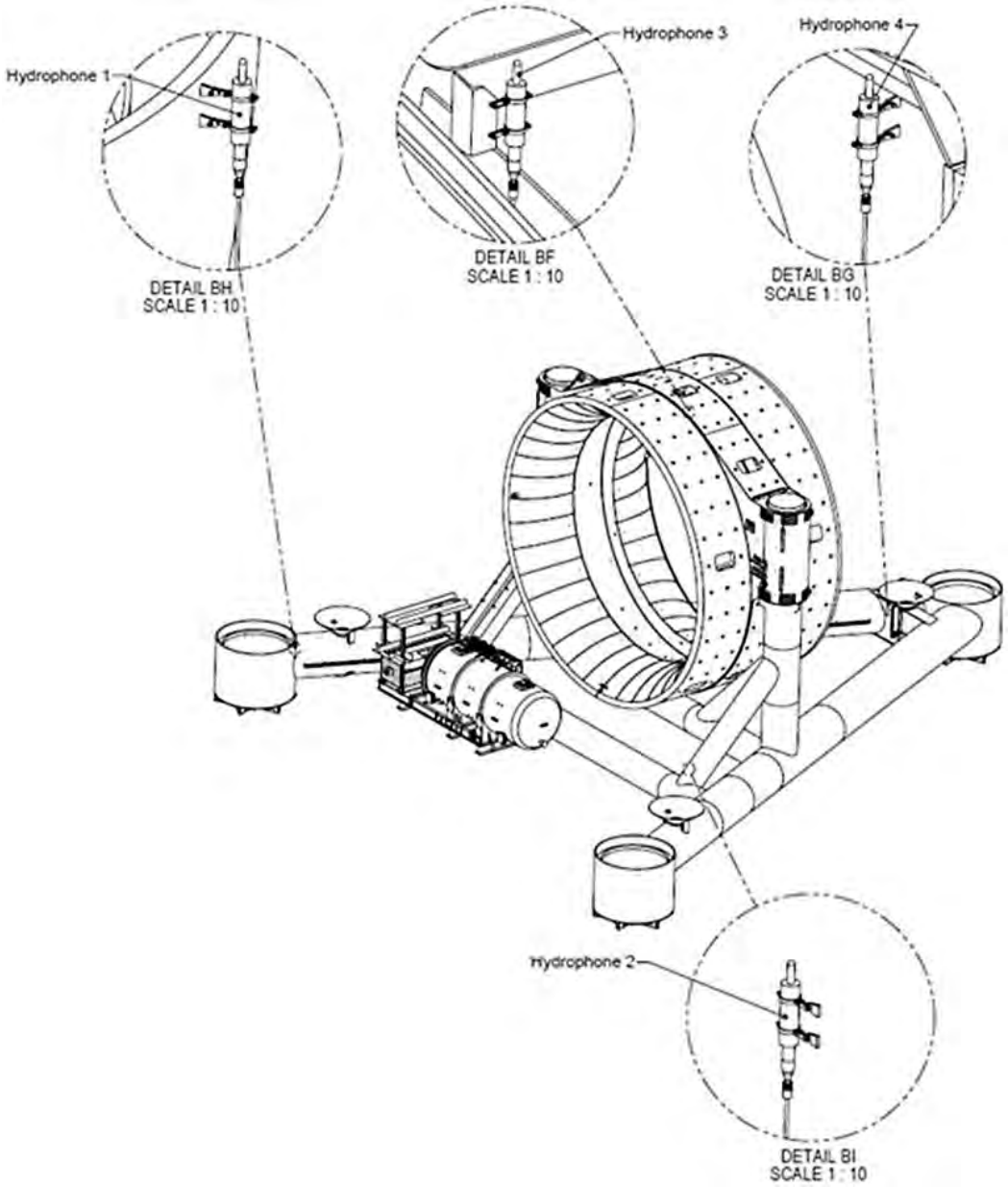

Figure 27. General arrangement drawing for the Open-Centre Turbine showing the locations of the icListen hydrophones. Hydrophone 1 was 8 m from the turbine rim. The cylinder at the lower left side of the turbine rim is the Turbine Control Centre.

A.1.3. icListen drifters

Hydrophone drifters based on the icListen were deployed by FORCE on 31 Aug 2016, 20 Oct 2016, and 27 Mar 2017. The icListen drifter is a lightweight device that uses a compliant suspension to hang the recorder 5 m below the surface. Some isolation from surface movement is provide by a compliant strength member and dampers (black cable and bristles in Figure 28).

All icListen trials employed two separate drifters sampling at 512 kHz. Each drift was 1–3 km long for which the start and stop locations and times are known. The 2016 drifts occurred before the turbine was deployed. Drifts on 20 Oct 2016 were interleaved with AMAR drifts (Appendix A.1.4) and occurred across the low tide slack tide. On 27 Mar 2017, eleven trials with two separate drifters were conducted throughout a flood tide while the turbine was free-spinning.

Figure 28. The icListen drifter being unloaded from the Tidal Runner (photo courtesy of Ocean Sonics Ltd.).

A.1.4. AMAR drifters

An AMAR recorder integrated into a drifting mooring was deployed by FORCE on 18 and 20 Oct 2016, before the installation of the OpenHydro turbine (Table 6).

The mobile recorder assembly employed a catenary mooring in a free-drifting arrangement (Figure 29). The mooring was designed to keep the acoustic recorder from moving in the vertical axis due to wave motions, since 1 cm of vertical motion results in a 120 dB re 1 µPa pressure change, which is 10-times the background sound pressure level in most ocean areas. If the design was successful, then the recorder would effectively be a water ‘particle’ drifting with the water mass and recording the actual sound levels rather than artificial pressure changes caused by the interaction of the recorder and the environment. Temperature depth (TD) loggers were included in the mooring (Figure 29) to verify that different aspects of the mooring were moving as expected. Unfortunately, these devices were not properly activated during deployment, so no TD data was recorded.

The catenary mooring consisted of a buoyant surface unit and an AMAR acoustic recorder (JASCO) attached below it on an alternately weighted and buoyed line 35 m long. The surface unit comprised a large spherical float with an upper mast and a counterweight below at the end of a rigid rod. A satellite beacon and VHF/strobe beacon were mounted on the upper mast to facilitate tracking and retrieval. A pick-up line with floats and a fabric sea anchor (not shown in Figure 29) were also attached to the surface float.

The AMAR was fitted with an M8E-35dB hydrophone (GeoSpectrum Technologies Inc.), duty cycled between 32,000 samples per second (sps) for 680 seconds (acoustic bandwidth: 10 Hz to 16 kHz) and 375,000 sps for 130 seconds (acoustic bandwidth: 10 Hz to 187 kHz, nominal sensitivity: −165 dB re 1 V/µPa).

Table 6. Deployment and retrieval locations and times of 8 recordings made by the AMAR catenary drifter on 18 and 20 Oct 2017. Data start and end times indicate the timeframe where no deployment/retrieval related noise occurred. The total data is the number of minutes during the recording where data was not impacted by deployment/retrieval related noise.

Date	ID	Deployment		Retrieval		Data start (UTC)	Data end (UTC)	Total data (min)
		Location	Time (UTC)	Location	Time (UTC)			
18 Oct 2017	18–01	45.368° N 64.443° W	12:32	45.357° N 64.408° W	13:01	12:36:30	12:54:30	18.00
	18–02	45.377° N 64.452° W	14:00	45.356° N 64.397° W	14:18	14:01:30	14:11:30	10.00
	18–03	45.372° N 64.455° W	15:35	45.352° N 64.389° W	15:54	15:36:00	15:47:30	11.50
	18–04	45.377° N 64.452° W	16:55	45.354° N 64.395° W	17:21	16:56:30	17:13:00	16.50
	18–05	45.361° N 64.421° W	18:17	45.364° N 64.445° W	19:06	18:19:15	19:00:00	40.75
20 Oct 2017	20–01	45.359° N 64.408° W	10:50	45.362° N 64.425° W	11:13	10:52:00	11:07:30	15.50
	20–02	45.363° N 64.419° W	12:27	45.365° N 64.428° W	12:45	12:27:45	12:40:00	12.25
	20–03	45.368° N 64.443° W	14:03	45.356° N 64.405° W	14:40	14:05:30	14:29:00	23.50

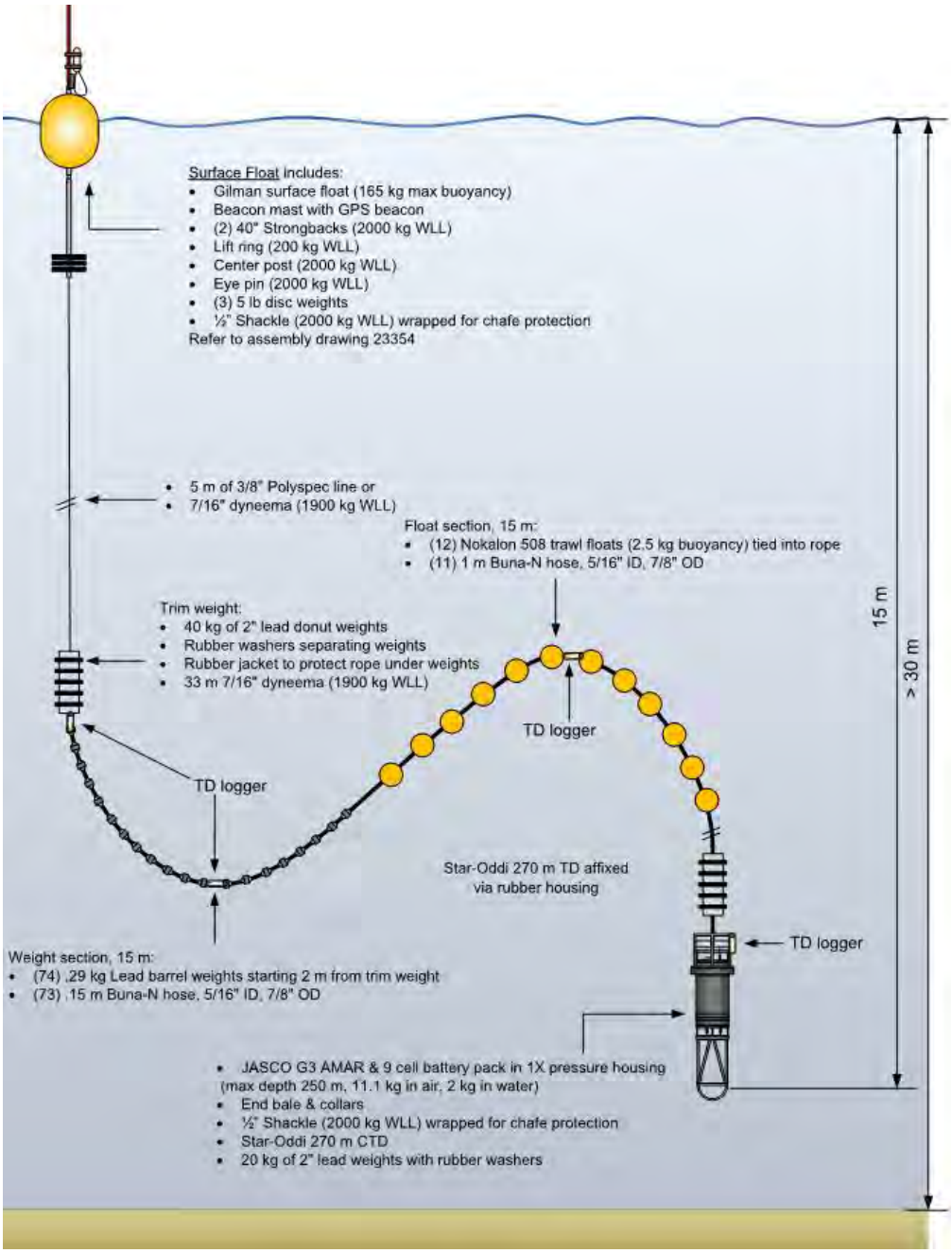

Figure 29. Catenary mooring diagram

A.2. Recorder Calibrations

Each AMAR was calibrated before deployment and upon retrieval with a pistonphone type 42AC precision sound source (G.R.A.S. Sound & Vibration A/S; Figure 30). The pistonphone calibrator produces a constant tone at 250 Hz at a fixed distance from the hydrophone sensor in an airtight space with known volume. The recorded level of the reference tone on the AMAR yields the system gain for the AMAR and hydrophone. To determine absolute sound pressure levels, this gain is applied during data analysis. Typical calibration variance using this method is less than 0.7 dB absolute pressure.

Figure 30. Split view of a G.R.A.S. 42AC pistonphone calibrator with an M36 hydrophone Manufacturers' calibrations were used for the icListen data.

A.3. Acoustic Metrics

This report uses the symbols and definitions for acoustic metrics from ISO standard 18405 [69]. An important element of the standard is the distinction between field quantities, such as sound pressure, and *level* quantities that are 10 times the logarithm of the field quantity, i.e., sound pressure l*evel*.

The most important metrics employed in this analysis are (see Table 7):

- Peak sound pressure level ($L_{p,pk}$) (note that the term peak SPL is deprecated).
- Sound pressure level over an averaging duration T ($L_{p,T}$), which may be referred to as the SPL;
- Sound exposure level over some period T ($L_{E,T}$), which may be referred to as the SEL; and
- Weighted sound pressure levels ($L_{p,W,T}$) where 'W' is a frequency band or frequency weighting function. The frequency bands employed are the decidecade bands (below), the marine mammal function hearing group auditory filters (Figure 4), and the inverted herring audiogram.

For most of the analysis in this report, a one-minute averaging time is employed. This duration is aligned with the time resolution of the tide and turbine state information, and it provides a tractable data size for analysis. Shorter time periods have high sound level variances than the one-minute integration time, and this information is not relevant for analysis of a continuous sound source such as the Open-Centre Turbine. For some analysis, a one-second averaging time is employed for understanding of effects that have shorter time durations, such as the sound levels versus range to the turbine when analyzing drifter data.

The distribution of a sound's pressure with frequency is described by the sound's spectrum (absolute value of the Fourier transform of the sound's time series), which shows the fine-scale features of the frequency distribution of a sound. The sound spectrum is split into of adjacent frequency bands whose width depends on the duration of the time series input to the Fourier transform. There are many excellent texts on Fourier Analysis; we recommend *Principles of Marine Bioacoustics* [70], which includes chapters on hearing, use and production of sound by marine life, and other relevant background information. Splitting a spectrum into 1 Hz wide bands, yields the pressure spectral density of the sound. These values directly compare to the Wenz curves, which represent typical deep ocean sound levels (Figure 2 [71]; note that Wenz averaged spectra over 200 seconds, and to be strictly comparable current projects should use similar durations).

In general animals perceive exponential increases in frequency rather than linear increases [72, 73]. Therefore, splitting the spectrum into 1 Hz bands is not representative of how animals perceive sound;

rather analyzing a sound spectrum with bands that increase exponentially in size gives data that are more meaningful. In underwater acoustics, a spectrum is commonly split into bands that are 1/10th of a decade where each decade represents a 10-fold increase in frequency. The centre frequency of the *i*th decidecade band, $f_c(i)$, is defined as

$$f_c(i) = 10^{i/10}, \quad (1)$$

and the low (f_{lo}) and high (f_{hi}) frequency limits of the *i*th decidecade-band are defined as:

$$f_{lo} = f_c(i) \cdot 10^{-1/20} \text{ and } f_{hi} = f_c(i) \cdot 10^{1/20} . \quad (2)$$

This definition is the same as the ANSI definition for 1/3-octave-bands (base 10) [69, 74]. The decidecade bands become wider with increasing frequency, and on a logarithmic scale the bands appear equally spaced (Figure 31).

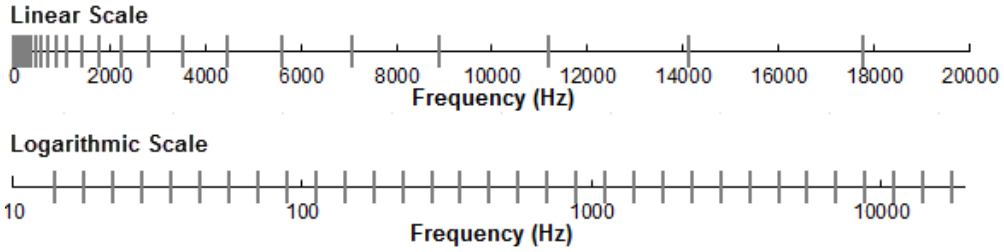

Figure 31. Decidecade bands shown on a linear frequency scale (top) and on a logarithmic scale (bottom).

The sound pressure level in the *i*th decidecade-band $L_{p,ddec\ i,T}$ is computed from the power spectrum $S(f)$ between f_{lo} and f_{hi}:

$$L_{p,ddec\ i,T} = 10 \log_{10} \left(\frac{1}{T} \int_{f_{lo}}^{f_{hi}} S^2(f) df / p_o^2 \right),$$

where T is the duration of time used to compute the power spectrum S(f) and p_o is the reference pressure. Summing the sound pressure level of all the decidecade bands yields the broadband sound pressure level:

$$\text{Broadband SPL} = 10 \log_{10} \sum_i 10^{L_{p,ddec\ i}/10} .$$

Table 7. Symbols and Abbreviations

Symbol/abbreviation	Definition	Units
Fundamental Values		
λ	Wavelength of a sound = c/f	m
c	Sound speed in water, nominally 1500 m/s	m/s
f	Frequency of a sound	Hz = 1/s
Acoustic Metrics [see 69]		
Peak sound pressure level ($L_{p,pk}$)	Ten times the logarithm of the ratio of the maximum instantaneous sound pressure level in a stated frequency band attained by an acoustic pressure signal, $p(t)$ divided by the reference value, P_{02} (normally 1 µPa²): $10 \log_{10} \frac{max(p^2(t))}{p_o^2}$. Note that L_{pk} is a poor indicator of a sound's loudness because the peak signal duration is often very short. The sound exposure level is a better indicator of loudness.	dB re 1 µPa²
Sound pressure level (SPL or $L_{p,T}$)	Ten times the logarithm of the ratio of the mean-square pressure level in a stated frequency band over a time window (T, s) containing the acoustic event to a reference value, P_{02}: (normally 1 µPa²) $10 \log_{10} \frac{1}{T} \int_T \frac{(p^2(t))}{p_o^2} dt$.	dB re 1 µPa²
Sound exposure level (SEL, $L_{E,T}$)	The sound exposure level is ten times the logarithm of the ratio of the time-integral of the squared pressure over the analysis duration (T), divided by the reference time T_0 (normally 1 s) and reference square pressure value P_{02} (normally 1 µPa²): $10 \log_{10} \left(\int_{T_{100}} p^2(t) dt \Big/ T_0 p_0^2 \right)$ where T_0 is a reference time interval of 1 s. The SEL represents the total acoustic energy received at some location during an acoustic event. By Parseval's theorem, this is also the variance in the signal assuming a mean pressure of zero.	dB re 1 µPa²·s
Weighted sound pressure level ($L_{p,W,T}$)	The sound pressure level computed using a frequency weighted spectrum (of data with time duration T) $10 \log_{10} (\frac{1}{T} \int_f \frac{(w(f)S(f))^2}{p_0^2} df)$, where w(f) is the frequency weighting function and S(f) is the Fourier transform of p(t).	dB re 1 µPa²
Mean-square sound pressure spectral density level ($L_{p,f,t}$)	Ten times the logarithm of the ratio of the distribution as a function of non-negative frequency of the mean-square sound pressure per unit bandwidth of a sound having a continuous spectrum, divided by the reference value reference square pressure value p02 (normally 1 µPa²): $10 \log_{10} \left(S(f)^2 \Big/ p_0^2 \right)$.	dB re 1 µPa²/Hz

Note: The units for sound pressure level in this table are given as dB re 1 µPa², however, many references continue to use dB re 1 µPa which is equivalent. The difference reflects how the analysis was performed. Here we show the calculation as $10\log_{10}$(pressure²), whereas many practitioners compute the sound pressure level as $20\log_{10}$(sqrt(pressure²))–which yields the same value but has units of dB re 1 µPa. Some of the figures in this report were generated with older versions of JASCO's analysis software that used the dB re 1 µPa units. Similarly, the pressure spectral density level is also called the power spectral density in some figures.

A.4. Cadence Analysis

Cadence analysis aligns the acoustic data with an external cadence such as the time of day, time of week or tidal cycle. For this project cadence analysis begins by referencing each minute of data to a point in the tidal cycle. Tide predictions are generated using the TBone web service (http://tbone.biol.sc.edu/tide/index.html). For these data the Cape Sharp, NS, (45.3667° N, 64.3833° W) station was used.

For the high-resolution cadence images, data were plotting for up to 780 minutes (13 hours) after a given tide reference point (low, high, or slack tide). Each available minute of data is compared to the tide prediction and then assigned to the bin corresponding to the same number of minutes following the chosen reference point. The cadence analysis was performed on the 1 Hz pressure spectral density data. Each time and frequency bin is divided by the total number of data points to get the average pressure spectral density for that bin. Pressure spectral density is plotted on a logarithmic frequency axis, so low frequencies are interpolated between the 1 Hz FFT points, and high frequencies are averaged across all 1 Hz bins that correspond to each pixel in the image.

This same underlying data is separately averaged across 15-minute time periods, again relative to the same tide reference points (low, high, or slack tide). Then the 15-minute average 1 Hz data is used to compute decidecade band values. These 15-minute decidecade values are stored in a comma-separated value (CSV) file for subsequent analysis and reporting.

A.5. General Additive Modelling of Received Levels

A General Additive Model is a statistical tool used to make inferences about an unknown function using known predictor variables. In this study, General Additive Models were fit to the long term acoustic measurements to predict turbine sound at all operating conditions and flow rates, using the available measurements at only some turbine conditions and flow rate. The models were created using the software package ‘mgcv’ [75] for the ‘R’ programming language. Additive models are sometimes referred to as ‘smoothers’ because they are spline functions that smoothly follow the measured data rather than being traditional linear models. The model used was ‘decidecade SPL ~ s(normalizedCurrentSpeed)’. Individual models were run for the six-identified tide and turbine states:

1. Turbine not spinning, flood tide.
2. Turbine not spinning, ebb tide.
3. Turbine free spinning, flood tide.
4. Turbine free spinning, ebb tide.
5. Turbine generating, flood tide.
6. Turbine generating, ebb tide.

The models were then used to predict the median sound levels for each decidecade band at normalized flow rates of 20, 40, 60, and 80% of the full flow. The models are only valid above 70% flow for the flood direction since the ebb flow rarely exceeds 70% of the maximum flood flow. Similarly, the sound levels at 100% of full flow were not included because we did not have sufficient examples of this operating state to develop a reliable model.

The models were used to create tables of expected sound pressure levels as a function of the six tide-turbine states and the normalized flow speed (1–99). These tables are included in this report in Appendix D.3.

A.6. Acoustic Propagation Modelling

Acoustic propagation modelling was used for two purposes in this analysis: 1) to estimate the propagation loss of the turbine signals arriving at the recorders; and 2) to estimate the ranges from the turbine that the turbine sounds would be above the ambient levels.

Our original intention was to employ high fidelity acoustic propagation modelling to estimate the propagation losses. This type of modelling accounts for the water depth, bottom shape and composition as well as sound speed profile in the water column to estimate the losses as a function of range and direction. The FORCE site is exceptionally challenging to model because:

- The seabed around the turbine is weathered basalt, which has a great deal of structure (ripples and boulders on the order of 2–3 m high) that is difficult to model.
- The basalt platform stands up above the local seabed that is composed of mixed rock and sediment with uncertain geoacoustic parameters
- The sound speed profile is poorly known.
- The water depth varies over a wide range due to the tides which would require a great many propagation modelling 'runs' to account for. Once the runs were completed the depth-appropriate transmission loss would need to be selected from moment to moment to estimate the losses.

The analysis of received sound levels from the icListen drifters deployed on 27 Mar 2017 performed by GTI (reported dated 5 Jan 2018) demonstrated that the distance from the turbine that the sound could be detected was on the order of 100's of meters, and that spherical spreading (20Log_{10}(Range)) was an appropriate propagation model (Figure 32). Therefore, we choose to use simple geometric spreading with an attenuation of 20Log_{10}(Range) for this analysis.

The propagation ranges under consideration here are less than 1 km, and the frequency range of interest is below 10 kHz. Therefore, we did not include an absorption term in the propagation modelling since it is at most 1 dB/km at 10 kHz, which is far below the uncertainty in other elements of our analysis.

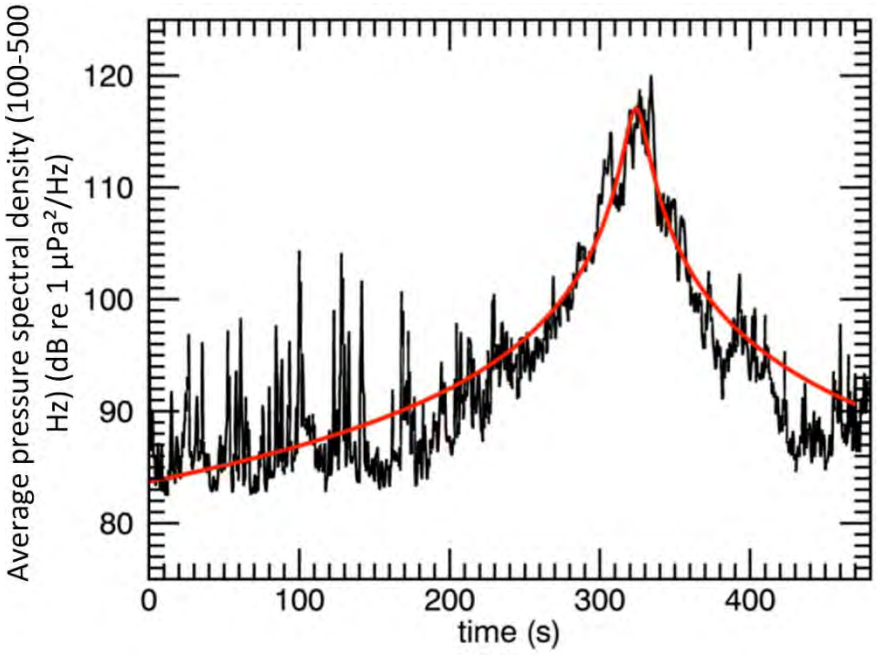

Figure 32. Average Pressure Spectral Density in the frequency range of 100–500 Hz vs time in file for icListen drifter 1658 on trial 7 on 27 Mar 2017. The drifter moved at ~4 m/s. The estimated range to the turbine at the closest range was 30 m. The red line is a best-fit of 20log10(range) (Figure 9 from GeoSpectrum Technologies Inc FORCE Turbine Analysis Report dated 5 Jan 2018).

A.7. Automated Click Detector for Porpoises

We applied an automated click detector/classifier to the high-frequency data from the autonomous AMAR data sampled at 375 kHz and the icListen data sampled at 512 kHz to detect clicks from porpoises (Figure 33). This detector/classifier is based on the zero-crossings in the acoustic time series. Zero-crossings are the rapid oscillations of a click's pressure waveform above and below the signal's normal level (e.g., Figure 33). Clicks are detected by the following steps (Figure 33):

1. The raw data is high-pass filtered to remove all energy below 8 kHz. This removes most energy from other sources such as shrimp, vessels, wind, and cetacean tonal calls, while allowing the energy from all marine mammal click types to pass.
2. The filtered samples are summed to create a 0.334 ms rms time series. Most marine mammal clicks have a 0.1–1 ms duration.
3. Possible click events are identified with a split-window normalizer that divides the 'test' bin of the time series by the mean of the 6 'window' bins on either side of the test bin, leaving a 1-bin wide 'notch'.
4. The maximum peak signal within 1 ms of the detected peak is found in the high-pass filtered data.
5. The high-pass filtered data is searched backwards and forwards to find the time span where the local data maxima are within 9 dB of the maximum peak. The algorithm allows for two zero-crossings to occur where the local peak is not within 9 dB of the maximum before stopping the search. This defines the time window of the detected click.
6. The classification parameters are extracted. The number of zero crossings within the click, the median time separation between zero crossings, and the slope of the change in time separation between zero crossings are computed. The slope parameter helps to identify beaked whale clicks, as beaked whale clicks increase in frequency (upsweep).
7. The Mahalanobis distance between the extracted classification parameters and the templates of known click types is computed. The covariance matrices for the known click types, computed from thousands of manually identified clicks for each species, are stored in an external file. Each click is classified as a type with the minimum Mahalanobis distance, unless none of them are less than the specified distance threshold.

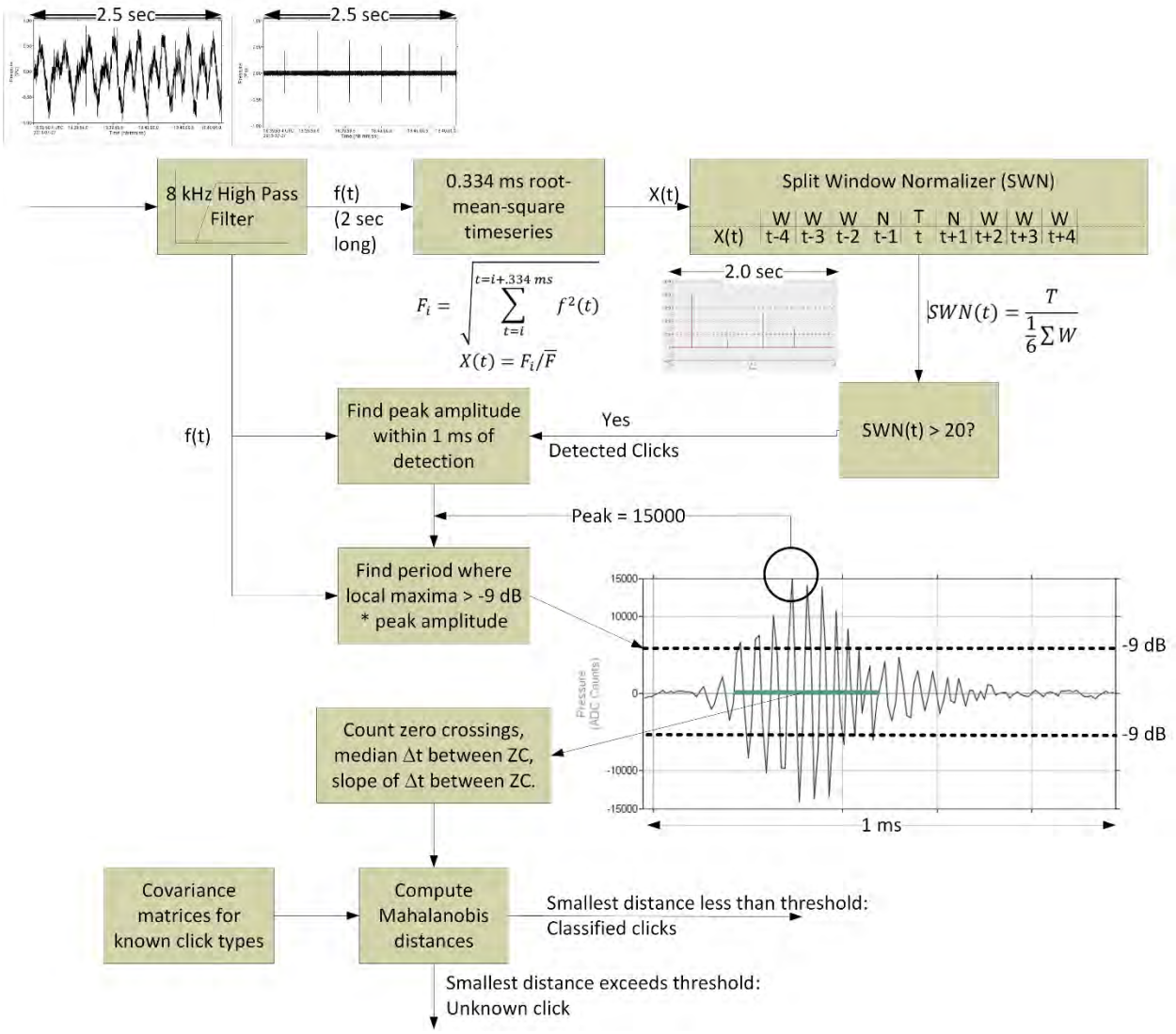

Figure 33. The click detector/classifier block diagram.

Appendix B. Results–Total Sound Levels

B.1. Non-Acoustic Data

Emera provided data with the minute-by-minute normalized current speeds (Figure 34), direction, and the turbine operating state (not spinning, free spinning, generating). Using this information, three time periods were selected for detailed analysis of sound levels while both the AMAR and icListen recordings are available:

- 24 Dec 2016–the maximum current speed on this day was 68% at 09:50 and represents a neap tide day.
- 16 Dec 2016–the maximum current speed was 100% at 02:43 and is a maximum spring tide.
- 01 Dec 2016–the maximum current speed was 83% at 02:43 and was chosen as a representative 'normal' day.

For each time the modelled (see Appendix C.2.2.2) and measured sound levels are compared. The range to the 150 dB SPL isopleth and the sound levels exceeding background levels are also estimated. The comparisons are made from the high tide time preceding the maximum current until the low tide following.

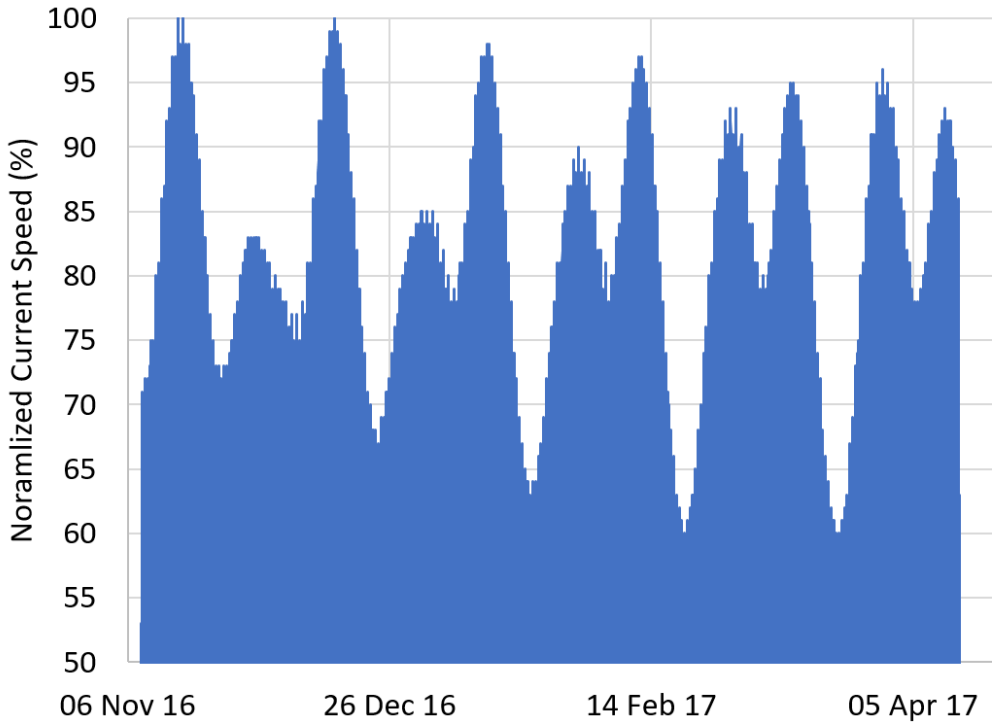

Figure 34. Normalized current speed data provided by Emera. Due to the large amount of data (by minute) this figure shows the maximum normalized current speed per tidal cycle.

B.2. Static Recorders

This section contains the total sound levels and variability in sound levels recorded at the autonomous AMAR (Stations 1 and 2), on two of the turbine mounted icListens, and the outer Bay of Fundy reference AMAR (Stn 1).

This section demonstrates that:

- Flow noise affects acoustic recordings in the Bay of Fundy. The effects are proportional to the current velocity. Similarly, the effects increase with height off the seabed.
- The Open-Centre Turbine generates sounds at frequencies as low as 60 Hz that can be easily distinguished from the background noise using a bottom mounted recorder 167 m from the turbine. There we chose to use the decidecade bands of 63 Hz and above for analysis and modelling of the turbine and environment.
- The Minas Passage environment has much higher sound levels in the kilohertz region than are recorded in low energy environments. This is due to sediment interaction noise, i.e., gravel and rock striking each other.

B.2.1. Outer Bay of Fundy Stn1

The long-term recording made under the traffic lanes in the outer Bay of Fundy is used as a reference for a 'normal' acoustic environment in the Bay of Fundy (Figures 35 and 36). The overall trend in the data are periods of low-frequency noise associated with variations in tidal current strength, as well as short periods of low-frequency noise associated with passing vessels. At frequencies above 1 kHz, the pressure spectral density (Figure 36 bottom) and decidecade sound pressure levels (Figure 36 top) both tend to decrease in amplitude as the frequency increases. Note that the decidecade levels above 1 kHz have a small quartile range (~6 dB) and are in the range of 90 dB re 1 µPa². We will see in the following sections that the decidecade levels in the Minas Passage are much higher and have greater inter-quartile ranges.

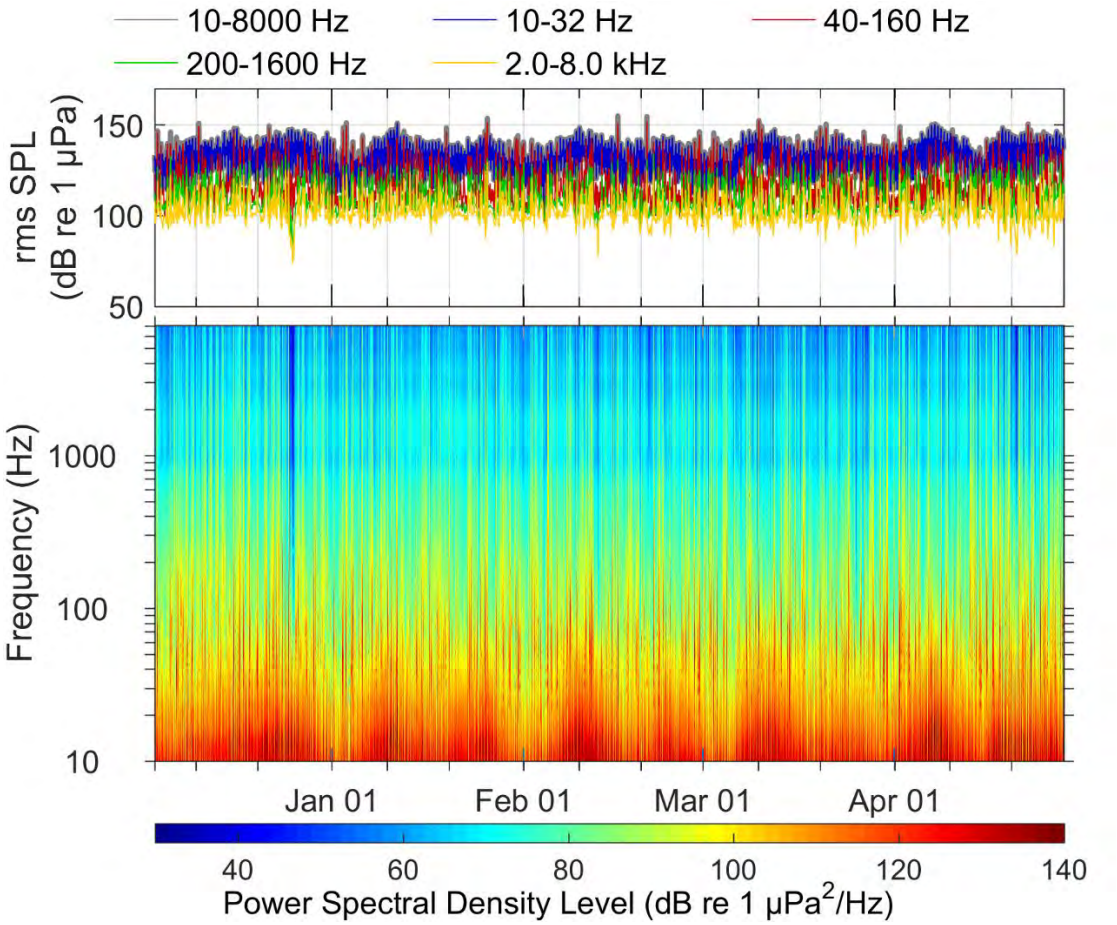

Figure 35. (Top) in-band SPL and (bottom) spectrogram for the AMAR deployed in the Bay of Fundy in 2015.

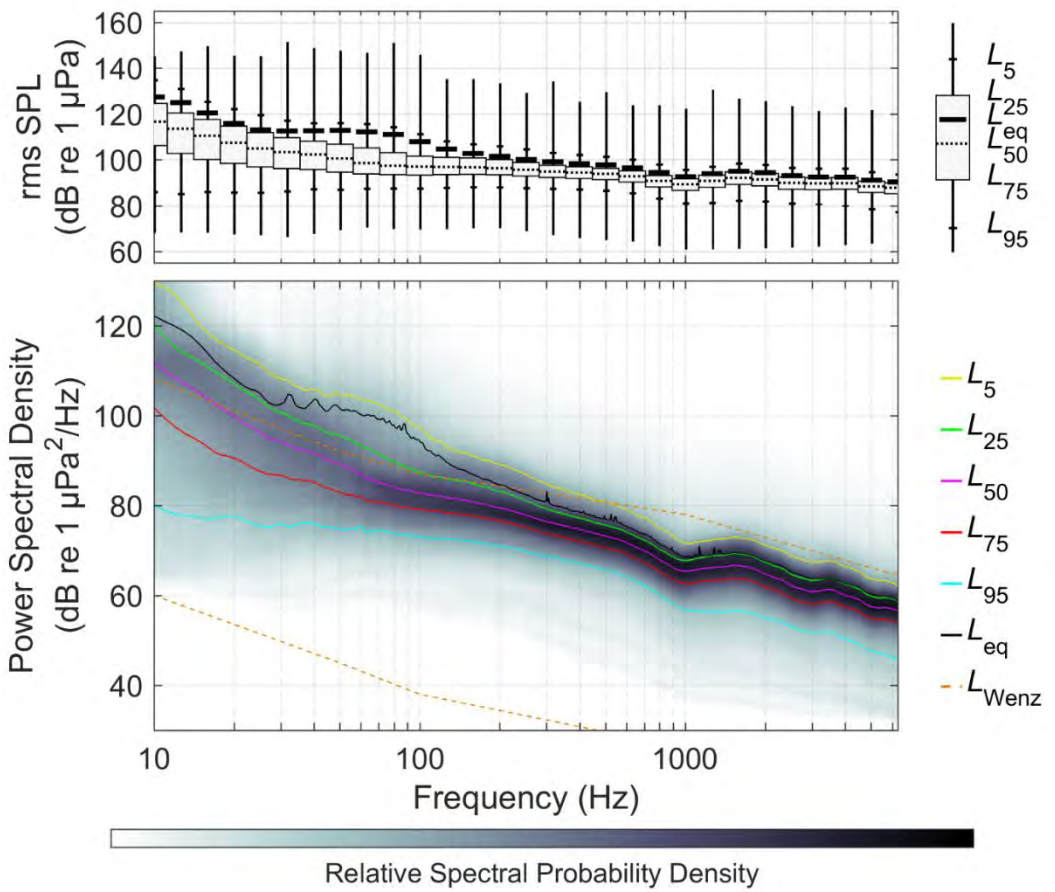

Figure 36. (Top) Exceedance percentiles and mean of the decidecade band SPLs and (bottom) exceedance percentiles and probability density (grayscale) of 1-min PSD levels compared to the limits of prevailing noise (Wenz 1962) for the AMAR deployed under the shipping lanes in the Bay of Fundy in 2015.

B.2.2. Autonomous AMAR

The complete measurement results for the autonomous AMAR are presented in Figures 37 and 38 for the deployment period (18 Nov 2016 to 19 Jan 2017). All results presented in this section are from hydrophone 1. The spectrogram and band level plot (Figure 37) shows that low-frequency noise contributed the most energy to the recordings, and that the highest low-frequency sound levels occurred on the days with the highest tidal currents (Figure 34). The differences over a short time in the band level plot indicate that there were large variations due to tide. Figure 38(bottom) shows the pressure spectral density (PSD) compared to the expected limits on prevailing noise. Typically, we compare the median, or L_{50}, to the prevailing noise limits to describe ambient noise conditions. In this area, the L_{50} exceeded or was very close to the upper limit on prevailing noise for all frequencies. There are peaks in the PSD in the range of 60–300 Hz and ~4 kHz that are likely associated with the turbine operations (see Appendix C). Based on Figure 38, data from frequencies less than 50 Hz are affected by flow noise most of the time; however, the flow noise can reach to ~200 Hz and above.

The decidecade band levels above 1 kHz are ~10 dB higher than in the outer Bay of Fundy and have an interquartile range of ~20 dB. This variability is due to the energy from sediment interactions, which is an important source at full tidal flows and stops at slack tide.

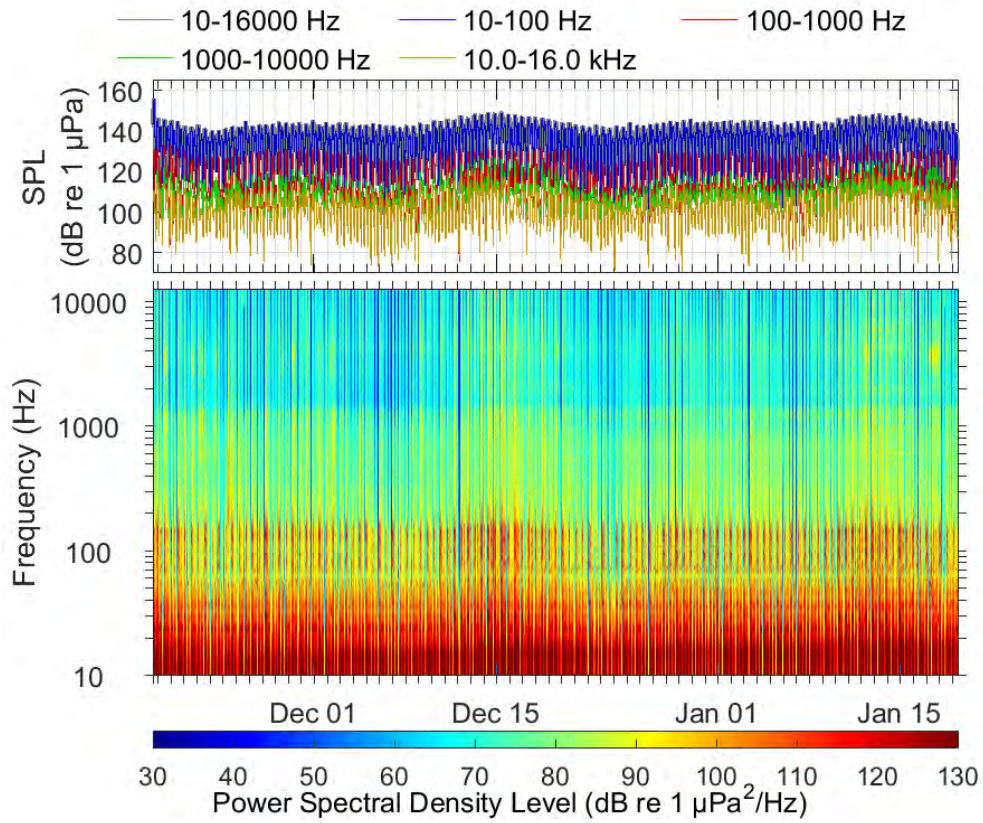

Figure 37. (Top) in-band SPL and (bottom) spectrogram for the autonomous AMAR.

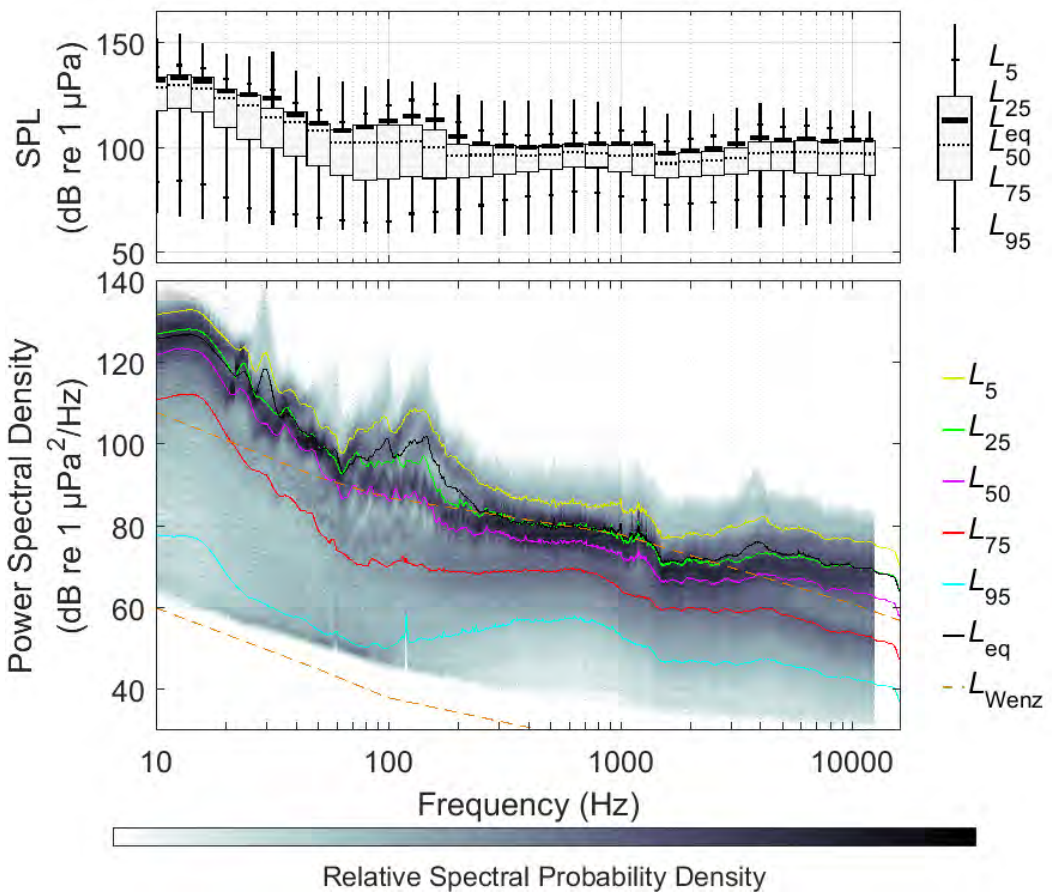

Figure 38. (Top) Exceedance percentiles and mean of the decidecade band SPLs and (bottom) exceedance percentiles and probability density (grayscale) of 1-min PSD levelscompared to the limits of prevailing noise (Wenz 1962) for the autonomous AMAR.

B.2.3. Turbine mounted hydrophones

B.2.3.1. icListen 1404-Forward-Port

The complete measurement results for the Forward-Port icListen are presented in Figure 39 and Figure 40 for the period sampled at 32 kHz (12 Nov 2016 to 08 Mar 2017). The spectrogram and band level plot (Figure 39) shows that low-frequency noise contributed the most energy to the recordings, and that the highest low frequency sound levels occurred on the days with the highest tidal currents (Figure 34). Figure 38(bottom) shows the pressure spectral density (PSD) compared to the expected limits on prevailing noise. Typically, we compare the median, or L_{50}, to the prevailing noise limits to describe ambient noise conditions. In this area, the L_{50} was 5–10 dB above the upper limit of prevailing noise for all frequencies. The peaks in the PSD in the range of 60–300 Hz and ~4 kHz that are likely associated with the turbine operations are less pronounced on the icListen than they are on the AMAR (Figure 38; also see Appendix C). Based on Figure 40, data from frequencies less than 200 Hz are affected by flow noise most of the time, however, the flow noise can reach to ~500 Hz. The high PSD levels above 1000 Hz are likely generated by real sound in the water from sediment interaction noise.

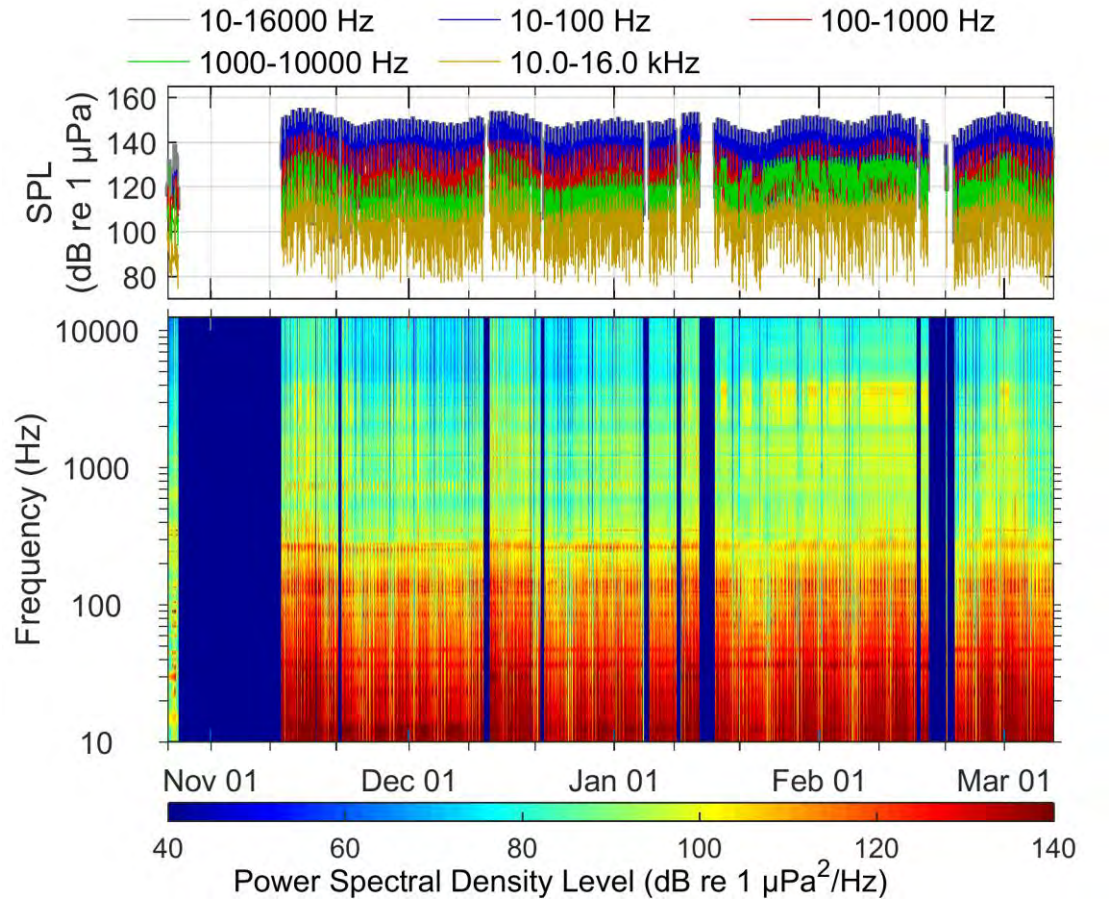

Figure 39. (Top) in-band SPL and (bottom) spectrogram for icListen 1404 hydrophone in the Forward-Port position.

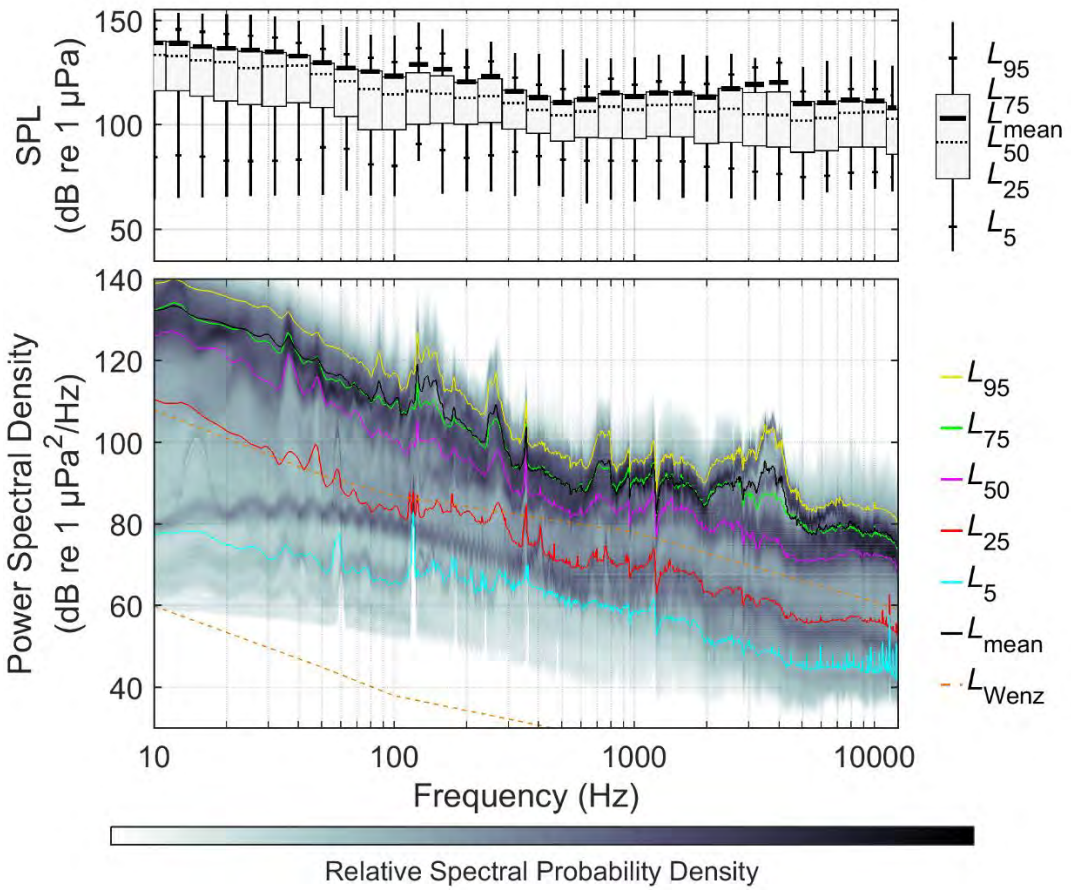

Figure 40. (Top) Exceedance percentiles and mean of the decidecade band SPLs and (bottom) exceedance percentiles and probability density (grayscale) of 1-min PSD levels compared to the limits of prevailing noise (Wenz 1962) for icListen 1404 hydrophone in the Forward-Port position

B.2.3.2. IcListen 1405–Turbine Top

The hydrophone placed at the top of the turbine (hydrophone 3, Figure 27) was operational for ~13 tidal cycles (Figure 41). The long-term spectrogram for this hydrophone has a short enough total duration that the differences between the ebb and flood tide speeds and its effect on flow noise is easily seen. The flow noise at this location affected the recorded sound levels up to 16 kHz (Figures 41 and 42). The decidecade bands above 1 kHz on this hydrophone (Figure 42) continue to decrease in amplitude with frequency, unlike those on the forward-port hydrophone (Figure 40) and the autonomous AMAR (Figure 38). This shows that the flow noise is still dominant at these frequencies and the effects of sediment interaction are not important in the recordings at this position. This data from this recording position are of limited value for assessing the sound emitted by the turbine.

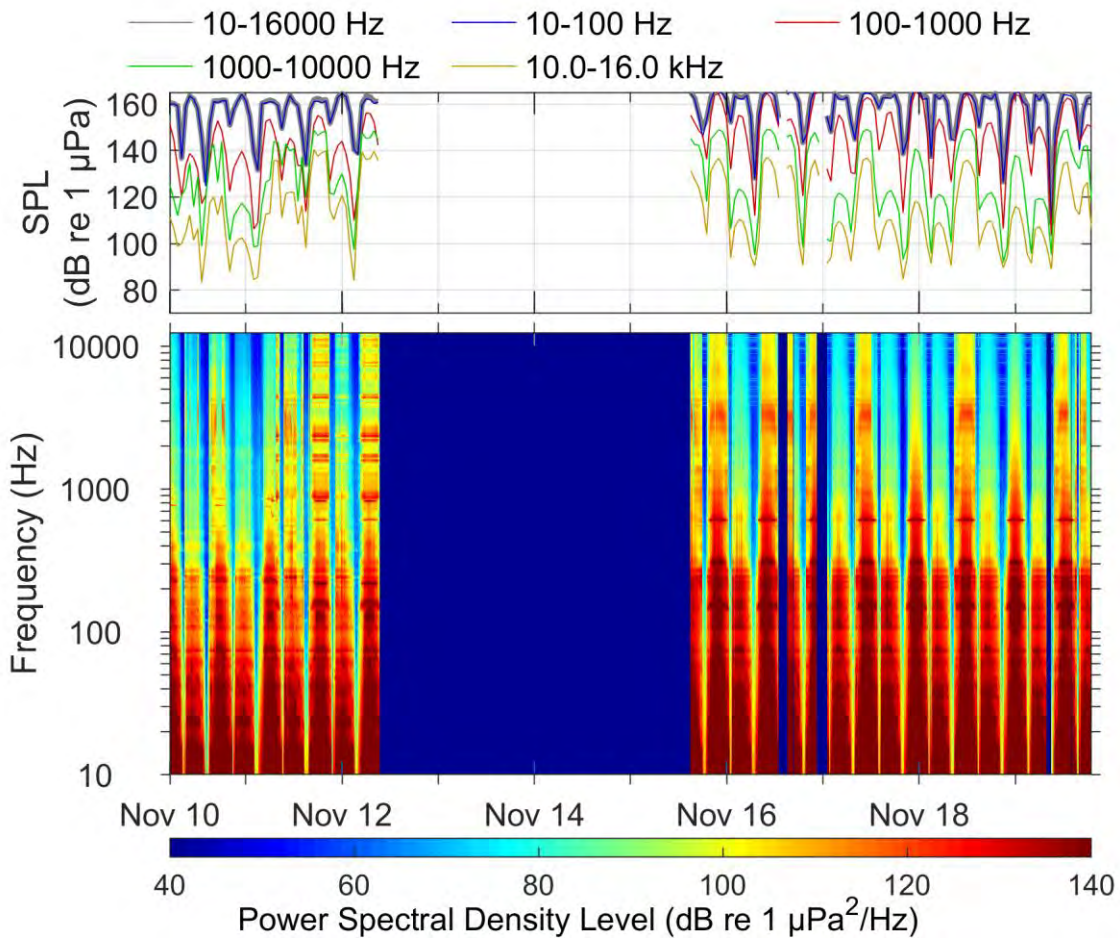

Figure 41. (Top) in-band SPL and (bottom) spectrogram for icListen 1405 hydrophone on top of the turbine.

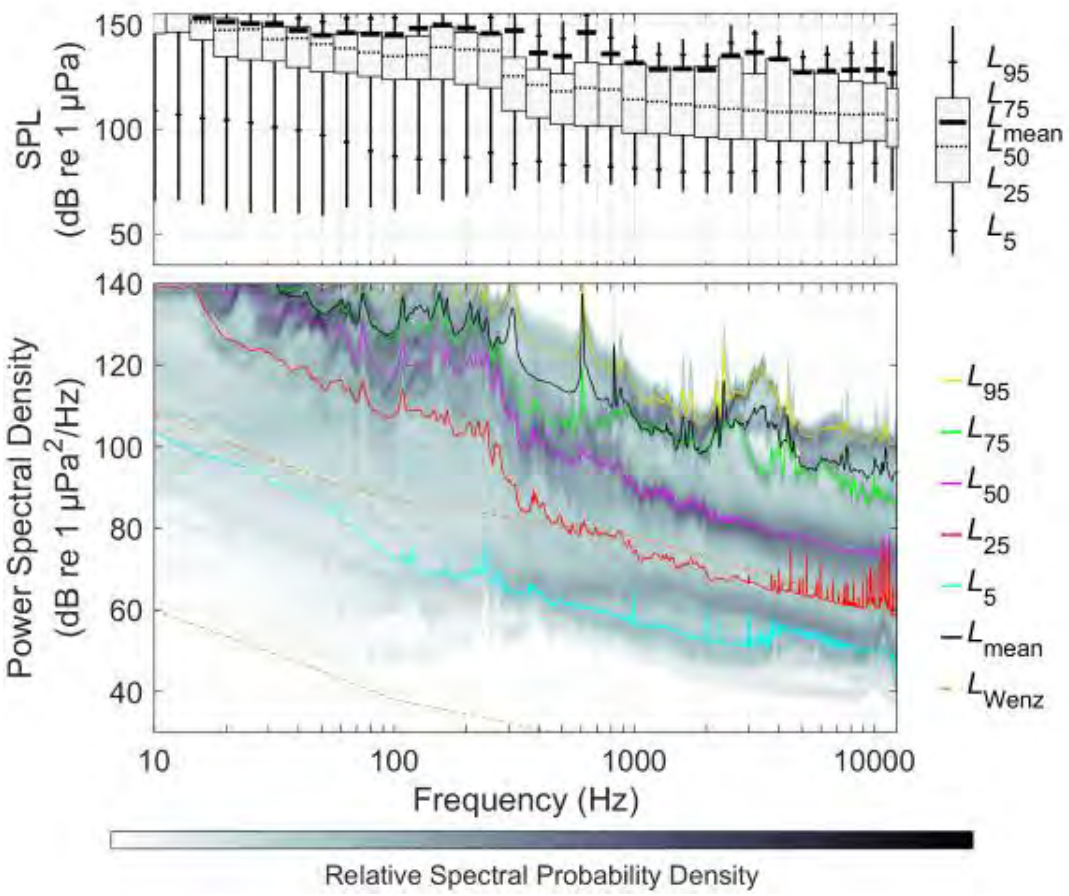

Figure 42. (Top) Exceedance percentiles and mean of the decidecade band SPLs and (bottom) exceedance percentiles and probability density (grayscale) of 1-min PSD levels compared to the limits of prevailing noise (Wenz 1962) for icListen 1405 hydrophone on top of the turbine.

B.2.3.3. High Frequency Noise Issues on the Cabled icListen

The icListen sampling rate was increased to 512 kHz on 24 Mar 2017. This high sampling rate data can be used to detect porpoises, whose clicks are centred near 130 kHz [13]. During meetings with Emera, concerns about the detection rate of porpoises on the icListen compared to CPOD detectors (Chelonia Ltd) lead us to investigate the high sample rate data. It was found that in the frequency band of 60–150 kHz the noise levels on the cabled icListen hydrophone were 15–25 dB above those on the on the drifting icListen hydrophone or the AMAR (Figures 43–47). The nature of the noise leads us to believe that the source is from switching power supplies that are providing power to the icListen. Further investigation of this noise is recommended before the turbine is redeployed. There were also impulsive sounds present in the data that were likely from the Gemini sonar.

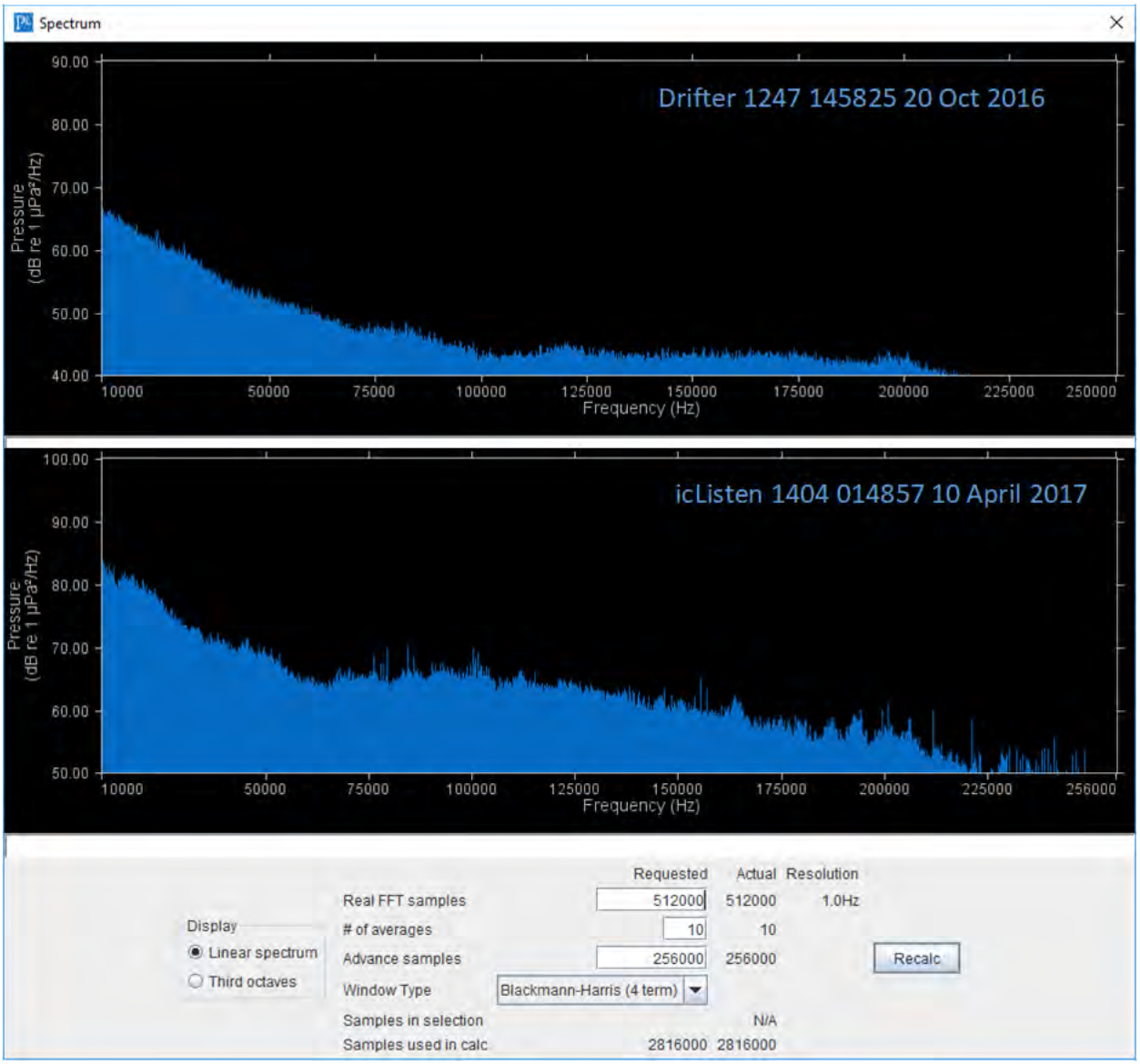

Figure 43. Comparing icListen noise floors. (top) icListen 1247 in a drifter mooring on 20 Oct 2016. (middle) icListen 1404 attached to the OpenHydro turbine platform. (Bottom) Processing Parameters.

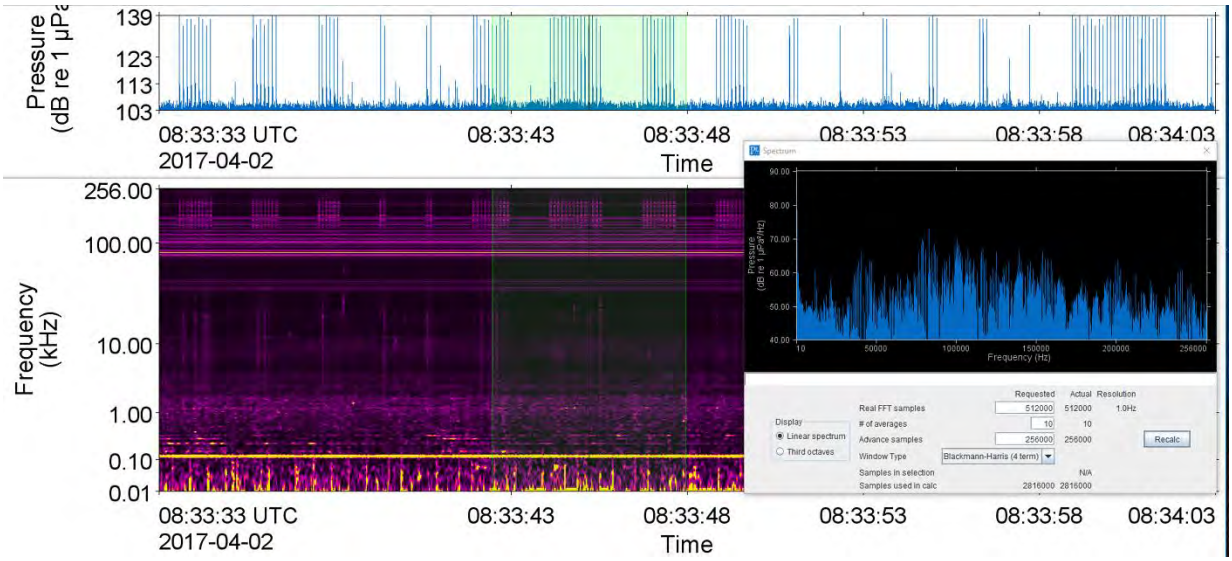

Figure 44. icListen 1404 data sampled at 512 kHz at slack tide on 2 April, showing impulsive signals (likely from the Gemini sonar) and continuous tones at high frequencies.

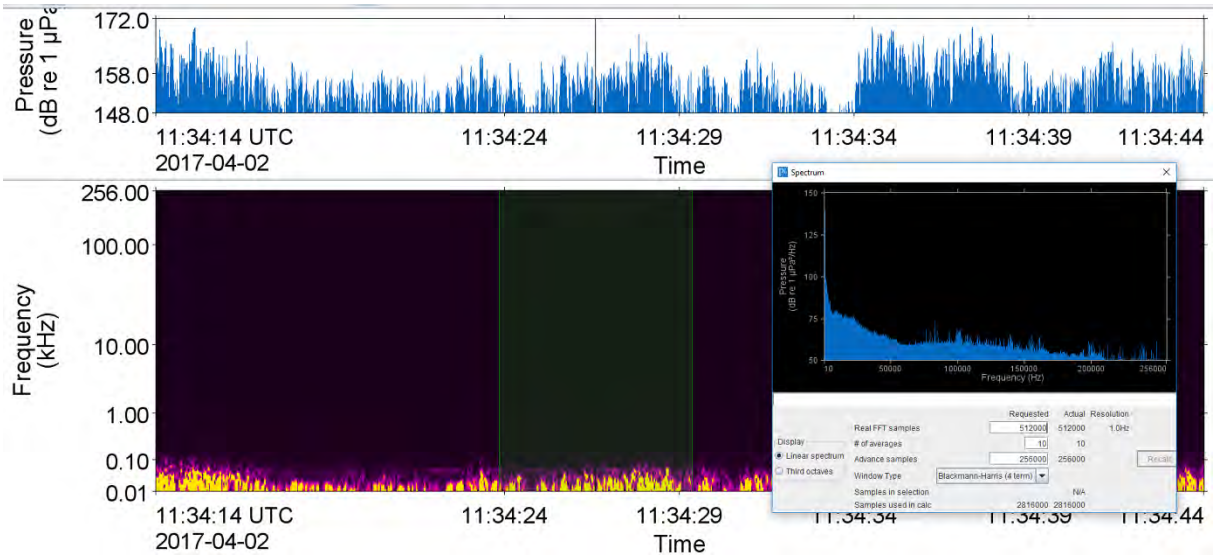

Figure 45. icListen 1404 data at full tidal flow 3 hours after the data in Figure 44; the increase in energy seen in Figure 43 is still present. This effect is not replicated for the AMAR (Figure 47)

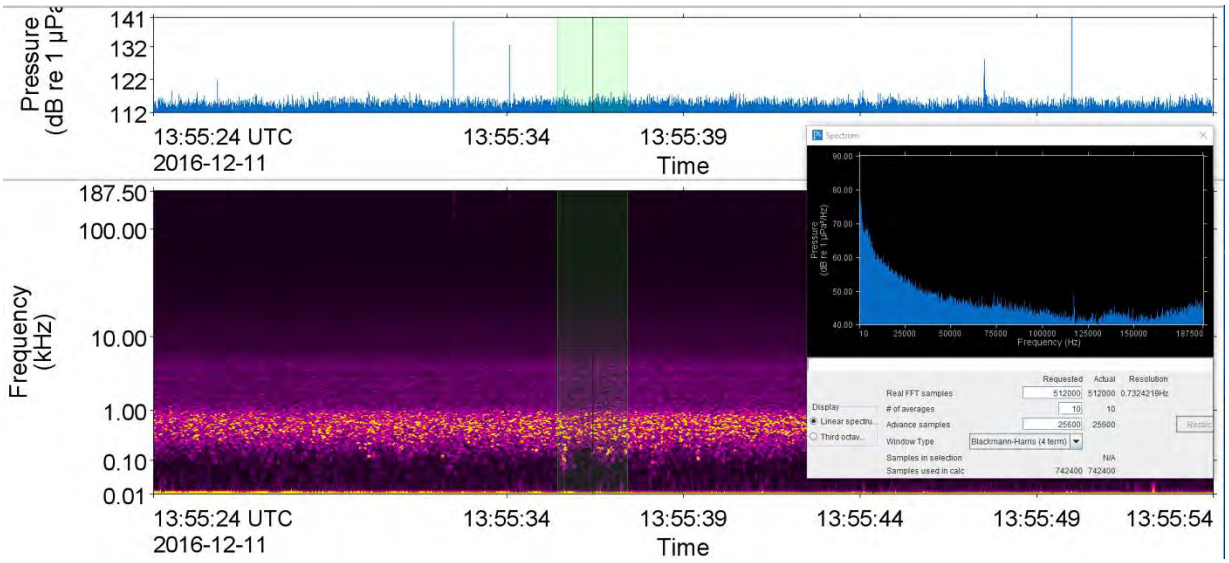

Figure 46. Autonomous AMAR data at slack time on 11 Dec 2016. The noise levels above 60 kHz are similar to those from the drifting icListen (Figure 43)

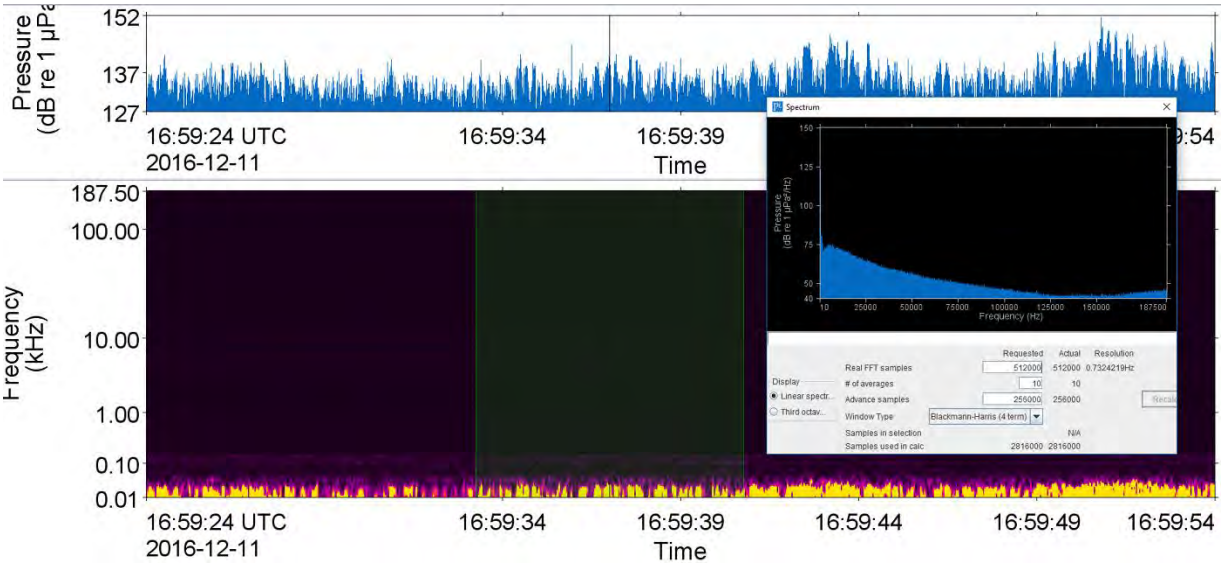

Figure 47. Autonomous AMAR data at full tidal flow on 11 Dec 2016, 3 hours after the data in Figure 46. The noise levels above 60 kHz did not change significantly.

B.2.4. Porpoise Detections

The autonomous AMAR sampled at 375 kHz for 1-minute out of every 8, and the forward-port icListen was switched to 512 kHz sampling on 24 Mar 2017; these data sets are suitable for detecting porpoises. Porpoise were detected sporadically in November 2016 to January 2017 on the bottom mounted recorder (Figure 49). Porpoise were detected on almost all days in the spring using the turbine mounted hydrophone (Figure 48). Further work will be needed to determine if the differences in detection are related to the recording method or the seasons. The AMAR high flow mooring cover may not allow the porpoise click frequencies to propagate to the hydrophone. We have verified its performance up to 32 kHz only. The CPOD data collected intermittently since 2012 appears to show that porpoise presence peaks in the spring and is at its lowest levels in December/January [76].

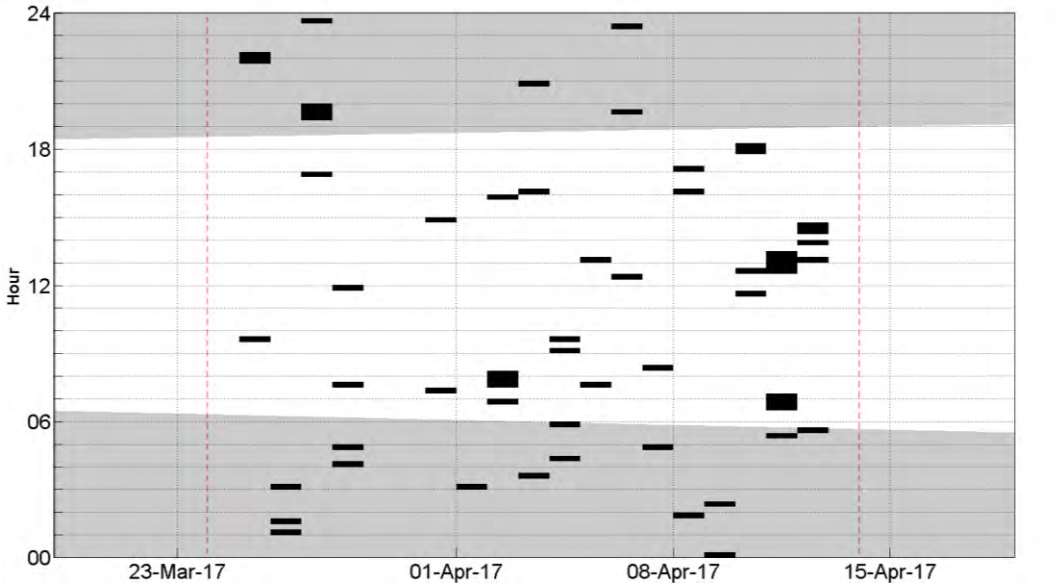

Figure 48. Automated porpoise click-trains detections on the 512 kHz sampled forward-port hydrophone data (24 Mar 2017 to 13 Apr 2017).

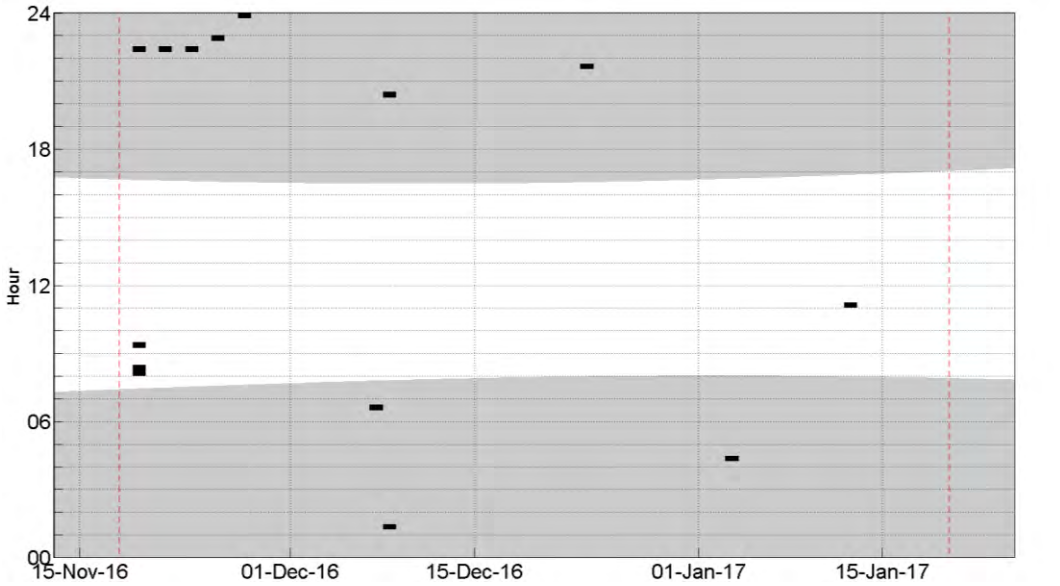

Figure 49. Automated porpoise click-trains detections on the 375 kHz sampled autonomous AMAR data (16 Nov 2016 to 19 Jan 17).

B.3. Drifters

Acoustic recordings are made with hydrophones that are sensitive to the small changes in pressure from sound waves travelling in the water. Large pressure changes can occur when water flows around the hydrophone—a problem for stationary hydrophones that is overcome by using drifters. However, drifters can move up-and-down in the water due to waves, which also causes large pressure changes. These pressure changes from hydrophone movement and currents are called flow noise. It is a measurement artifact that must be minimized during data collection and accounted for during data analysis.

Two sets of drifter measurements were considered in this analysis–the combined icListen and AMAR drifts on 20 Oct 2016 and the icListen drifts on 27 Mar 2017. The data are summarized in Figure 50.

On 20 Oct 2016, the AMAR and icListen measured similar sound levels (Figure 50 left). In this data set, the high-frequency cetacean mammal weighted sound pressure levels (frequency > ~10 kHz, see Figure 4) rise in parallel with the low frequencies are only a few decibels below the broadband sound levels for most of the tidal cycle. This means that the strongest source of sound is at high frequencies, i.e., from sediment interactions. Near slack tide, vessel noise caused the low-frequency sound levels to increase independently of the high frequencies. In this data set, the icListen drifter had regular, low intensity and low-frequency impulsive sounds (Figure 51). We believe the source of this sound is movement of the hydrophone due to surface wave action that couples to the hydrophone (mooring shown in Figure 28). The AMAR drifter, which has a catenary mooring (Figure 29) did not have these impulses (Figure 52).

On 27 Mar 2017, the icListen data showed a nearly constant low-frequency sound level while the high-frequency sound level rises and falls with the tidal cycle (right hand side of Figure 50). The seventh drift, at around 14:00, was analyzed in detail both by GeoSpectrum and in this report (see Appendices A.6 and D.1) to assess the turbine sound level as a function of range. These data proved valuable for validating the sound level model derived from the autonomous AMAR data (Appendix C.2). The increase in sound levels as the drifter passed the hydrophone is not apparent here because Figure 50 uses data with a 1-minute averaging time. The source of the low-frequency noise on 27 Mar 2017 appears to be far higher levels of surface-wave induced noise that made data below 150 Hz unsuitable for analyzing environmental or turbine sound levels (Figure 53).

From these data sets, we conclude:

1. The value of drift measurements is in obtaining the sound level versus range to validate source level models.
2. Either acoustic recorder is suitable for drift measurements. If the AMAR is used in the future, it should be programmed to record continuously at the higher sampling rate rather than duty cycling.
3. Drifters must include an effective means of isolating the hydrophone from surface wave action.
4. Drifters must have a GPS logger attached that records the location at least once per minute, higher logging rates are recommended.

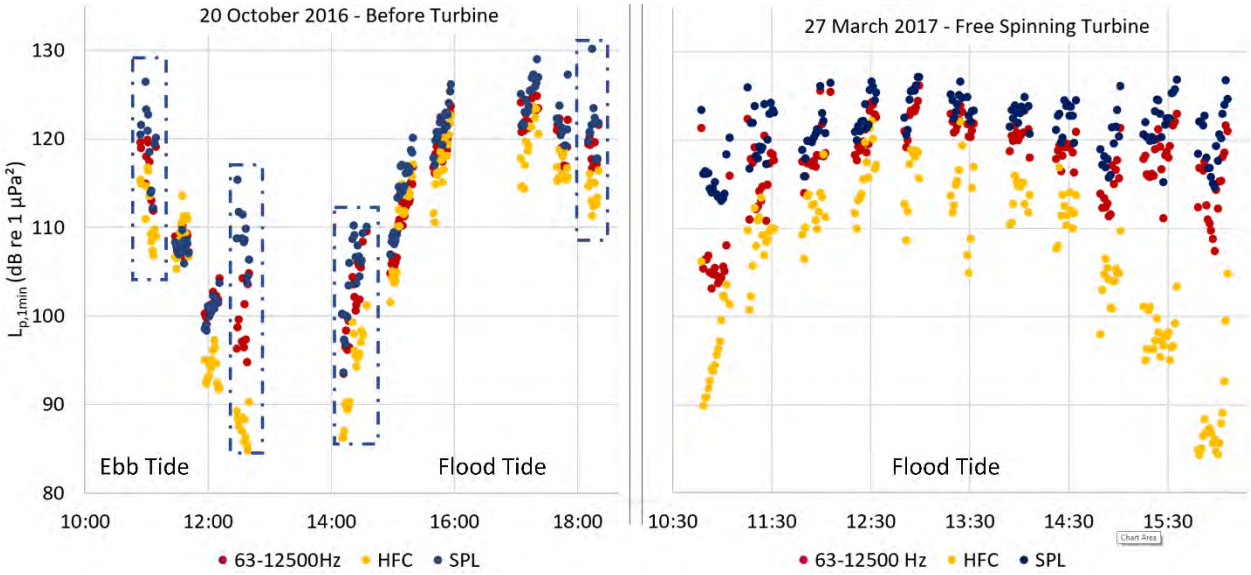

Figure 50. Comparing drifting hydrophones results. (left) one-minute SPL measured on 20 Oct 2016 before the turbine was installed. Drifts with boxes around them were made with the AMAR drifter. (Right) the 11 drift trials made on 27 Mar 2017 using the icListen drifters with the turbine free-spinning.

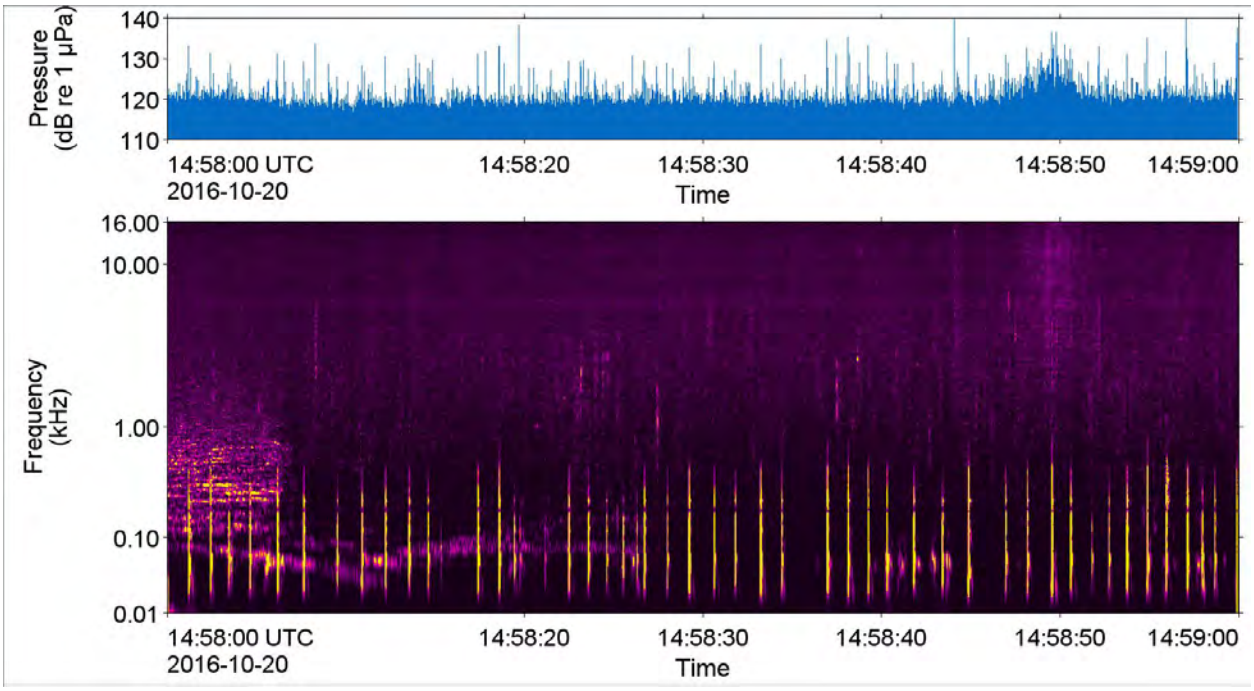

Figure 51. Time-series (top) and spectrogram (bottom) of one-minute of data from icListen drifter 1247 at 14:58 on 20 Oct 2016. The data were high-pass filtered at 5 Hz to remove the extreme low-frequency noise that was present. The vertical yellow impulses from ~10 Hz–300 Hz are likely due to the mooring line coming tight and the hydrophone moving upwards in the water column.

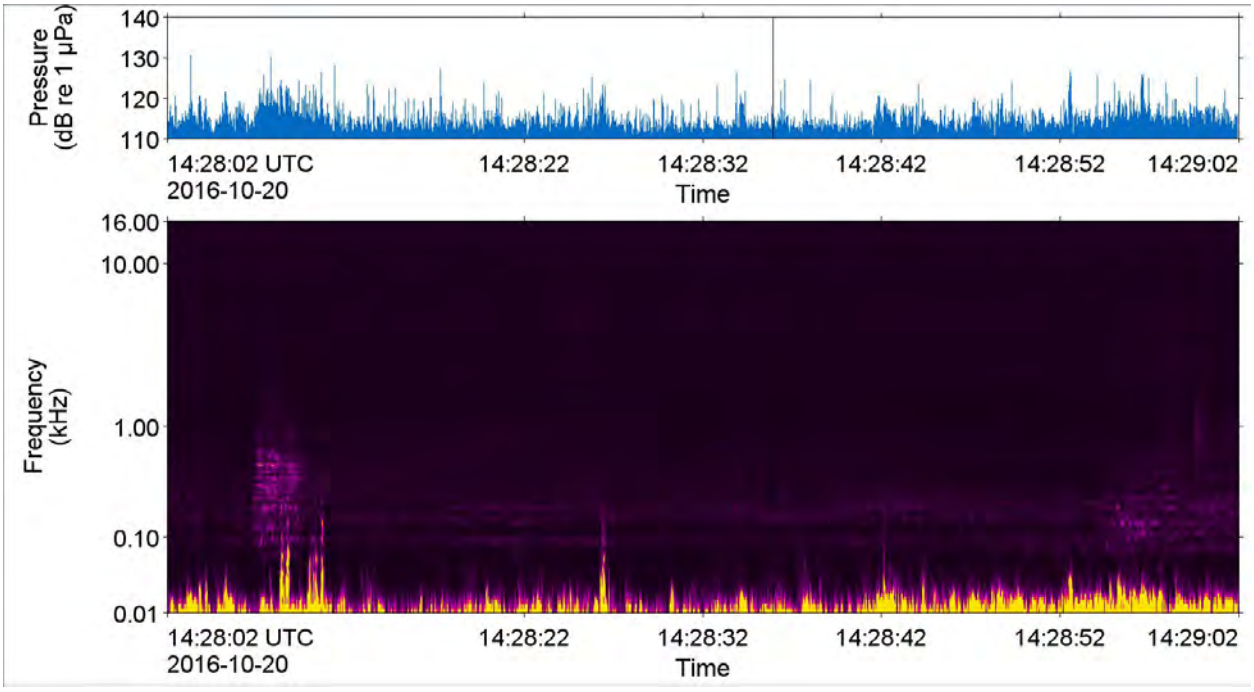

Figure 52. Time-series (top) and spectrogram (bottom) of one-minute of data from the AMAR drifter at 14:28 on 20 Oct 2016.

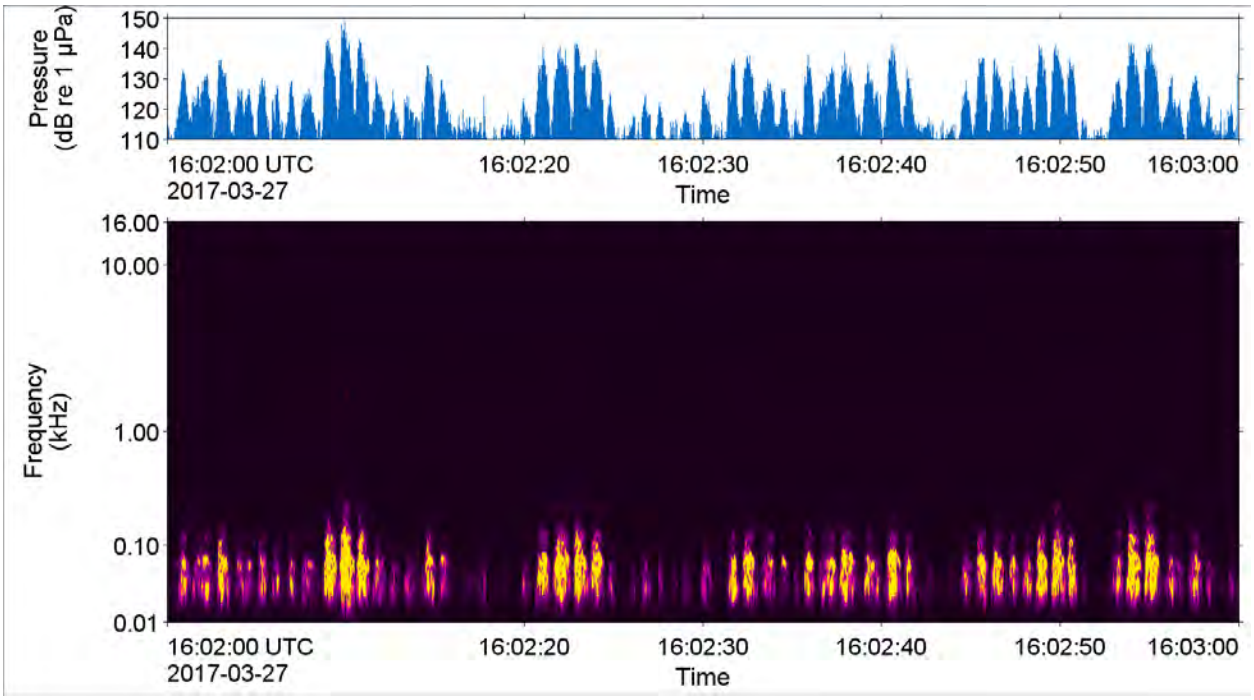

Figure 53. One-minute SPL time-series and spectrogram from icListen drifter 1658 at 16:02 on 27 Mar 2017. Conditions on this day resulted in longer movement noises than were observed on 20 Oct 2016. These data were high pass filtered at 5 Hz.

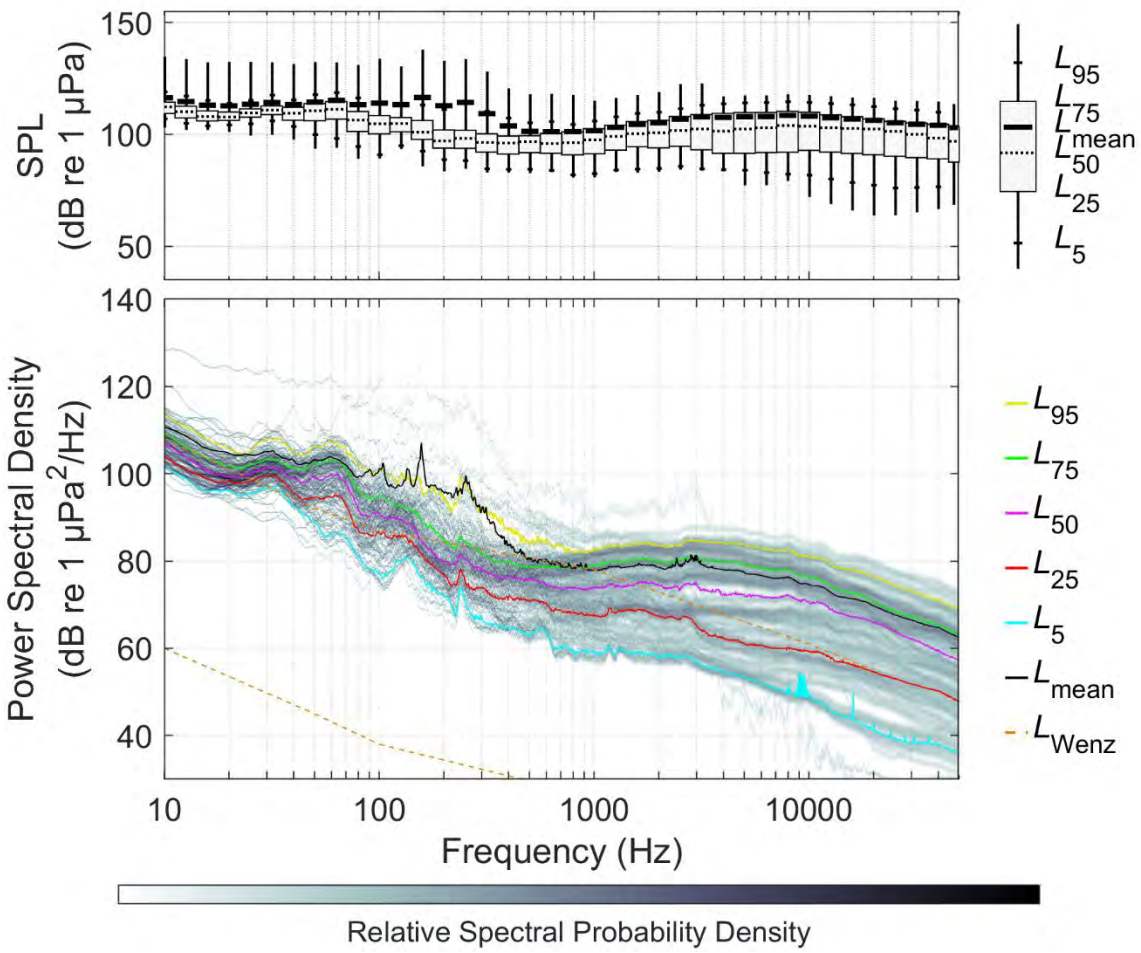

Figure 54. (Top) Exceedance percentiles and mean of the decidecade band SPLs and (bottom) exceedance percentiles and probability density (grayscale) of 1-min PSD levels compared to the limits of prevailing noise (Wenz 1962) for icListen 1658 drifter hydrophone deployed on 27 March. This figure is based on 158 minutes of data across a single flood tidal cycle shown on the right side of Figure 50.

B.4. Comparing Median Spectra

We compared median pressure spectral densities (from Figures 36, 38, 40, 42, and 54) as an indicator of the flow noise recorded at with different monitoring methods (Figure 55). Turbulent flow noise is expected to have a slope of frequency$^{-5/3}$ which is included in the figure for comparison [65, 66].

It is clear from Figure 55 that all recording locations considered are affected by flow noise to varying amounts. For frequencies greater than 60 Hz, the autonomous AMAR data appears to be representative of sounds in the water rather than flow noise. The autonomous, shielded, and bottom mounted location of the autonomous AMAR was 5–20 dB quieter than the hydrophone in the forward-port location, and 10–40 dB quieter than the turbine top location. The drifter was affected by vertical movement noise up to ~150–200 Hz on 27 March (Figure 53), but it had similar sound levels to the AMAR from ~50–1000 Hz. Above 1000 Hz sediment movement noise in the Minas Passage increased measured sound levels compared to the outer Bay of Fundy. The sediment noise may have had higher levels on recordings made above the seabed compared to the autonomous bottom mounted recorder. For quiet long-term recordings, the high flow mooring AMARs appear to be the preferred monitoring solution.

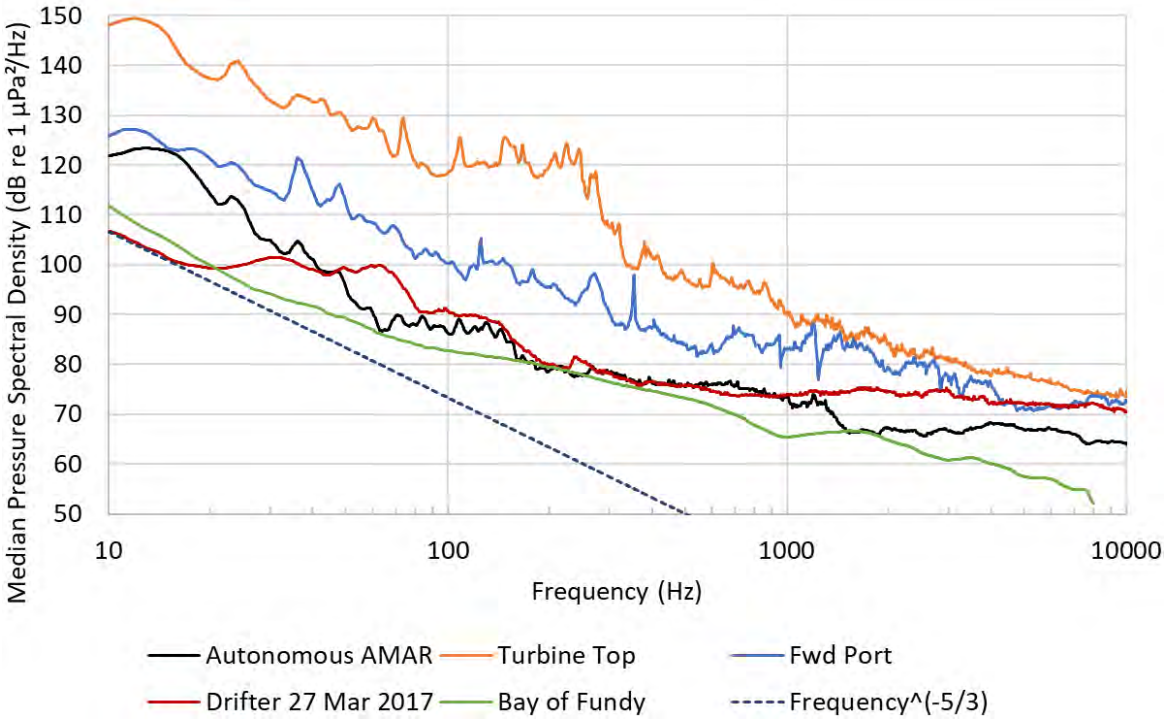

Figure 55. Median pressure spectral densities for three different long-term recording positions, the reference recording from the outer Bay of Fundy as well as the drifter measurements from 27 Mar 2017. Frequency$^{-5/3}$ is the expected slope for turbulent flow noise.

Appendix C. Received Turbine Sound Levels

The sound levels received at autonomous AMAR and the forward-port icListen were analyzed in detail to determine the received sound levels from the Open-Centre Turbine. The objective of the analysis was determining the sound level for each combination of turbine operating and tidal states. The received levels will be converted to source levels that can then be used for predicting the noise footprint of the turbine (Appendix D).

The turbine operating states are not spinning, free spinning and generating. The tidal state is composed of two variables–the tidal direction (ebb and flood) and the current speed (Figure 34). Thus, there were six basic cases–ebb and flood tides for the three tidal states. Two types of analysis to group the data as a function of tidal speed were completed. In the first case the current speed was ignored and only the tidal increment time (e.g., time since high tide, see Appendix A.4) was used to collect similar data (Section Appendix C.1). In the second case the tidal increment time was ignored and only the current speed was used to collect similar data (see Appendix C.2).

C.1. Collecting Data by Tidal Increment

The data were collected by tidal increment (i.e., time since high tide) in two ways–by the median power spectral density for each minute, and by the median decidecade sound pressure level for every fifteen minutes after high tide. The 1-minute power spectral density analysis provides insights into variability of individual frequencies; however, it is more difficult to employ for forward modelling of the range at which the turbine sound exceeds the background levels and thresholds for effects of noise on marine life. The decidecade values for every 15 minutes are more appropriate for forward modelling.

C.1.1. Median Power Spectral Densities by Minute

Table 8 contains six long-term-spectral-average figures where the horizontal axis is time since high tide. The *predicted* high tide times for Parrsboro were used to generate these figures, and they will be updated using the FORCE tidal gauge data in the future. All figures were generated using the same colour-to-PSD mapping. The columns of Table 8 are for the three turbine operating states. The top row of Table 8 are the measurements made at 167 m from the turbine at the autonomous AMAR. The bottom row are the measurements made by the forward-port cabled hydrophone that was 8 m from the turbine rim.

Each figure includes two energy peaks, where the first period is the ebb tide and the second is the flood tide. Times without sufficient data samples are blocked out in red. Important results in these figures are:

1. In all turbine operating states, the flood tides have higher sound levels than the ebb tides
2. The generating state produces sounds in the 1–4 kHz range that are not present in the free-spinning state.
3. The large block of red in the not-spinning data shows that the turbine was always free spinning at high currents (i.e., during flood tides).
4. The blocked-out times near slack tide for the free-spinning and generating cases indicate that the turbine needs approximately 15% normalized current speeds to begin rotating. In the range of 20–300 Hz the turbine produces discrete tonal sounds that are shown as the horizontal bands of energy

5. The turbine produces discrete tones in the frequency range of 20–300 Hz that are shown in the figures as horizontal bands of energy in the forward-port hydrophone recordings. On the autonomous AMAR recordings, the lines are inclined, which is due to multipath interference where the sound arriving directly from the turbine adds constructively and destructively with the sound reflected from the surface. The frequencies with constructive interference create higher energy. Those frequencies depend on the wavelength of the sound and its relationship to the difference in path length for the direct and reflected energy. As the tide goes out, the water depth decreases, and the path length difference becomes shorter. Thus, the interference happens at lower frequencies (deeper water) at high tide than low tide, which makes the inclined lines ‘point’ upwards toward the middle of the figures which is low tide.
6. There is an indication that during the first hour of the ebb tide the turbine sound increases then drops slightly before increasing again, especially when measured by the forward-port hydrophone.

Table 8. Power spectral density versus tidal increment time, turbine state, and recorder. The horizontal axis is time in hours since high tide. Times with less than 30 samples of data are blocked out in red.

	Not spinning	Free spinning	Generating
AMAR Stn 2	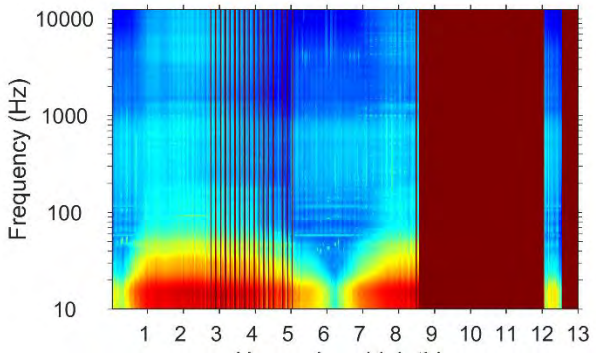	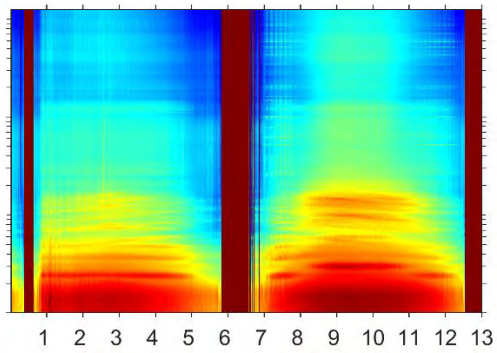	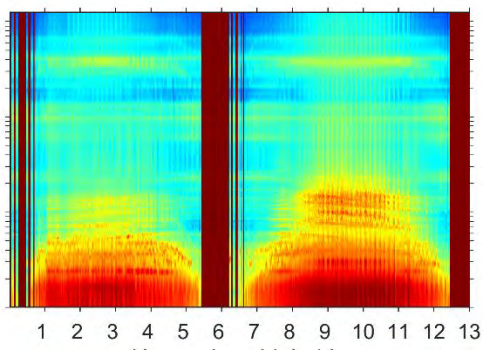
IcListen 1404	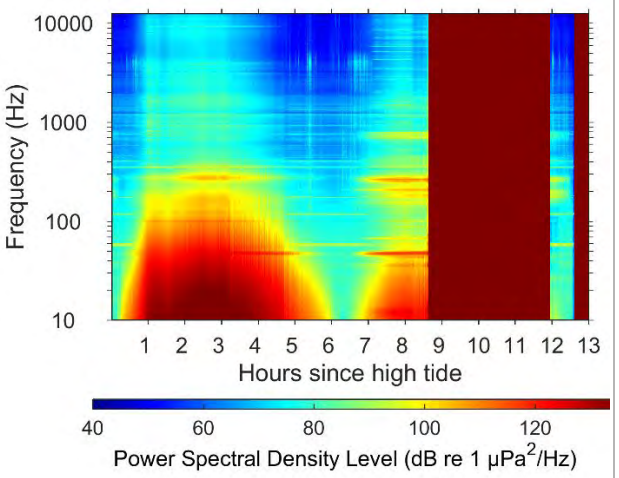	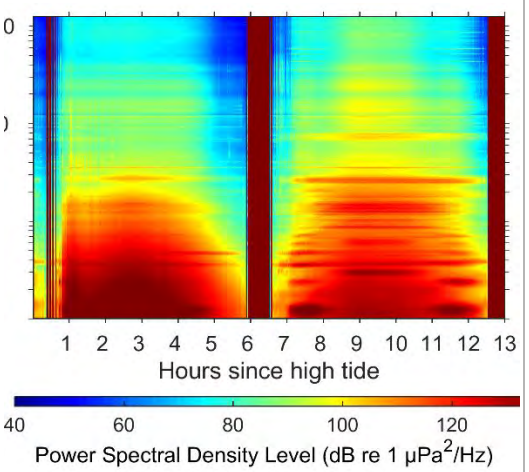	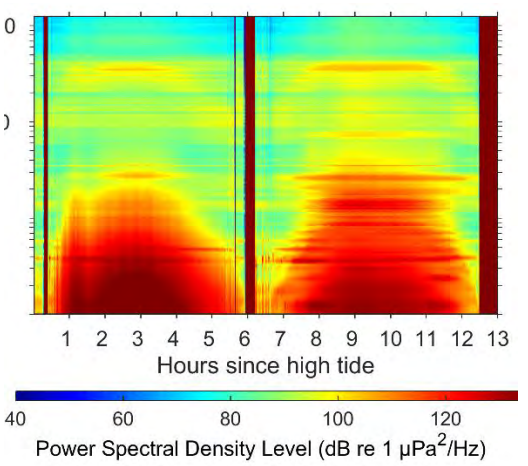

C.1.2. Decidecade Band Levels by 15-minute Increment

The pressure spectral density figures in Appendix C.1.1 have a frequency resolution of 1 Hz, and a time resolution of 1 minute–this is too fine a resolution to be managed for most visualizations and subsequent use in acoustic footprint modelling. Decidecade band levels at a lower time resolution are much easier to manage and visualize. In particular, we want to understand how the three turbine operating states sound levels compare across time, across frequency, and by recording location (the autonomous AMAR and forward-port icListen). For the autonomous AMAR, Figure 56 (ebb tide) and Figure 57 (flood tide) have a panel for each 15-minute time increment, and the horizontal axis for each panel is the decidecade frequency. Figure 58 has a panel for each decidecade and the horizontal axis is time across the full tidal cycle with high tide at the left-hand edge of each panel. Figures 59, 60, and 61 repeat these figures for the forward-port icListen hydrophone. Each panel in all figures has three curves corresponding to the different turbine operating states.

Important results from these figures are:

1. For the autonomous AMAR recordings (Figures 56–58), the sound generated by the turbine is distinct from the ambient noise for decidecades of at least 40 Hz and above. The turbine sound is most pronounced in the bands of 63–250 Hz for both free spinning and generating states, and in the band 100–1250 Hz and 3150–4000 Hz for generating only.
2. At the turbine mounted hydrophone, the low-frequency sound (63–250 Hz) does not separate from the flow noise. The higher-frequency sound is well separated from the background noise levels in the frequency band of 1000–6300 Hz but is most prominent in 1000–1250 Hz and 3150–4000 Hz bands.
3. The 63–250 Hz sound increases over a 40-dB range as a function of current speed, whereas the 1000–1250 Hz sound has a nearly constant sound level. The 3150–4000 Hz sound levels vary over a 10-dB range as function of current speed.
4. For all frequency bands, the data recorded on the bottom mounted hydrophone has higher sound levels during flood tide than during ebb. During the ebb tide the turbine mounted hydrophone has higher sound levels for frequencies of 63 Hz and below than during the flood tide. We propose that this is due to additional turbulence in the water mass as it exits the turbine and interacts with the hydrophone (see Figure 27 for hydrophone placement). This reversal of the low-frequency energy pattern can also be seen in Table 8.

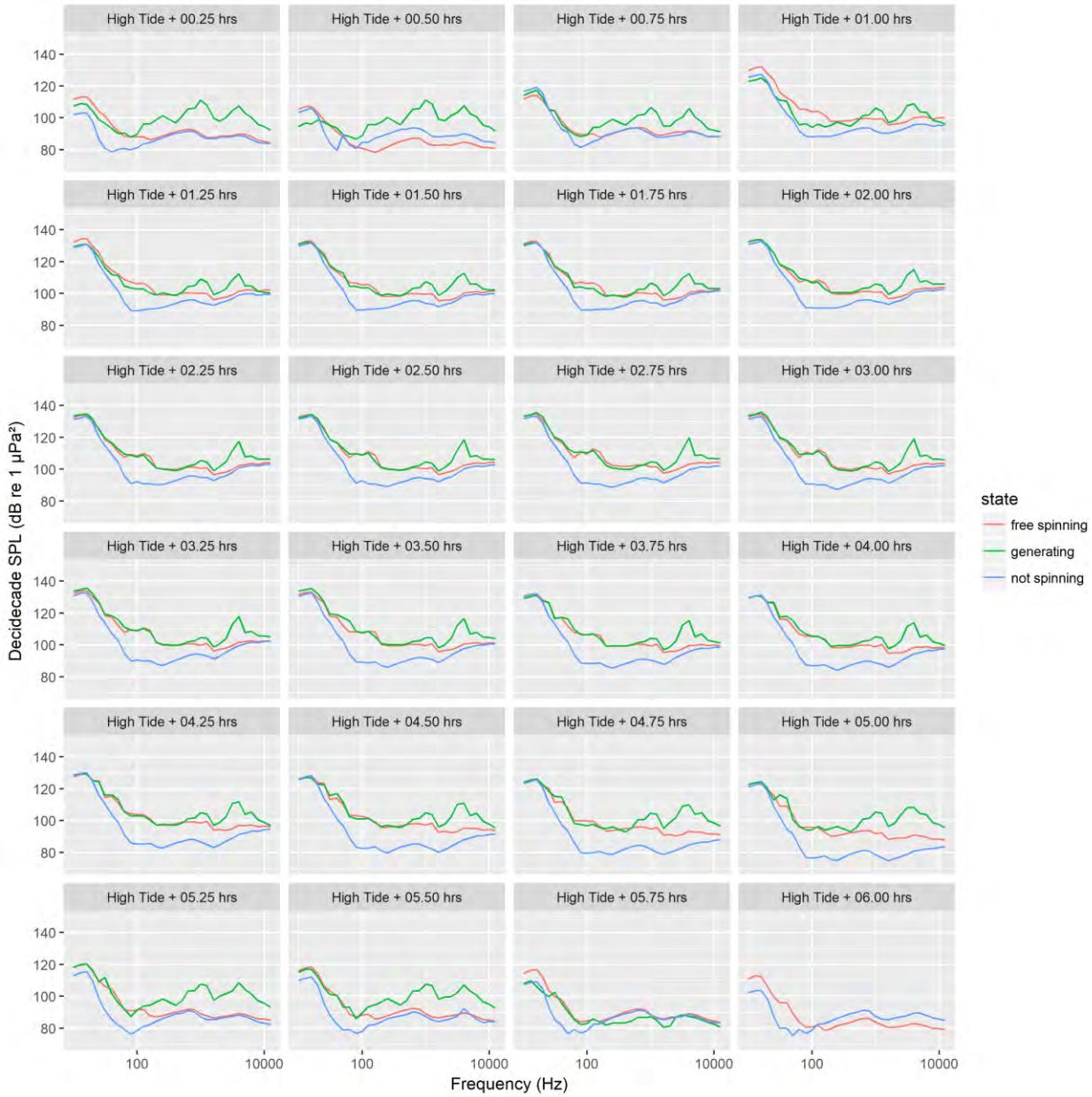

Figure 56. Median decidecade band SPL for each 15-minute time increment during ebb tide using data from the autonomous AMAR. The turbine state is shown by the curve colours.

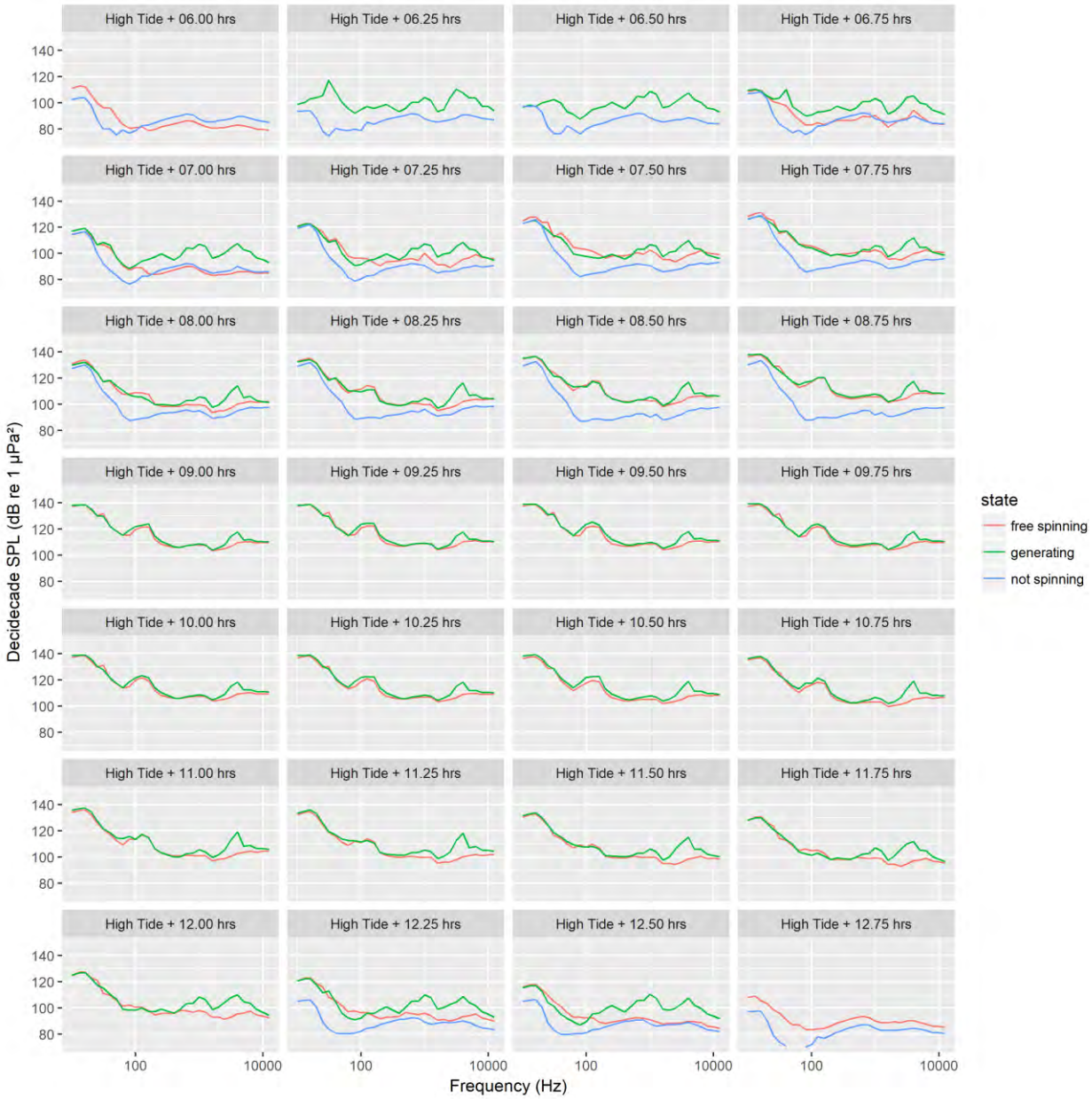

Figure 57. Median decidecade band SPL for each 15-minute time increment during flood tide using data from the autonomous AMAR. The turbine state is shown by the curve colours.

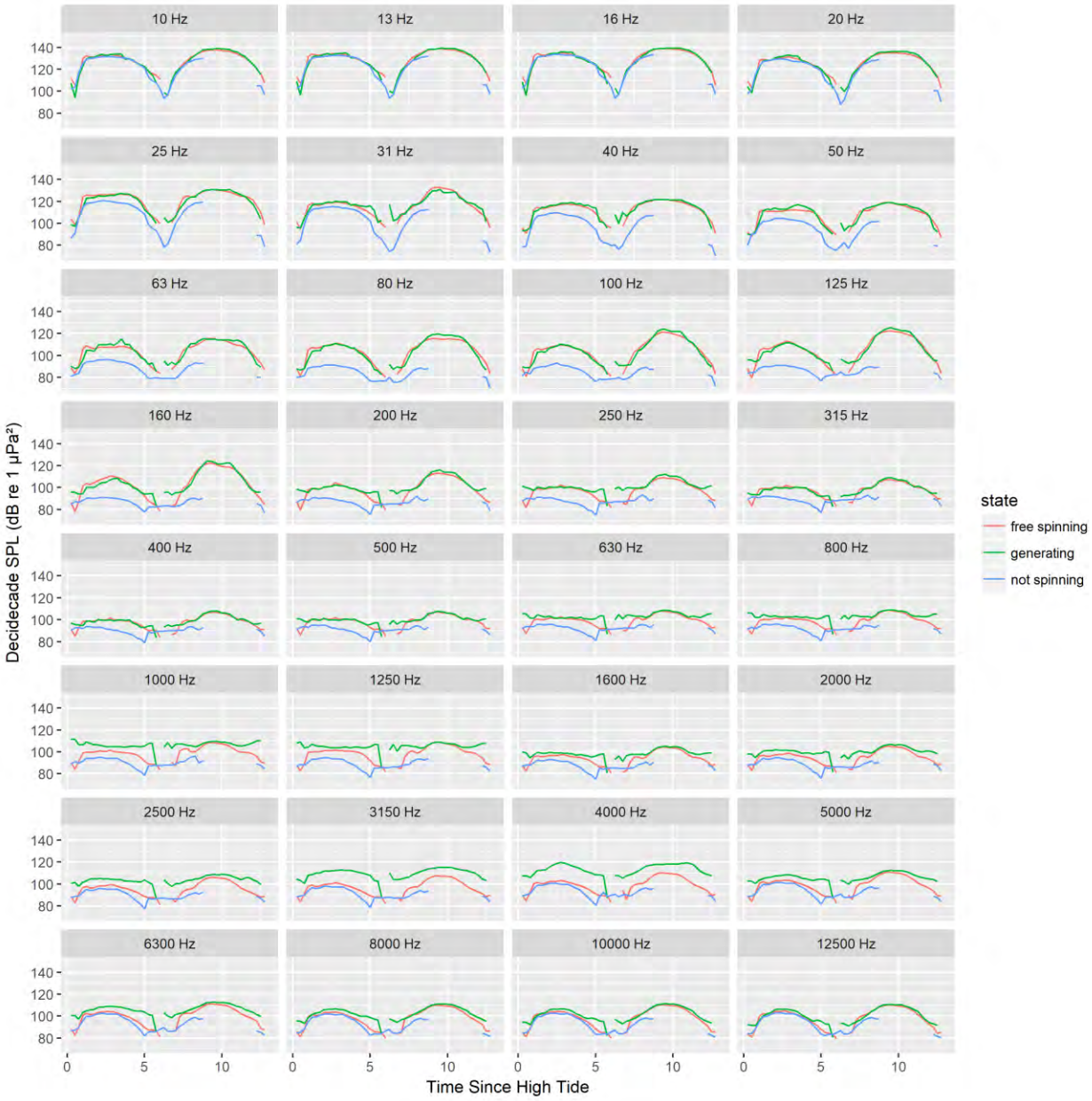

Figure 58. Median decidecade band SPL for each decidecade using data from the autonomous AMAR. The turbine state is shown by the curve colours.

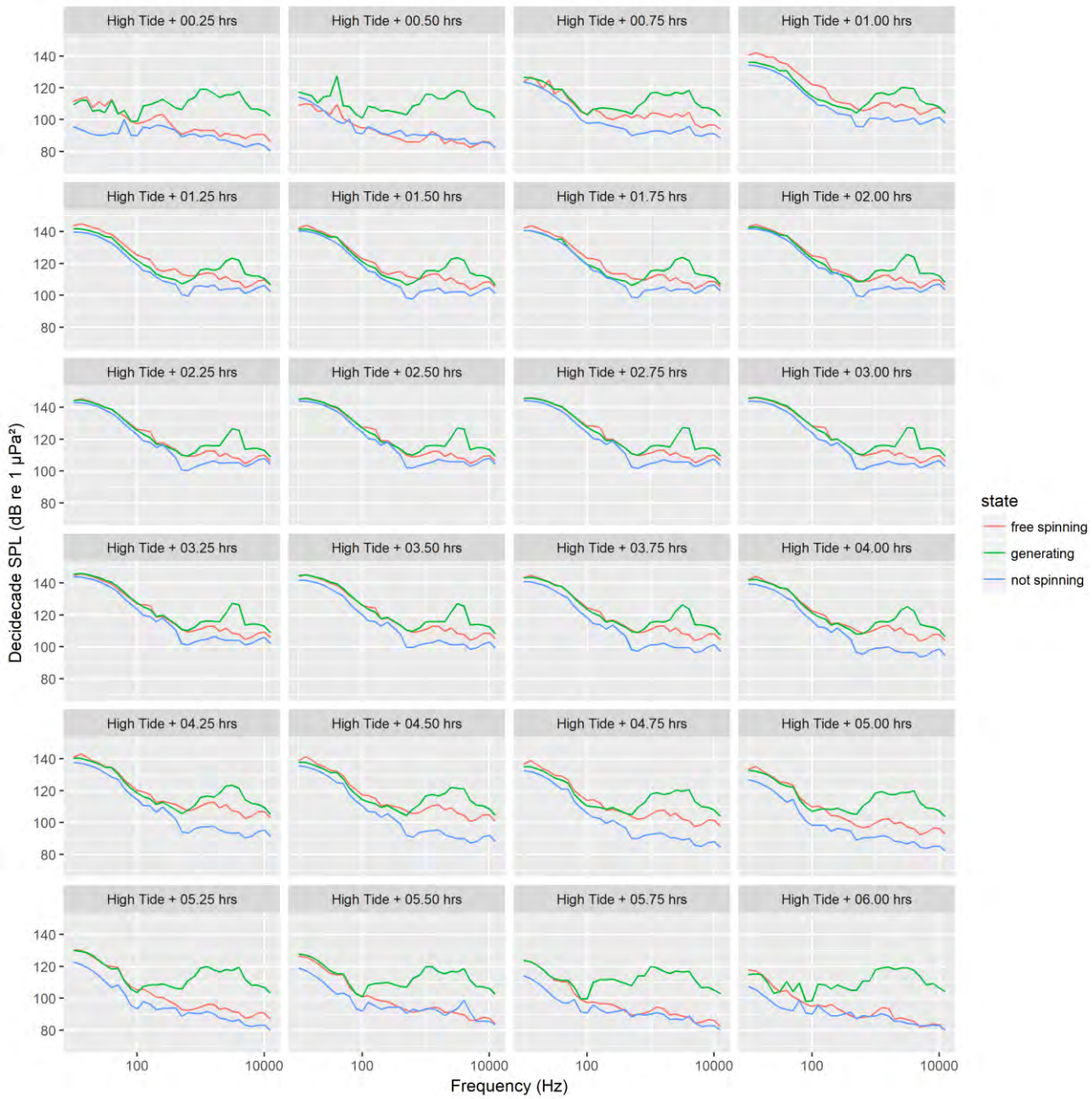

Figure 59. Median decidecade band SPL for each 15-minute time increment during ebb tide using data from the forward-port icListen hydrophone. The turbine state is shown by the curve colours.

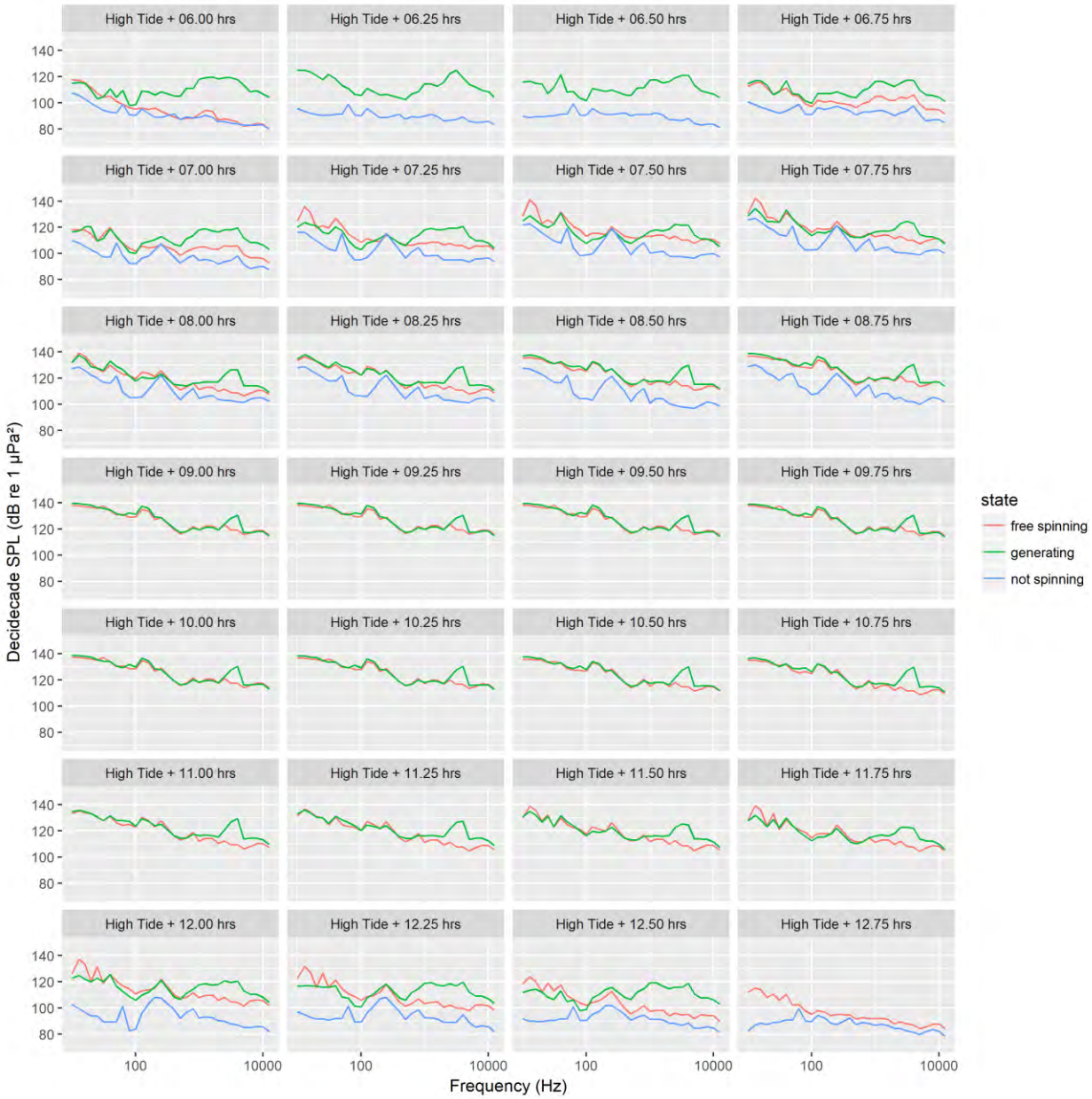

Figure 60. Median decidecade band SPL for each 15-minute time increment during flood tide using data from the forward-port icListen hydrophone. The turbine state is shown by the curve colours.

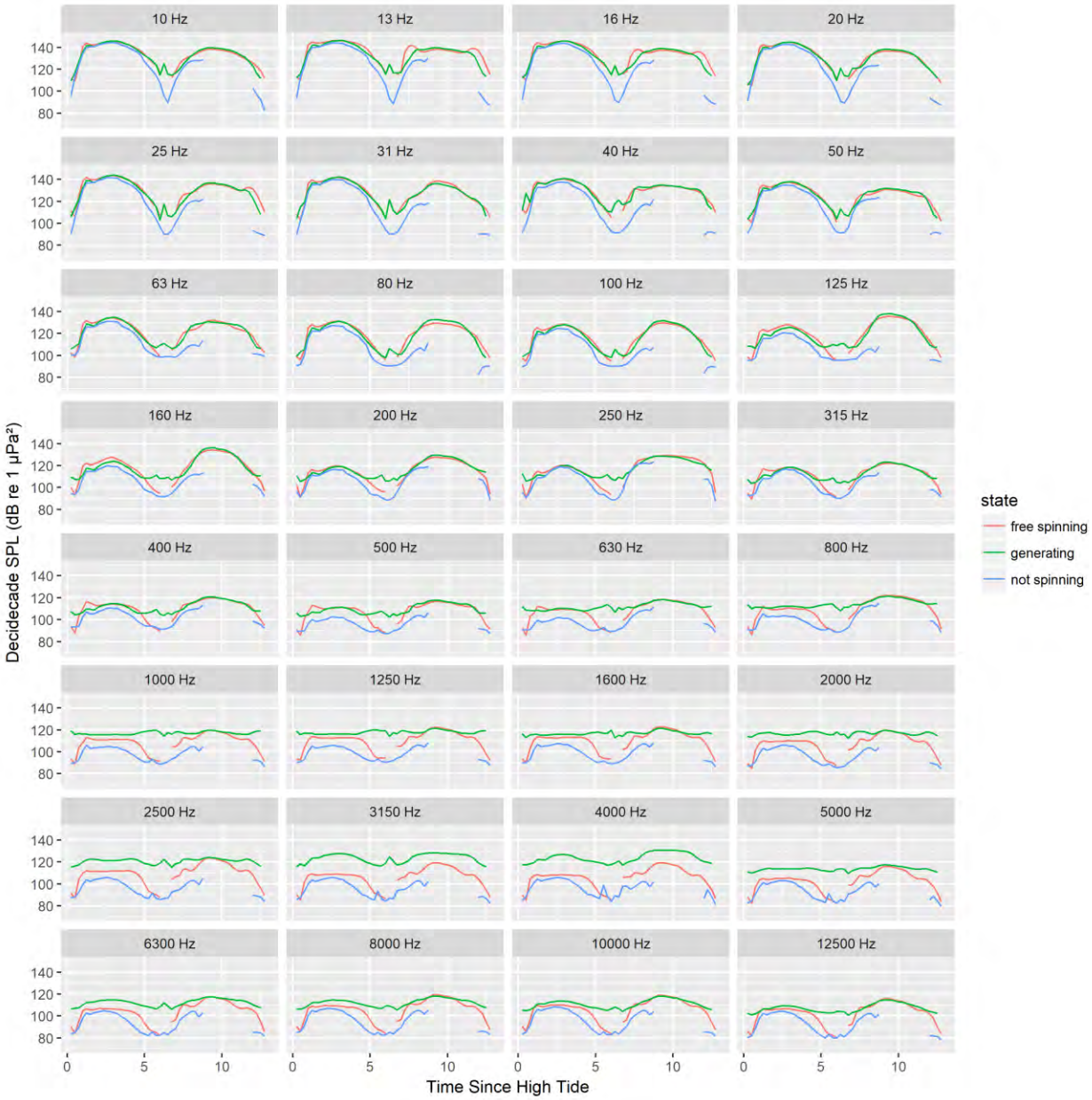

Figure 61. Median decidecade band SPL for each decidecade using data from the forward-port icListen hydrophone. The turbine state is shown by the curve colours.

C.2. General Additive Models of Decidecade Sound Pressure Levels

C.2.1. Model Development

The results from Appendix C.1 showed that the sound levels from the environment (flow noise and sediment interaction noise) and from the turbine depend on current speeds. However, the current speeds are highly variable in time both within the lunar cycle and across lunar cycles (see Figure 34). Therefore, an analysis based on the current speed rather than tidal time increment has the potential to provide more accurate representations of the sound levels.

As described in Appendix A.5, Generalized Additive Models (GAMs) of the 1-minute decidecade band sound pressure levels vs current speed were created for each combination of tide direction (ebb, flow) and each turbine operating state (not spinning, free spinning, generating). Typical result are shown in Figures 62–64 which provide an overview of the sound levels received at the autonomous AMAR. The red curves through the data are the general additive models. The reasons for choosing the GAMs vs a linear model are evident from the results–the not spinning sound pressure level appear to increase linearly with current speed, however the free spinning and generating sound levels do not. The black dots in Figures 62–64 are the measured data; the relative density in the measured data clouds indicate that for 18 Nov 2016 to 19 Jan 2017 the turbine was free-spinning much more that it was generating.

The differences in behaviour of the sound pressure levels as a function of frequency that were observed in the time increment analysis are also evident in the current speed analysis. For example, at 160 Hz (Figure 62) the flood generating sound levels increase over a 30-dB range, are nearly flat at 1000 Hz (Figure 63), and increase over a 10 dB range at 4000 Hz (Figure 64).

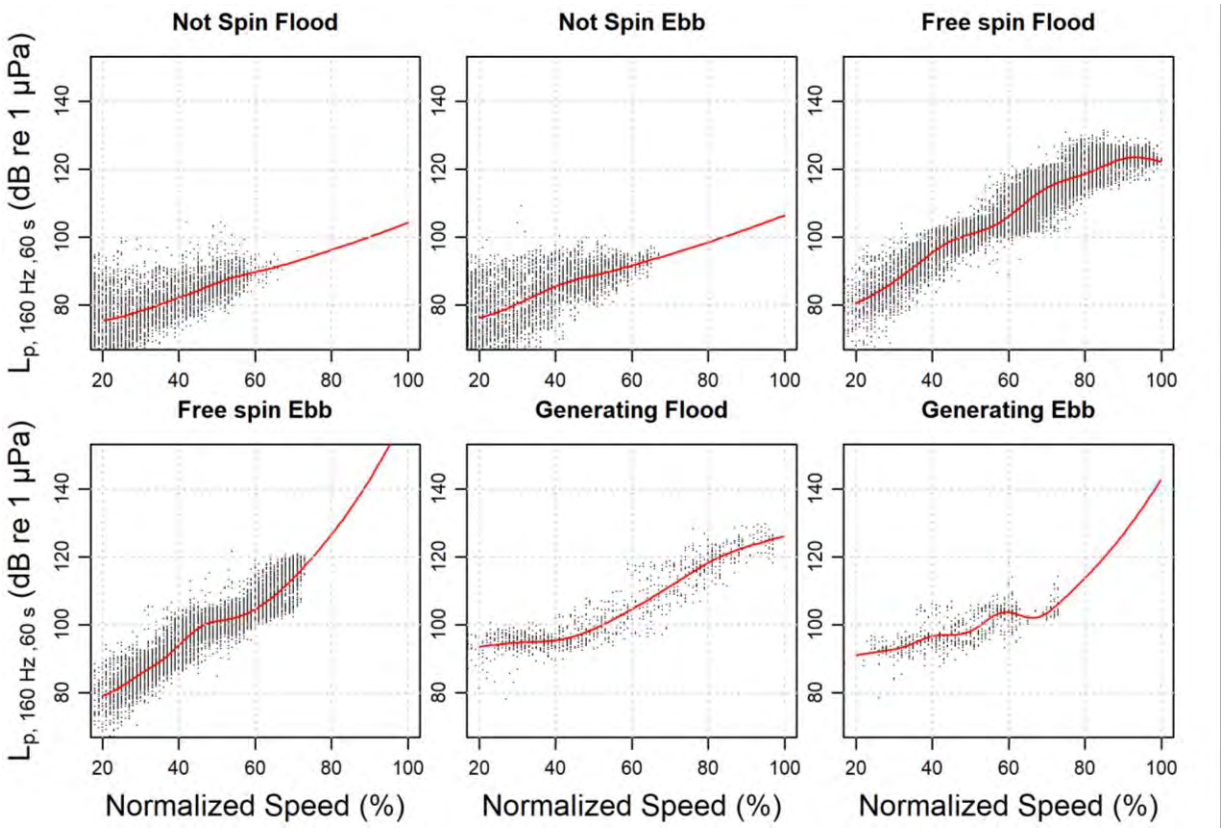

Figure 62. Received 160 Hz decidecade band sound pressure levels from the autonomous AMAR (18 Nov 2016 to 19 Jan 2017) plotted versus normalized current speed for each tide-turbine state. Red lines are the general additive model SPL ~ s(normalizedCurrentSpeed).

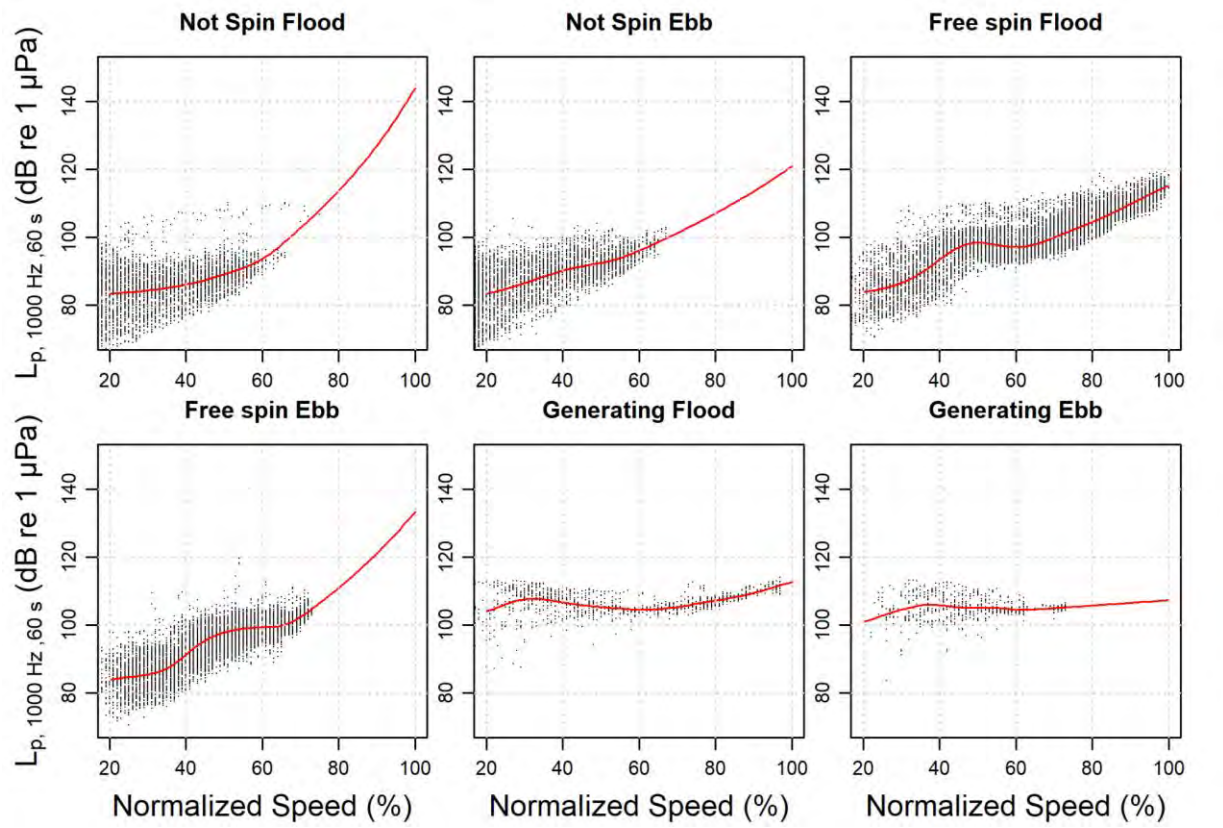

Figure 63. Received 1000 Hz decidecade band sound pressure levels from the autonomous AMAR (18 Nov 2016 to 19 Jan 2017) plotted versus normalized current speed for each tide-turbine state. Red lines are the general additive model SPL ~ s(normalizedCurrentSpeed).

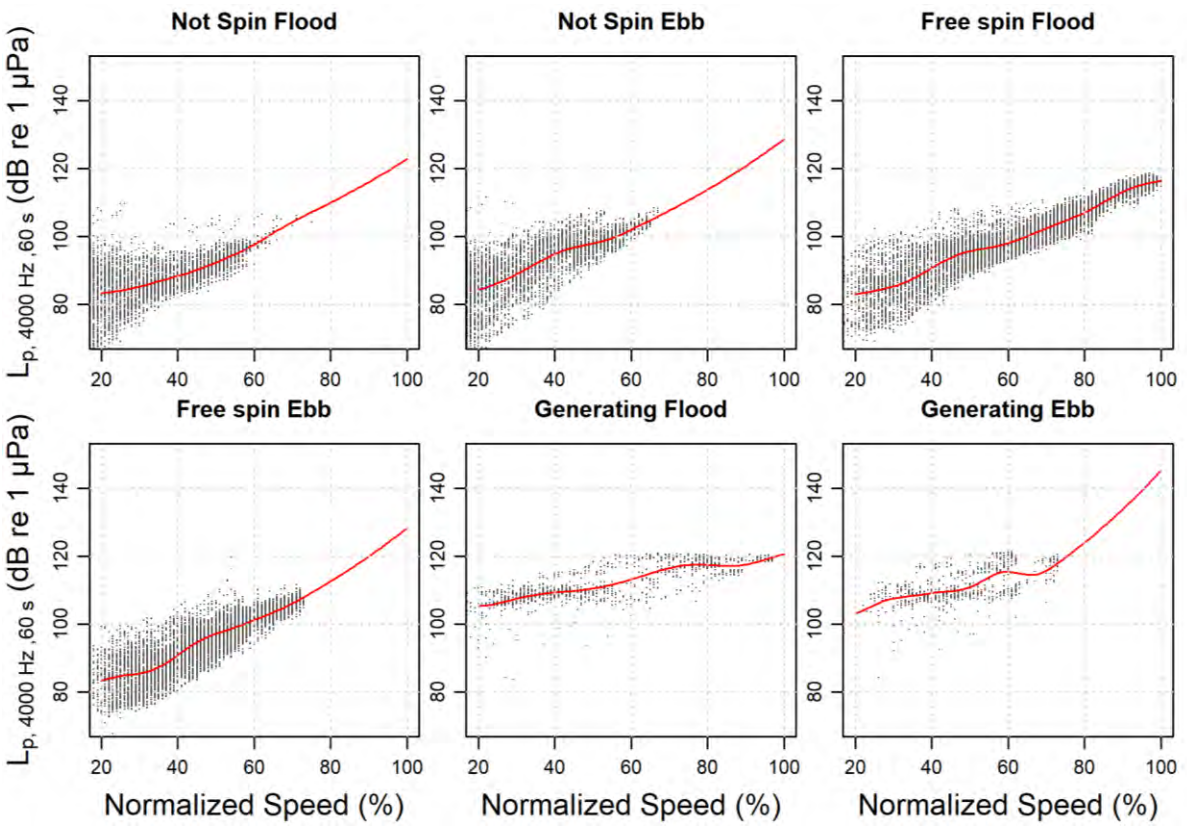

Figure 64. Received 4000 Hz decidecade band sound pressure levels from the autonomous AMAR (18 Nov 2016 to 19 Jan 2017) plotted versus normalized current speed for each tide-turbine state. Red lines are the general additive model SPL ~ s(normalizedCurrentSpeed).

C.2.2. Assessing Model Accuracy

Two approaches were used to assess the received sound pressure level model accuracy: 1) plotting the distributions of model-measured sound pressure level errors and 2) plotting an example of the modelled and measured sound levels for three sample tidal cycles described in Section B.1.

C.2.2.1. Model-Measure sound pressure level Errors

The GAMs were used to predict the received sound pressure level for each turbine state, decidecade band and percent normalized flow (1 to 99). For each minute of data from the autonomous AMAR the predicted sound pressure level was extracted from this table. The measured sound pressure level was subtracted from the modelled sound pressure level to compute the error. Boxplots of these error distributions were then generated for three sound pressure levels:

1. 63 Hz and above (Figure 65), which is the sum of the 63–12500 Hz decidecade bands; 63 Hz was chosen as the lower cut-off for the frequency band containing turbine sounds well above the background sound level (See Appendices B.2 and C.1).
2. High-frequency cetacean Weighted (HFC, Figure 66): the sum of the decidecade bands from 10–16000 Hz weighted by the HFC auditory filter which is relevant for the ability of porpoise to hear the turbine (see Section 2.2 and [28])
3. The sound pressure level weighted by the inverted herring audiogram (Figure 67), which represented the sound levels herring, gaspereau, and shad are likely to hear.

The error figures for each of the measurements show median errors of ~5 dB when the turbine is not spinning for normalized flows rates below 20%. This makes sense because other factors, such as wind, waves and vessel presence contribute to the sound levels when the currents are low and the model does not account for these factors. For the free-spinning and generating states, the modelled sound pressure levels are within 1–2 dB of the median measurements for normalized flow speeds above ~15%, which is 90% of the tidal cycle (based on the data provided by Emera, see Appendix B.1). The figures also indicate that there is very little free spinning or generating data for normalized flow speeds below 15%, as expected. From these results we conclude that the models may be used to estimate the turbine sound levels and the ambient sound levels for normalized flow rates above 20%.

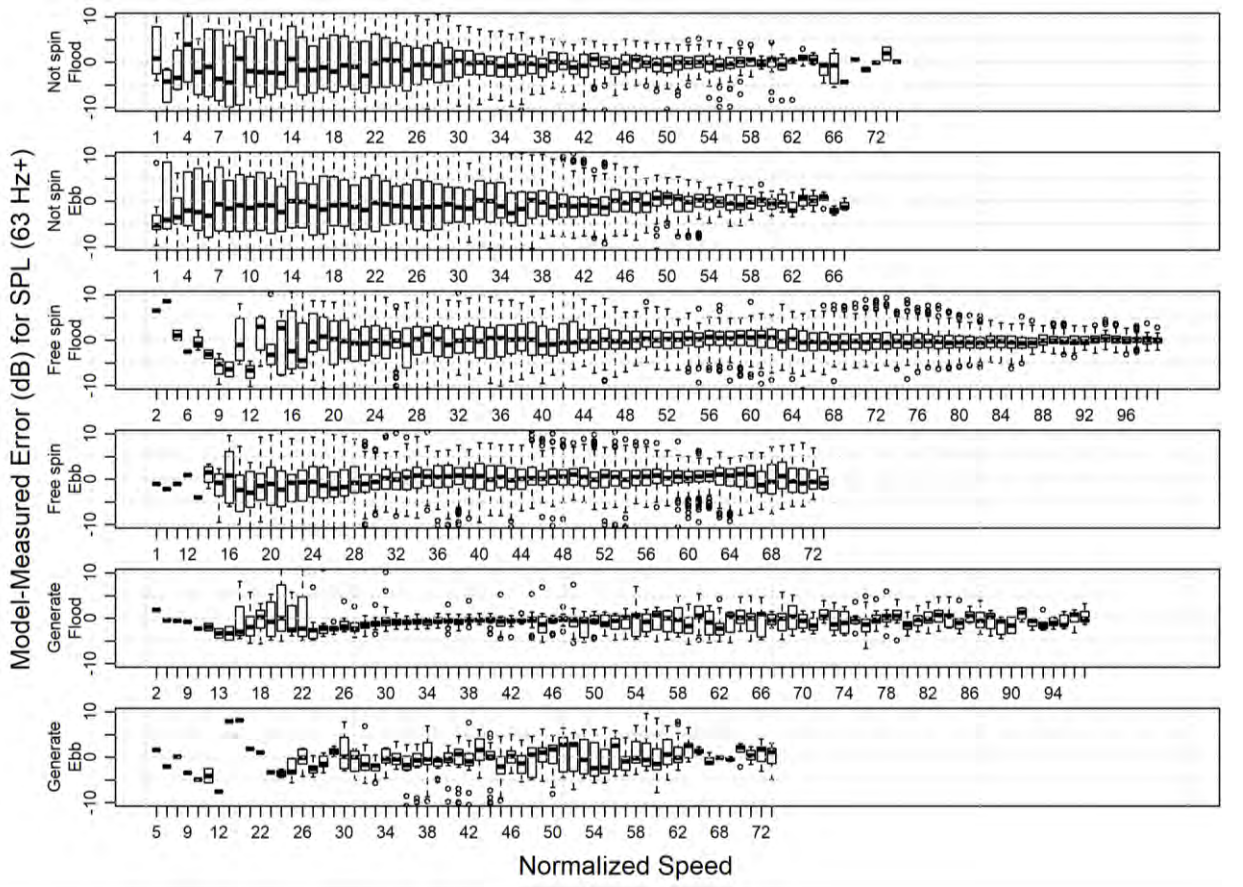

Figure 65. Difference between modelled sound pressure levels from 63–12500 Hz and all the per-minute data measured on the autonomous AMAR for each tide-turbine state combination.

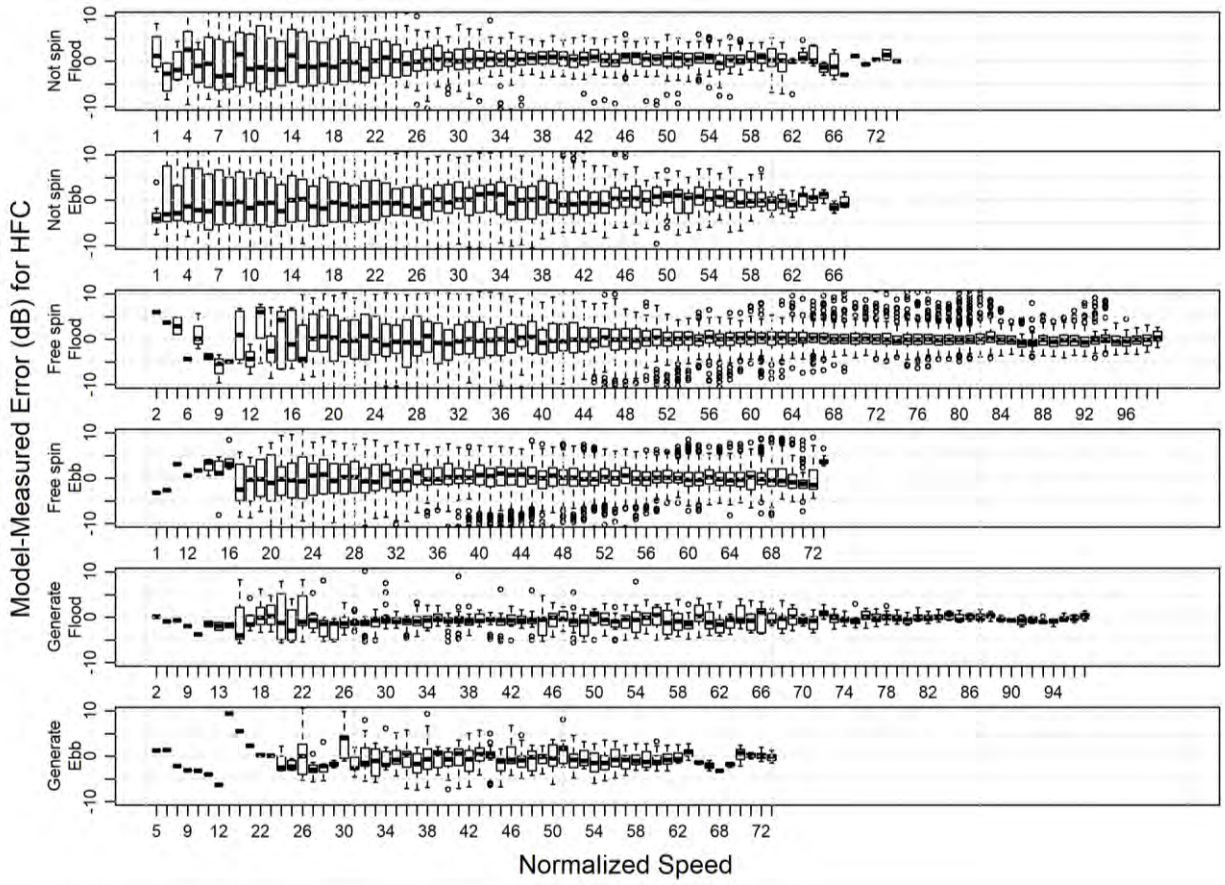

Figure 66. Difference between modelled high-frequency cetacean weighted sound pressure levels and all the per-minute data measured on the autonomous AMAR for each tide-turbine state combination.

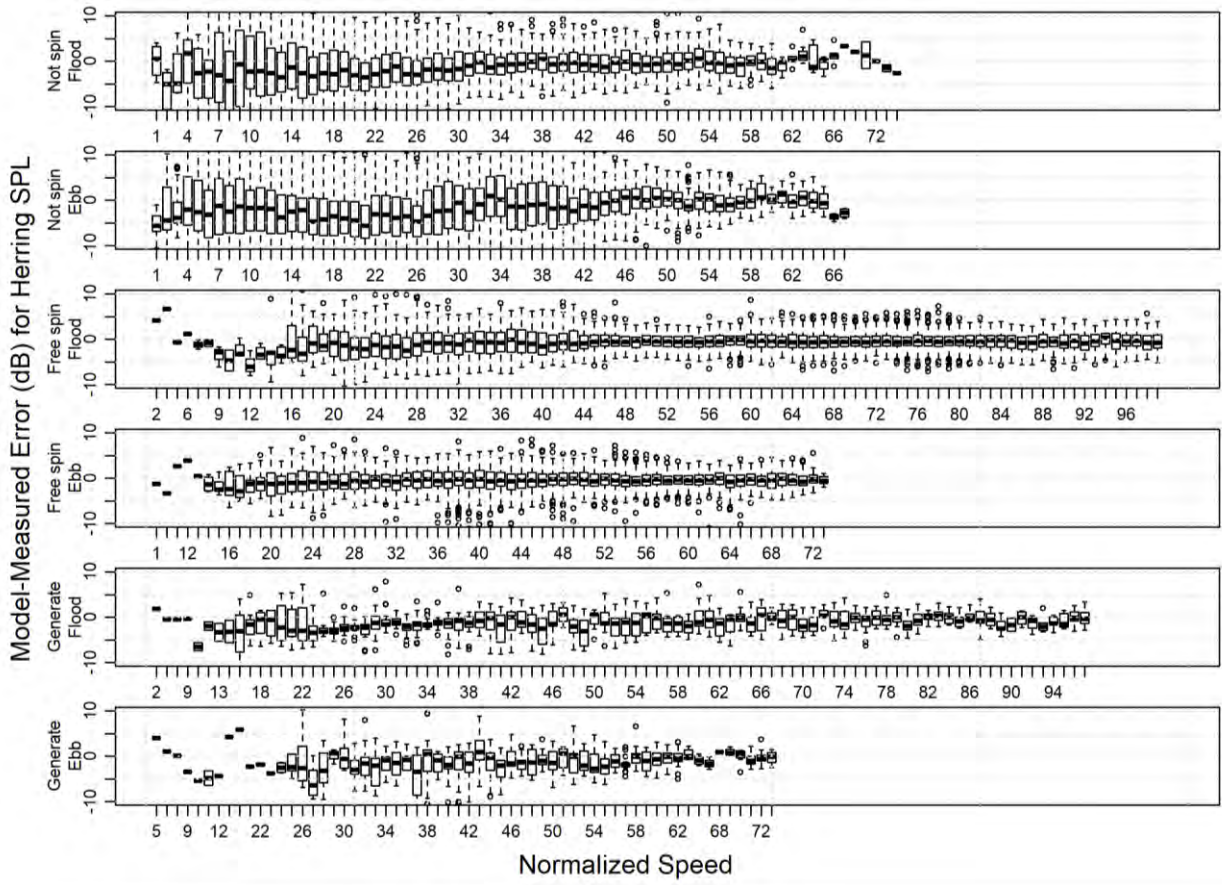

Figure 67. Difference between modelled sound pressure levels from 10–12500 Hz and all the per-minute data measured on the autonomous AMAR for each tide-turbine state combination

C.2.2.2. Representative Model-Measure Data

This section provides representative examples of the measured per-minute sound pressure levels and the predicted levels for three tidal cycles, selected to represent neap (Figure 68), normal (Figure 69), and spring (Figure 70) tides (see Appendix B.1). As shown by the boxplots in Appendix C.2.2.1, the agreements are very good for periods with higher flow speeds but less accurate around slack tide.

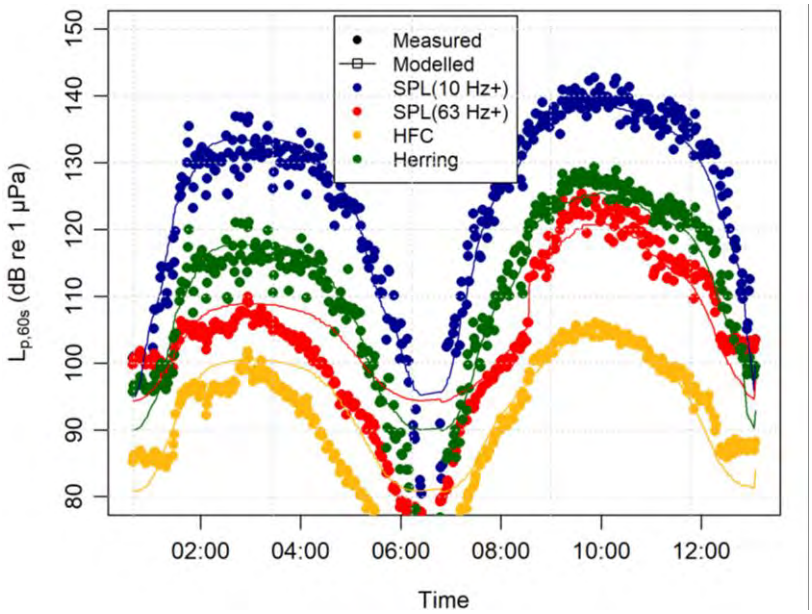

Figure 68. Neap tides on 24 Dec 2016: Comparing the modelled sound pressure levels (lines) and measured sound pressure levels (points). High tide shown on the left side.

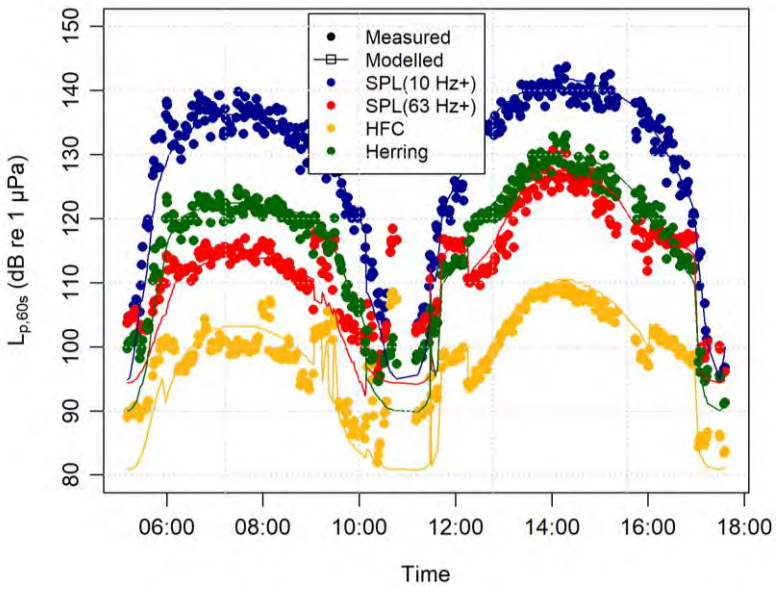

Figure 69. 'Normal' tides on 16 Dec 2016: Comparing the modelled sound pressure levels (lines) and measured sound pressure levels (points). High tide shown on the left side.

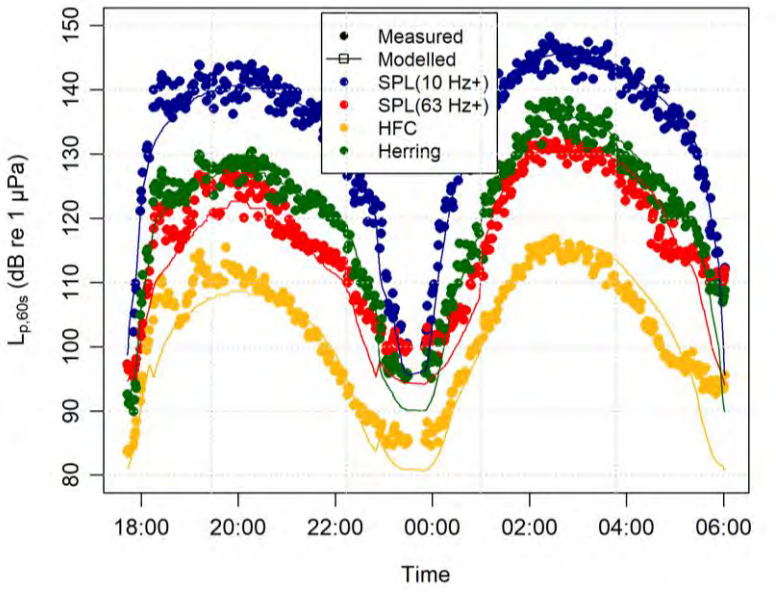

Figure 70. Spring tides on 30 Nov–1 Dec 2016: Comparing the modelled sound pressure levels (lines) and measured sound pressure levels (points). High tide shown on the left side.

C.2.3. Modelled Sound Pressure Levels

The models were used to predict the median sound pressure levels for each decidecade band for normalized current speeds of 20, 40, 60, and 80%, which were then plotted for all six tide-turbine state combinations (Figures 71 and 72). The sound pressure levels are plotted in the top row of each figure, and as a difference from the sound pressure levels measured under the traffic lanes of the outer Bay of Fundy (see Appendix B.2.1) in the bottom rows.

The important results derived from these figures are:

1. The sound levels in all three turbine states does not depend strongly on the current direction, only on the current speed.
2. The free spinning state is 5–25 dB quieter than the generating state, especially at low current speeds.
3. The ambient conditions in the Minas Passage at frequencies below 1 kHz are up to 25 dB quieter than the sound levels in the outer Bay of Fundy underneath the shipping lanes.
4. The 1000–1250 Hz sound produced by the turbine while generating shows a nearly constant sound level, a result similar to what was found from the tidal time increment analysis. The 3150–4000 Hz sound levels increases with current speed.
5. At normalized currents of 80% the sound levels are 10–30 dB above the levels recorded in the outer Bay of Fundy.
6. The differences in sound levels on the icListen hydrophone that depend on current direction (i.e., sound levels are higher during ebb tide at low frequencies) applies to the not spinning case, as well as the spinning cases. This suggests that the turbine is adding turbulence to the water column.
7. The icListen hydrophone on the turbine platform has energy at electrical power generation frequencies that are not present on the AMAR (e.g., 60, 120, and 300 Hz). The relative amplitude of the signals at these frequencies appears to change with flow speeds.
8. The turbine sound levels received at the icListen are higher than those on the autonomous AMAR, which makes sense since the icListen is much closer to the turbine.

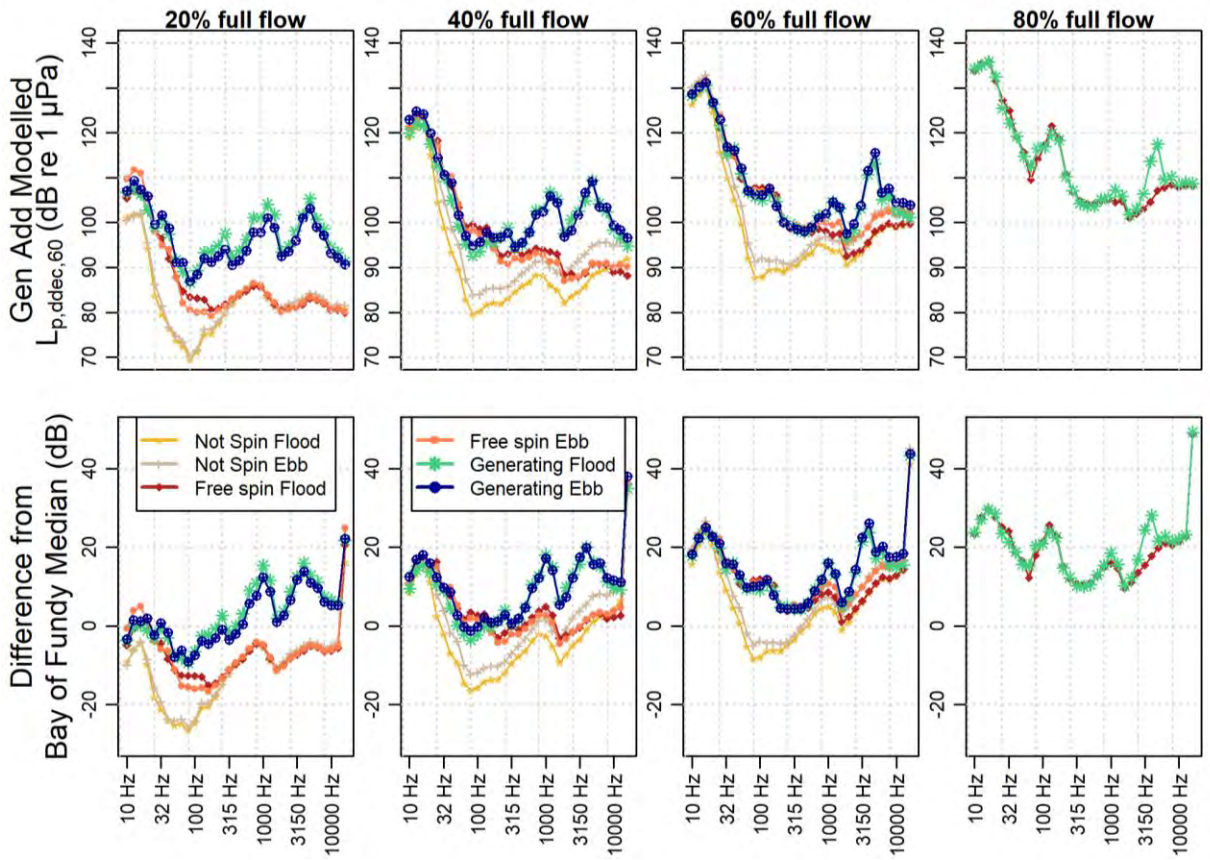

Figure 71. General additive modelled decidecade sound pressure levels received at the autonomous AMAR for normalized current speeds of 20, 40, 60, and 80% of full flow. (Top row) the modelled sound pressure levels. (Bottom row) the difference between the median decidecade sound pressure level measured under the shipping lanes in the Bay of Fundy and the conditions measured in the Minas Passage.

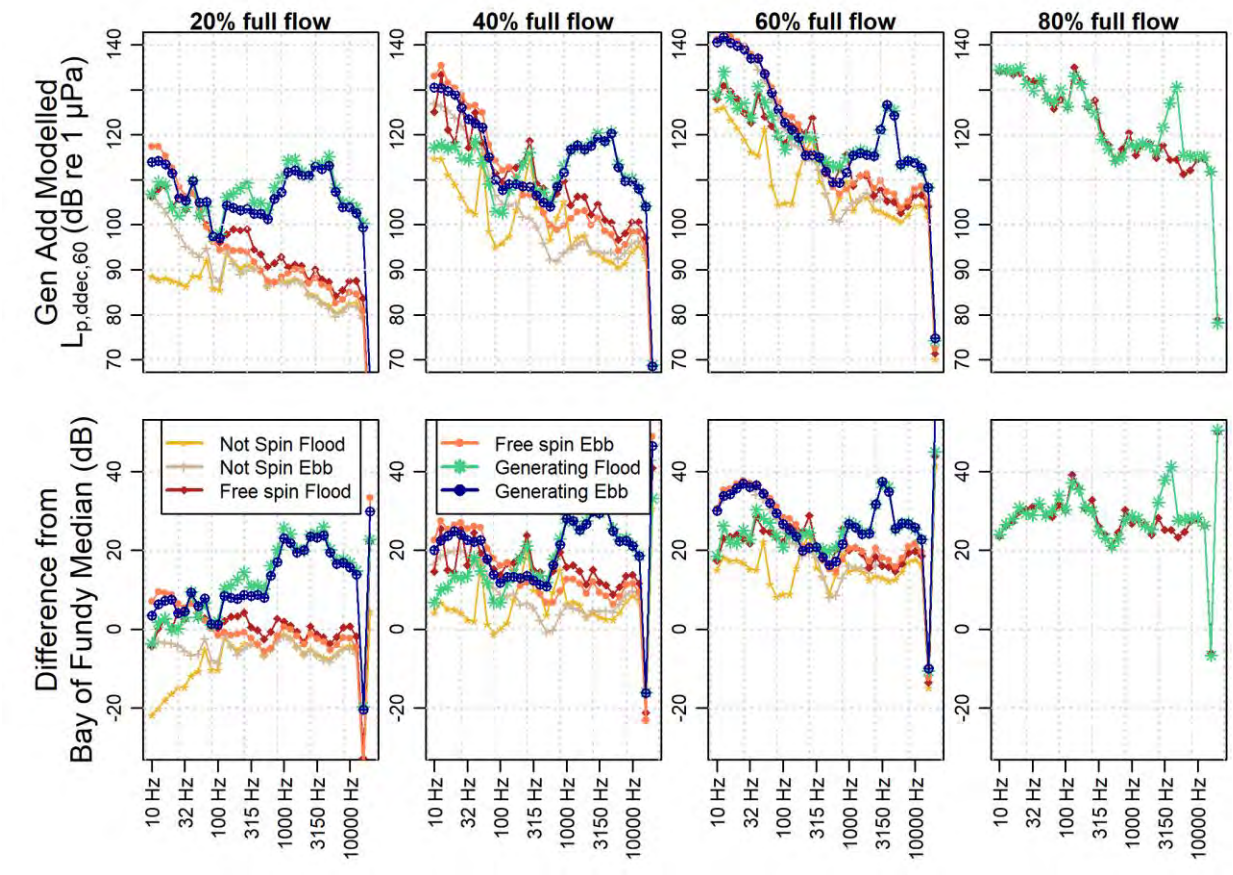

Figure 72. General additive modelled decidecade sound pressure levels received the forward-port hydrophone location for normalized current speeds of 20, 40, 60, and 80% of full flow. (Top row) the modelled sound pressure levels. (Bottom row) the difference between the median decidecade sound pressure level measured under the shipping lanes in the Bay of Fundy and the conditions measured in the Minas Passage.

Appendix D. Open-Centre Turbine Source Levels

A highly desirable outcome of this analysis is a turbine source level model that may be used to estimate the radius around the turbine where the turbine could affect marine life, as well as where the sound exceeds the background sound levels. The GAM received level models developed in Appendix C.2 were converted to source level models by adding $20\log_{10}$(range), where the range from the turbine to the autonomous AMAR was 167 m.

D.1. Model Evaluation

To evaluate whether the model is accurate, the icListen 1658 drifter pass on Trial 7 of 27 Mar 2017 was analyzed. This data had previously been analyzed by GTI (see Appendix A.6) which indicated that the drifter likely passed within 30 m of the turbine. Given that this measurement was made near high tide, this range means that the drifter passed directly over the turbine. To assess the model the track of the drifter was linearly interpolated between the known start and end points, which predicted a closest point of approach to the turbine of 30 m–in agreement with the GTI model. The 1-second sound pressure levels were computed and plotted as function of estimated range to the turbine (Figure 73). During those drift measurements the turbine was free-spinning in a flood tide. The modelled sound levels were computed from the sum of the not-spinning and free-spinning flood tide median sound pressure levels estimated for the known current speed for each minute. The free spinning source levels were used, minus $20\log_{10}$(range). Only the 63–400 Hz decidecades were summed which is the overlap of the frequencies where turbine is well separated from the environmental noise while free spinning.

In summary, Figure 73 indicates that the modelled sound level for the turbine and environmental noise closely tracked the sound levels measured by a drifter. This is a remarkable success given the uncertainties in the analysis:

- The models were developed using a bottom mounted recorder, but the measurements were made with a drifter.
- The range from the AMAR to the turbine is likely only accurate to ±20 m;
- The track of the drifter was highly uncertain because we only had the start and end points of the track; and
- The drifter recorded significant surface/movement noise.

The measured data in Figure 73 contains two peaks, one ~100 m before the turbine CPA and one ~250 m after CPA. These are due to multipath interference between the direct path and surface reflected path (Lloyd's mirror effect), as well as changes in the turbine sound emissions (see Figure 74).

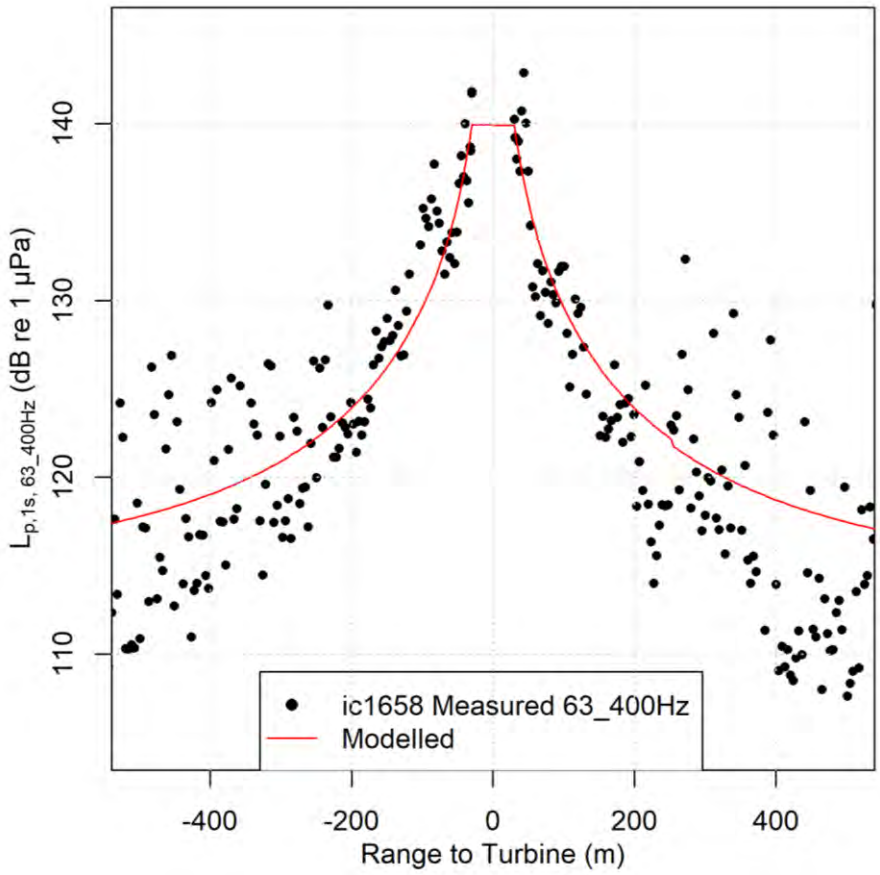

Figure 73. Received and modelled sound pressure levels for Trial 7 of icListen drifter 1658 on 27 Mar 2017.

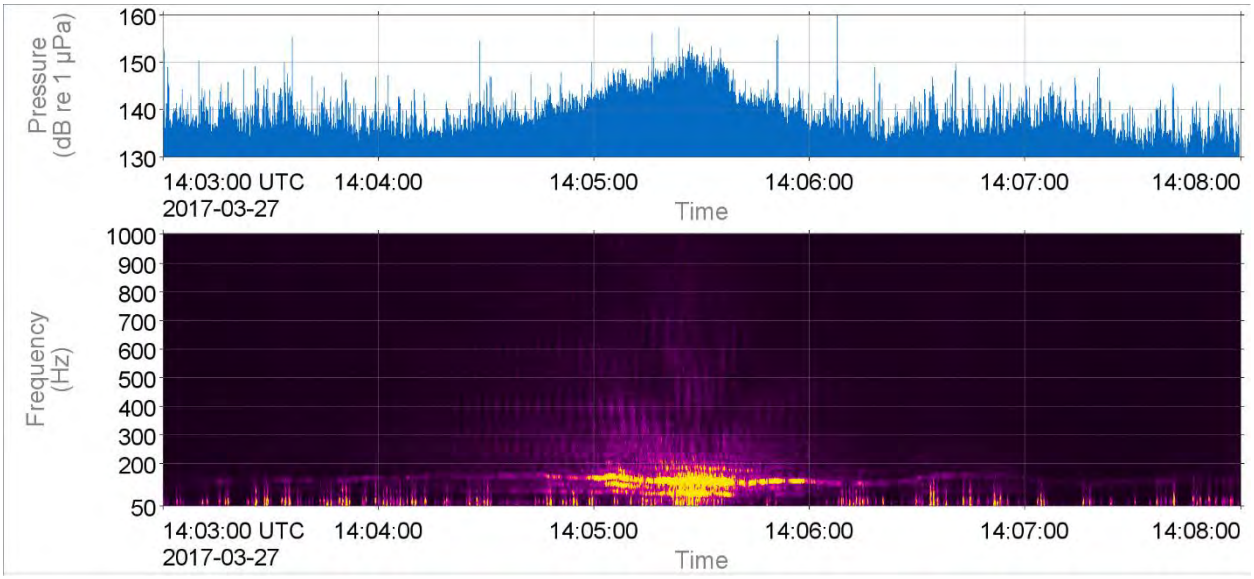

Figure 74. Five minutes of data centred on the closest point of approach of the ic1658 drifter to the turbine during trial 7 on 27 Mar 2017. The banding pattern in the data is due to multipath interference and is often called the Lloyd's mirror effect.

The comparison with the drifter demonstrates the reliability of the model when used within it's bounds. For the free-spinning case the valid frequency range are the 63–400 Hz decidecade bands. For the generating case, the range is the 63–10000 Hz decidecade bands. To understand the amplitude of the turbine source levels, we have compared it to a typical fishing vessel at 10 knots and a typical tugboat at 10 knots (Figure 75) [67]. Below 4 kHz the turbine has a much lower source level than the vessels. In the generating case the 4000 Hz decidecade has a similar source level as the typical vessel. Since the maximum source level of the turbine is ~165 dB re 1 µPa² and the vessels are ~180 dB re 1 µPa² at low frequencies we can expect that fish will detect and be affected by vessels at 7–10 times the range as the turbine.

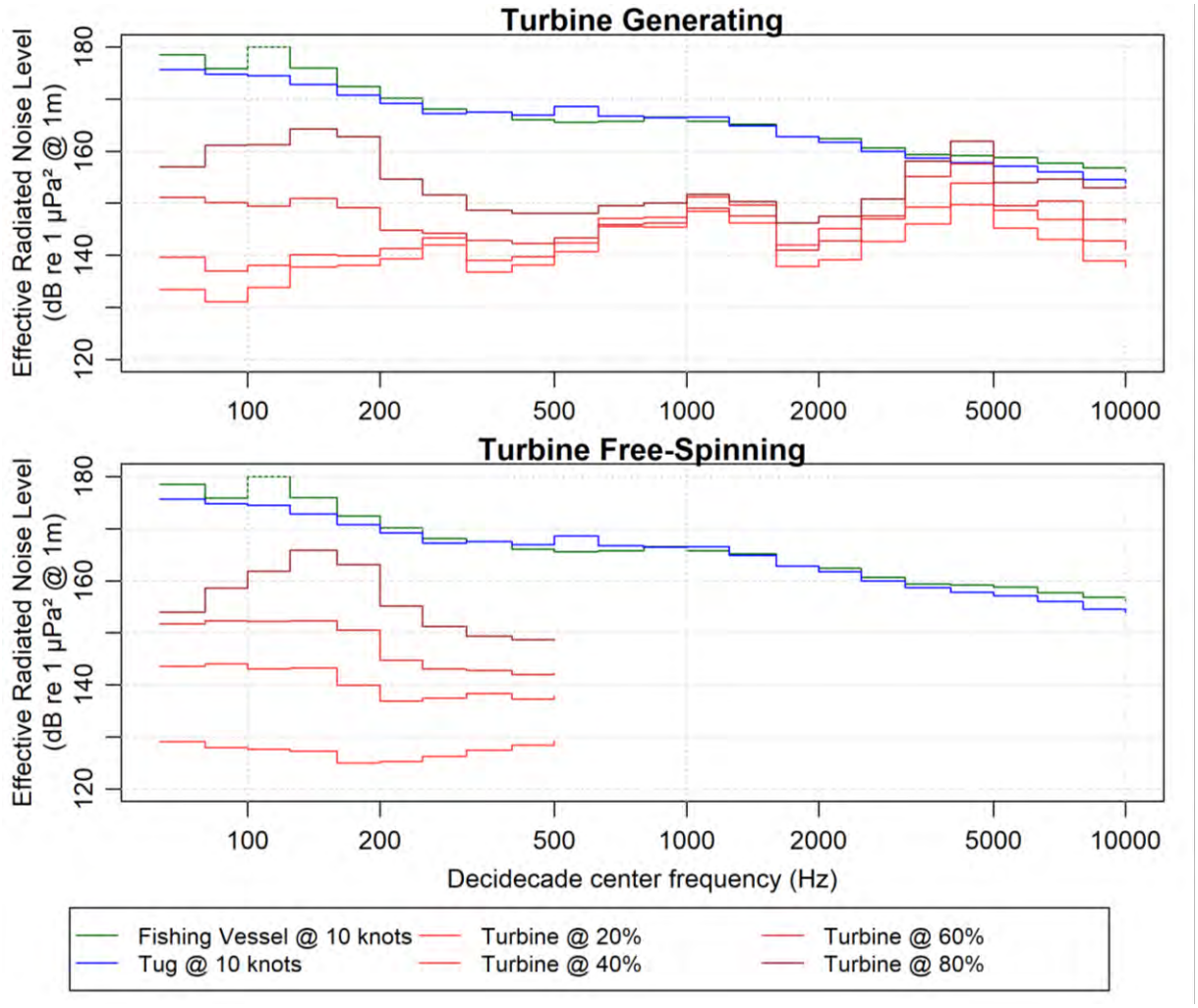

Figure 75. Comparing the turbine source levels to typical fishing and tugboat source levels. Above 400 Hz the turbine does not generate sounds in free-spinning mode that are measurable above background at 167 m.

D.2. Distances to Effects of Sound Radii

The model was used to estimate the distance to five threshold conditions:

1. The range where the 63 Hz and above sound pressure levels exceed 150 dB re 1 µPa which the range often specified for behavioural disturbance of fish.
2. The range where the 63 Hz and above sound pressure levels exceed the ambient background.
3. The range where the herring auditory filter weighted turbine sound levels exceed the herring-auditory-filter-weighted ambient background.
4. The range where the high-frequency cetacean marine-mammal auditory filter weighted sound pressure level exceeds background, which is the maximum range at which turbine sound could mask sounds a porpoise may hear.
5. The daily high-frequency cetacean weighted sound exposure level and the range to the temporary threshold shift criteria of 153 dB re 1 µPa²·s.

Both the environmental sound levels and turbine sound levels are highly variable due to the turbulence in the tidal flows. To capture this variability in the threshold ranges, we treated the sound levels measured at the AMAR as a variable source level. The calculations were:

1. Each minute of recordings where the normalized flow speed was greater than 20%, we assumed the signal at the AMAR was dominated by the turbine, and $20\log_{10}(167\text{ m})$ was added to the received level to convert the sound to as a source level (SL).
2. The ambient noise for the flow direction and normalized flow speed was extracted from the received level tables for the 'not spinning' turbine state (AN).
3. The threshold range is:

   $$R_T = 10^{(SL-AN)/20}\ .$$

   In the case of the 150 dB re 1 µPa² threshold the AN term is replaced by 150. The factor of '20' accounts for the spherical spreading in this environment (see Figure 73 and Appendix A.6).

The large set of results obtained may then be plotted using boxplots to provide an estimate of the variability in the threshold ranges (Figures 76–80). These figures show that:

1. The turbine sound only exceeds the threshold for behavioural disturbance to fish (150 dB re 1 µPa) at very short ranges and only at the highest current speeds on the flood tide (Figure 76).
2. The range where the turbine could be audible to herring, or mask sounds a herring could hear, was 1000 m (upper inter-quartile values in Figure 78). For most turbine states and current speeds, the range was 500 m or less.
3. The range where the turbine could be audible to porpoise, or mask sounds a porpoise could hear, was 800 m (Figure 79). The ranges were generally less than 300 m in the generating state and 150 m in the free-spinning state.
4. In the free-spinning state, the turbine was detectable above the background at a maximum of 500 m (Figure 77).
5. The high-frequency content in the generating sound results in longer ranges where the sound is greater than the ambient background than the free-spinning case; however, the sound is very constant, which results in a limited variability in the ranges where the turbine sound is above ambient for both the broadband and high-frequency cetacean weighted sound pressure levels.
6. The range where the turbine could cause temporary hearing shifts in porpoise, if one stayed beside the turbine for 24 hours, was 150–250 m on most days and increased to 500 m during spring tides (Figure 80). Based on the porpoise detection durations (Figure 49), it is highly unlikely that a porpoise would remain near the turbine for longer than one hour, and therefore TTS is not expected to occur.

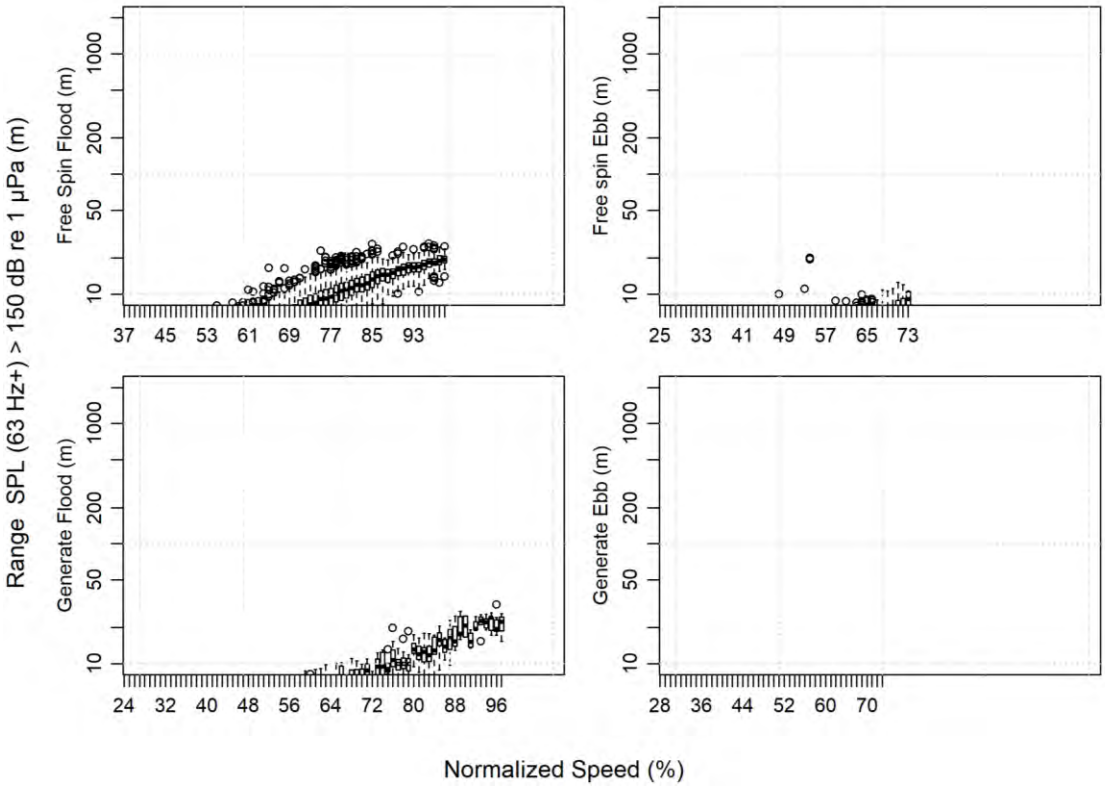

Figure 76. Threshold ranges for possible behavioural disturbance to fish.

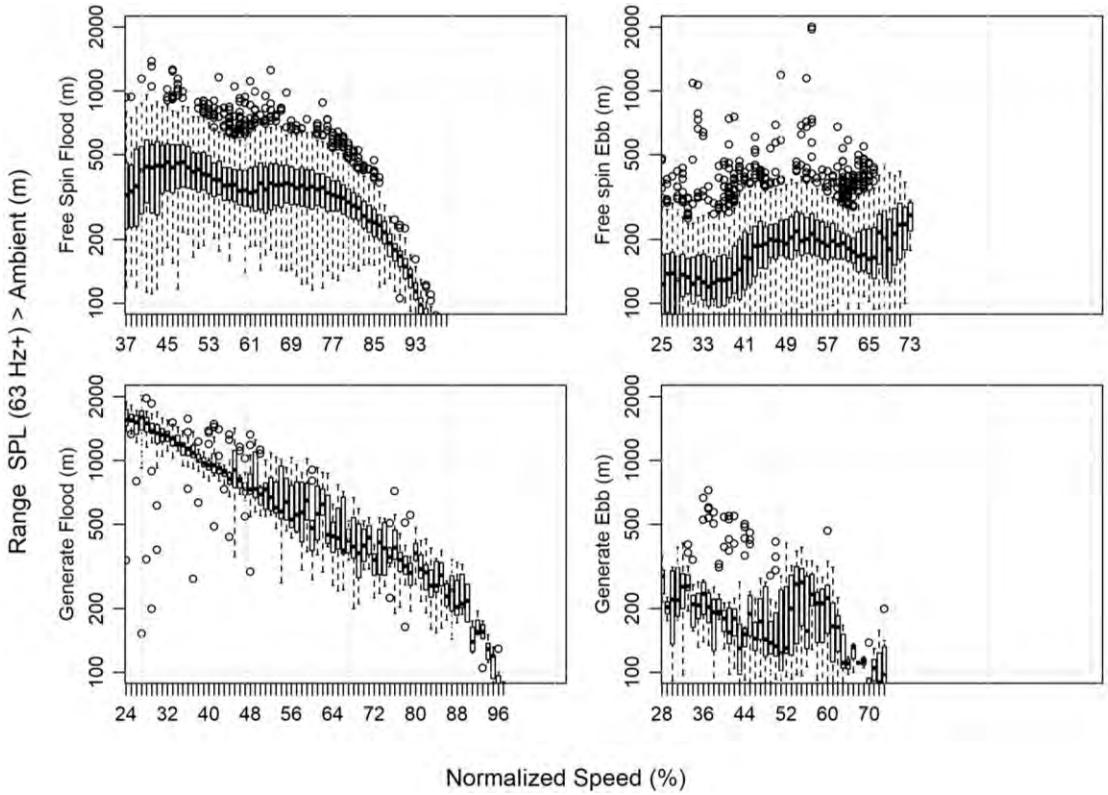

Figure 77. Threshold ranges where the turbine sound exceeds ambient background (63 Hz and above).

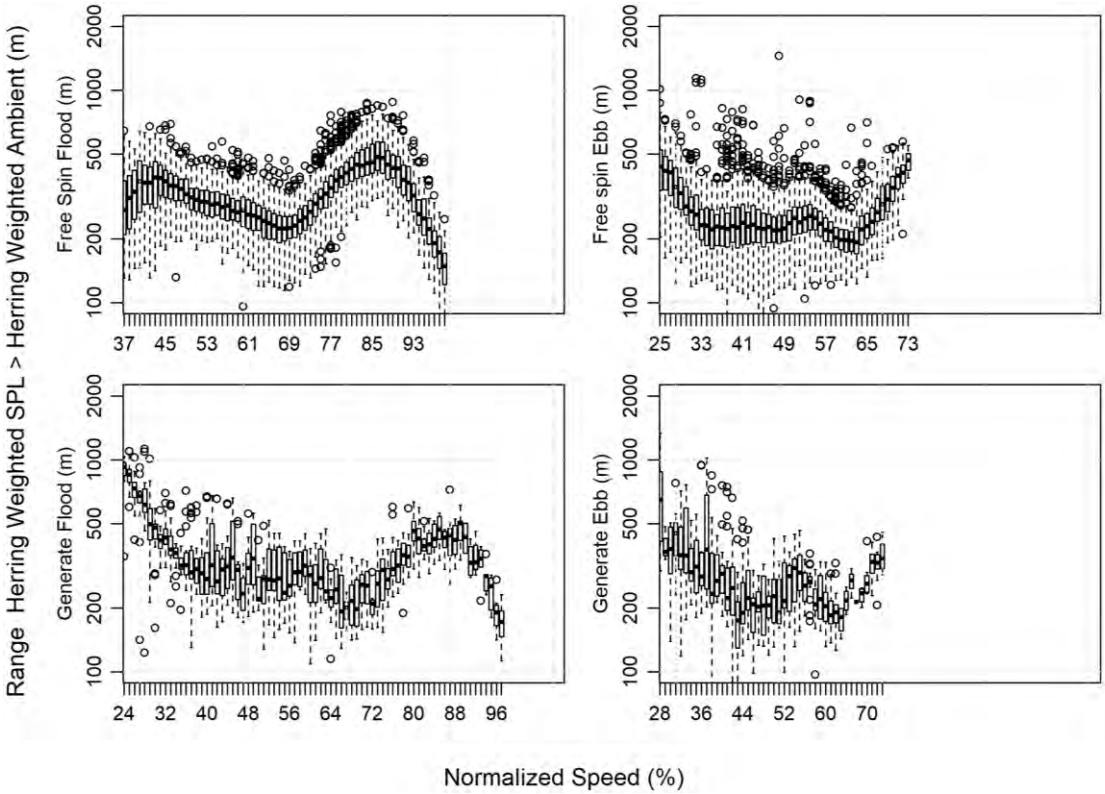

Figure 78. Threshold ranges where the herring audiogram weighted turbine sound exceeds the herring audiogram weighted background

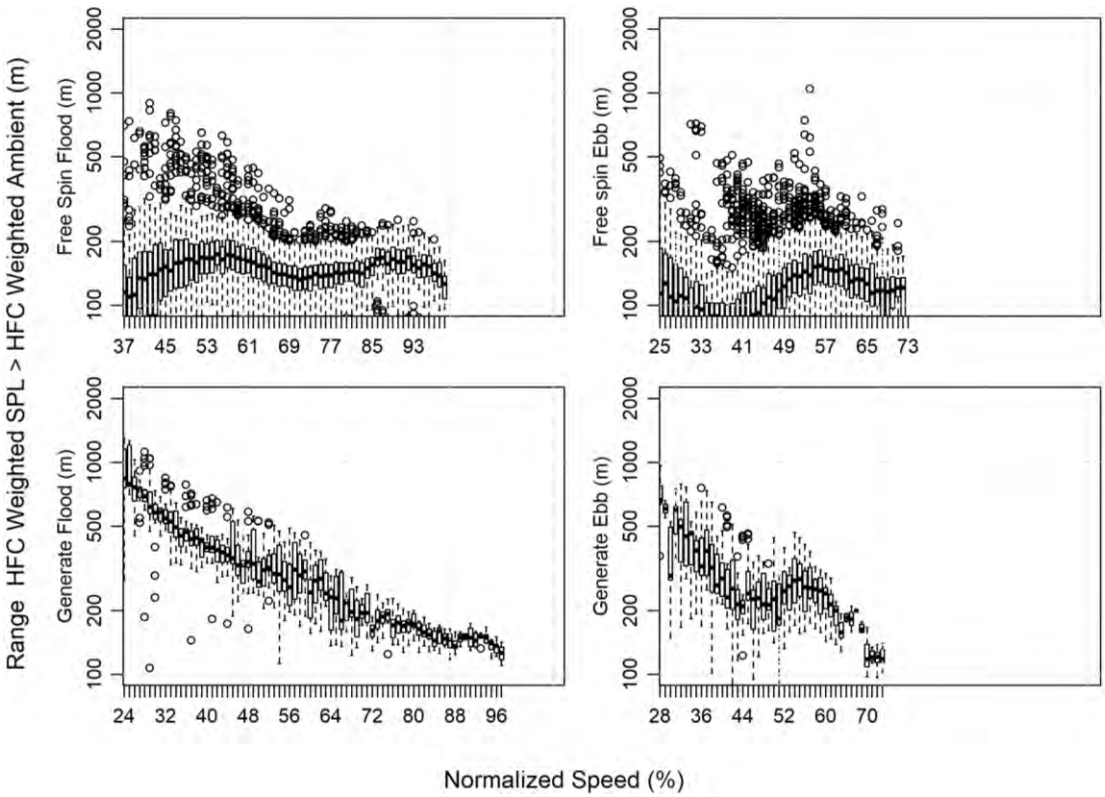

Figure 79. Threshold ranges where the HFC weighted turbine sound exceeds the HFC weighted background.

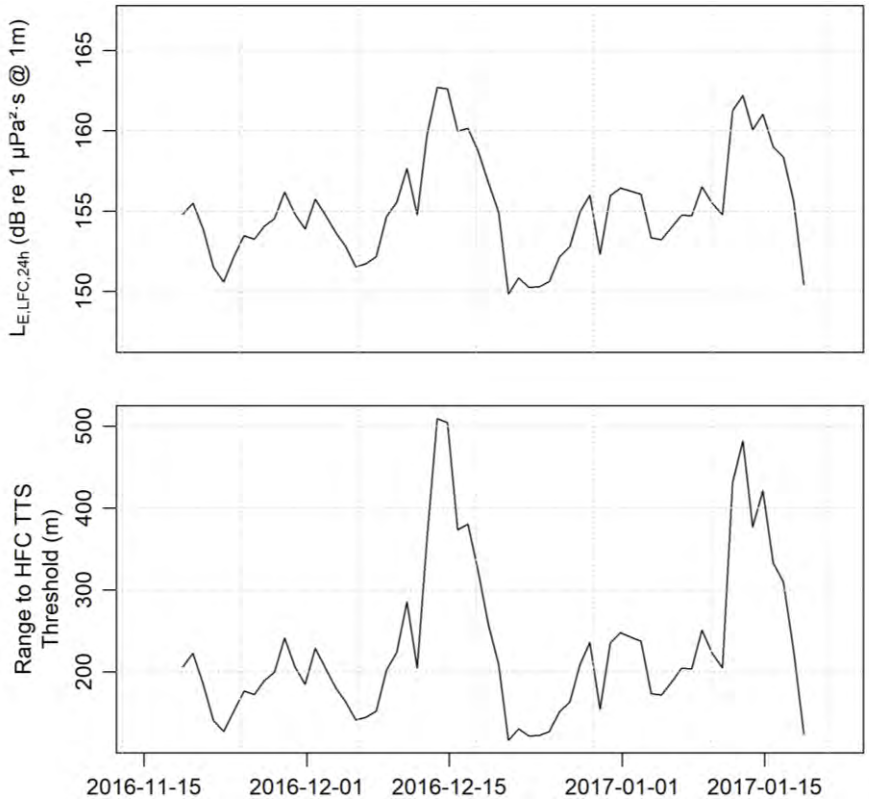

Figure 80. High-frequency cetacean weighted daily sound exposure levels and range to possible TTS.

D.3. Model Tables

This section contains embedded spreadsheets with the median sound pressure levels for each decidecade band and flow speed. The limits on using these models are:

- The free-spinning and generating models are only recommended for flow speeds above 20%.
- The not-spinning flood tide model should be used cautiously above 50% flow speeds.
- For ebb tides only use the data for flow speeds up to 70%.
- For the free-spinning state only use decidecades from 63–400 Hz; above 400 Hz the model is mostly environmental noise.
- For the generating state only use the decidecades from 63–10000 Hz.

D.3.1. Not Spinning Ebb

modelledSLsEbbNo
tSpinning_modelR_

D.3.2. Not Spinning Flood

modelledSLsFloodN
otSpinning_modelR

D.3.3. Free Spinning Ebb

modelledSLsEbbFre
eSpinning_modelR_

D.3.4. Free Spinning Flood

modelledSLsFloodF
reeSpinning_modelF

D.3.5. Generating Ebb

modelledSLsEbbGe
nerating_modelR_16

D.3.6. Generating Flood

modelledSLsFloodG
enerating_modelR_1